THE UNIVERSITY OF MICHIGAN

INDUSTRY PROGRAM OF THE COLLEGE OF ENGINEERING

THE EQUILIBRIUM OF SOLID CARBON DIOXIDE WITH ITS VAPOR IN THE PRESENCE OF NITROGEN

Richard E. Sonntag

A dissertation submitted in partial fulfillment
of the requirements for the degree of
Doctor of Philosophy in The
University of Michigan
1960

October, 1960

IP-469

Doctoral Committee:

Professor Gordon J. Van Wylen, Chairman
Professor Herbert H. Alvord
Assistant Professor Bernard A. Galler
Professor Joseph J. Martin
Professor G. Brymer Williams

ACKNOWLEDGMENTS

The author heartily expresses his gratitude to Professor Gordon J. Van Wylen, Chairman of the Doctoral Committee, for his constant encouragement and counsel during the course of the project.

The valuable assistance of Professors Herbert H. Alvord, Bernard A. Galler, Joseph J. Martin, Edgar F. Westrum, and G. Brymer Williams is gratefully acknowledged.

The advice of Professor John A. Clark and Mr. Herman Merte, Jr., and the assistance of Mr. Gene E. Smith are also appreciated.

The financial aid and support of the National Science Foundation, the Mechanical Engineering Department, and the Horace Rackham Graduate Fellowships and Scholarships are readily acknowledged.

Use of the facilities of the Heat Transfer and Thermodynamics Laboratory of the Mechanical Engineering Department and those of the Computing Center is appreciated.

The author also expresses his thanks to Miss Joyann Munson for the typing and to the Industry Program of the College of Engineering for the final preparation and reproduction of the manuscript.

TABLE OF CONTENTS

TABLE OF CONTENTS (CONT'D)

TABLE OF CONTENTS (CONT'D)

LIST OF TABLES

LIST OF FIGURES

LIST OF FIGURES (CONT'D)

NOMENCLATURE

A	Helmholtz function
A	Beattie-Bridgeman constant
a	Beattie-Bridgeman constant
B	Second virial coefficient
B	Beattie-Bridgeman constant
B*	Reduced second virial coefficient
b	Beattie-Bridgeman constant
b_o	Lennard-Jones force constant
C	Third virial coefficient
C*	Reduced third virial coefficient
c	Beattie-Bridgeman constant
D	Fourth virial coefficient
D1, D2, ..., D22	Functions, Beattie-Bridgeman equation solution
E	Lennard-Jones force constant
F	Arbitrary function
f	Fugacity
f	Function defined by (3-22)
G	Gibbs function
g	Molar Gibbs function
k	Arbitrary constant
k	Boltzmann's constant
N	Avogadro's number
n	Number of moles
P	Pressure

R	Gas constant (.08206 LIT-ATM/GM-MOLE-°K)
r	Molecule separation
S	Entropy
s	Molar entropy
T	Temperature
T*	Dimensionless temperature
U	Internal energy
V	Volume
v	Molar volume
y	Mole fraction
β	Second virial in Beattie-Bridgeman equation
γ	Third virial in Beattie-Bridgeman equation
δ	Fourth virial in Beattie-Bridgeman equation
ϵ	Enhancement factor
Θ_B	Second virial generalized function
Θ_C	Third virial generalized function
φ	Intermolecular force
σ	Lennard-Jones force constant
ω	Acentric factor

Subscripts

1	Component 1 (Carbon Dioxide)
2	Component 2 (Nitrogen)
3	Combination of 1 and 2
C	Critical state

i	i-th component or counter
R	Reduced
M	Mixture

Superscripts

g	Gas phase
s	Solid phase
◘	Saturation state
*	Ideal gas state
———	(over property) - Partial molar property

I. INTRODUCTION

A. Purpose

The purpose of this investigation is to determine the effect of gaseous nitrogen on the solid-vapor equilibrium of carbon dioxide in the temperature range 140-190°K, at up to 100 atmospheres pressure. The experimentally determined gas-phase composition is to be compared with that predicted by three different methods that have been used in the past on similar systems.

Temperatures as high as 190° are of particular interest in this study in order to be able to fully evaluate the simplifying assumptions made in one of the two solutions determined for each of the three equations of state. The upper limit of pressure has been chosen so as to give a gas phase density somewhat greater than that for which the equations of state are intended, especially at the lower temperatures.

B. Previous Work

A great deal of information has been published in past literature regarding the increase in apparent vapor pressure of a condensed phase when exposed to an inert gas pressure. It is perhaps somewhat more realistic to refer to this effect as the solubility of the condensed phase in the inert gas, the gas being termed inert because in many systems it dissolves in the condensed phase to only a very small degree. In many of the references mentioned below, this is the case, and in any event the gas phase composition was of principal interest.

In 1880, Hannay and Hogarth[1] studied the solubility of solid potassium iodide in alcohol and other vapors. More recently, Pollitzer and Strebel[2] determined the effects of nitrogen or hydrogen on the carbon dioxide liquid-vapor equilibrium, and also that of air, nitrogen or hydrogen on water liquid-vapor at various pressures and temperatures. Bartlett[3] also presented results of the solubility of water in hydrogen, and also other gases. Braune and Strassmann[4] investigated the effect of carbon dioxide on the vapor pressure of iodine at up to fifty atmospheres total pressure. In 1934, Saddington and Krase[5] studied water liquid-vapor in the presence of nitrogen at as high as three hundred atmospheres. Perkins[6] considered the influence of helium, argon or nitrogen on the decomposition of $Ba\,Cl_2 \cdot 8NH_3(s)$. In 1941, Kritchevsky and Koroleva[7] determined the effects of nitrogen, hydrogen, methane or carbon dioxide on the liquid-vapor methanol equilibrium at up to seven hundred atmospheres. In the same year, Wiebe and Gaddy[8] worked with the system water-carbon dioxide at high pressures. The following year, Kritchevsky and Gamburg[9] investigated benzene in nitrogen gas. Gratch[10] considered the effect of air on solid carbon dioxide, a system very similar to the present one, but at pressures up to fifty atmospheres. In 1948, Diepen and Scheffer[11] published results of the remarkable influence of ethylene gas on naphthalene, in which the apparent vapor pressure was as much as 25,000 times its value for pure naphthalene. Ipatev, et. al.[12] studied the benzene equilibrium, as in Reference 9, but under the influence of hydrogen gas. In 1950, Webster[13] found the effect of air on the water solid-vapor and liquid-vapor equilibria. He continued his work[14] on carbon dioxide-air as in (10), but at pressures

as high as two hundred atmospheres. In much of this work, the air was in the liquid rather than the vapor phase. In a particularly interesting study, Dokoupil, Van Soest, and Swenker[15] determined the influence of hydrogen on the solid-vapor systems nitrogen, carbon monoxide, and nitrogen-carbon monoxide at up to fifty atmospheres, and also made some theoretical predictions of the gas compositions. Another investigation of interest is that of Ewald,[16] who determined the solubility of solid xenon in nitrogen, hydrogen, and helium, and also solid carbon dioxide in hydrogen and helium. He also made theoretical calculations of the composition, but by methods different from those of the preceeding reference.

The systems discussed above were all of a similar nature to the present one, although in many of these the condensed phase was liquid rather than solid. There have also been a number of similar investigations carried out on systems comprised of more complex organic molecules.

Inasmuch as the present study involves carbon dioxide, a brief mention will also be made of recent work in the area of two-component two-phase equilibria, even though that type of system is not under consideration here. The majority of this recent work involving carbon dioxide has been the phase equilibrium with one or more hydrocarbons.

Poettman and Katz[17] presented the phase diagrams for carbon dioxide with propane, butane and pentane, respectively. Clark and Din[18] were concerned with carbon dioxide-acetylene, including three-phase equilibrium. Haselden, Newitt and Shah[19] investigated the systems carbon dioxide-ethylene and carbon dioxide-propylene, and in 1953 Bierlein and Kay[20] studied carbon dioxide-hydrogen sulfide. The following year,

Donnelly and Katz[21] considered the liquid-vapor and three-phase loci of carbon dioxide-methane, with very interesting results. In 1959 Sobocinski and Kurata[22] worked with the same system as (20) but also included a three-phase study.

Regarding the mutual solubility of liquid carbon dioxide with other liquids, Thiel and Schulte[23] published some results in 1920. Quinn and Jones[24] later presented a more complete discussion on the subject, and Francis[25] published mutual solubilities for 261 different liquids with liquid carbon dioxide in 1954. None of these included nitrogen, however, due to the low critical temperature of nitrogen.

Only a fairly small number of investigations have been concerned with the properties of the carbon dioxide-nitrogen system. Of these, two have been found which deal with the solubility of solid carbon dioxide in liquid nitrogen, those of Ishkin and Burbo[26] and also Fedorova.[27] Abdulaev[28] and also Mills and Miller[29] considered the liquid-vapor phase diagram of this system, but the results were quite incomplete.

From the theoretical viewpoint, that of predicting gas phase composition in the condensed phase-inert gas type of system, Dokoupil[15] used a simplified solution involving the Beattie-Bridgeman equation of state with very good results, although pressures were limited to fifty atmospheres. In 1953 Robin and Vodar[30] performed calculations for the data of References 3, 4, 5, 7, 8, 9, 12, and others, using a Statistical Mechanics virial-form of equation, and assuming the Lennard-Jones potential to be valid. The equation was limited to only the second virial coefficient, but results were generally quite good, except for systems

involving either water as the condensed phase or hydrogen as the inert gas. The same year, Webster[31] discussed his work[13,14] from a theoretical standpoint. Still in 1953, Ewald, Jepson and Rowlinson[32] made calculations for the data of References 11, 14, and others, also using a virial-form equation of state with the Lennard-Jones potential and empirical combination of the critical constants, resulting from the theorem of corresponding states. Their equation included terms through the third virial coefficient, and the results were reasonably good, at least for systems of fairly simple molecules.

Ewald[16] later improved upon this method by using intermolecular force constants determined from experimental virial coefficients, instead of estimating them by empirical relations with the critical constants. He then made semi-empirical combinations of these pure substance force constants to enable calculation of the interaction coefficients for gas mixtures.

Prausnitz[33] presented a new method for determining interaction coefficients for the second and third virial terms, his method based on the principle of corresponding states and tables compiled from generalization of mixture behavior.

Prausnitz considered an isotherm of (11) as one application of his method, with good correlation.

Ziegler[34] has made very extensive calculations for the solid-gas and liquid-gas equilibria of methane-hydrogen, using the methods of Dokoupil,[15] Ewald,[16] and others.

The methods and procedures discussed briefly here will be presented in detail in Section III, in order to obtain solutions of the theoretical equations of the following section.

II. DERIVATION OF THEORETICAL EQUATIONS

A. General

For a pure substance, the thermodynamic property relation

$$dU = TdS - PdV + \bar{G}_1 dn_1 + \bar{G}_2 dn_2 + \ldots \tag{2-1}$$

becomes

$$dU = TdS - PdV + gdn \tag{2-2}$$

Consider the Helmholtz and Gibbs functions:

$$A = U - TS \tag{2-3}$$

$$G = U + PV - TS \tag{2-4}$$

Differentiating (2-3) and (2-4),

$$dA = dU - TdS - SdT \tag{2-5}$$

$$dG = dU + PdV + VdP - TdS - SdT \tag{2-6}$$

Substituting these relations into (2-2) yields

$$dA = - SdT - PdV + gdn \tag{2-7}$$

$$dG = - SdT + VdP + gdn \tag{2-8}$$

B. Pure Substance Solid-Vapor Equilibrium

Expanding Equation (2-8),

$$d(ng) = ndg + gdn = -nsdT + nvdP + gdn$$

or

$$dg = -sdT + vdP \tag{2-9}$$

It has been shown, according to the methods of Gibbs, that for a solid-vapor equilibrium at a given temperature and pressure (the sublimation pressure $P_1^{\square}$)

$$g^s = g^g \tag{2-10}$$

If the vapor behaves ideally,

$$v = \frac{RT}{P} \tag{2-11}$$

Then, from (2-9) and (2-11) at constant temperature,

$$dg = \frac{RT}{P}\, dP = RTd\ (\ln P) \tag{2-12}$$

In order to preserve this form for a real gas, the quantity fugacity is introduced by the definition:

$$dg = RTd\ (\ln f) \tag{2-13}$$

with the realization that a real gas approaches ideal behavior as $P \to 0$, so that

$$\lim_{P \to 0} (f/P) = 1 \tag{2-14}$$

Therefore, the criterion for equilibrium can be written

$$f^s = f^g = f^{\square} \tag{2-15}$$

where the superscript $\square$ refers to the value at the vapor (sublimation) pressure of the pure substance.

C. Solid-Vapor Equilibrium in the Presence of an Inert Gas

Denoting the substance appearing in both phases by the subscript 1, the requirement for equilibrium in this case is

$$g_1^s = \overline{G}_1^g \tag{2-16}$$

where $\overline{G}_1^g$ denotes the partial free energy of component 1 in the gaseous phase.

For component 1 of the mixture, Equation (2-13) is written

$$d\overline{G}_1 = RT\ d(\ln \overline{f}_1) \tag{2-17}$$

where the fugacity of 1 approaches the partial pressure as the total pressure tends to zero, or

$$\lim_{P \to 0} \left(\frac{\bar{f}_1}{y_1 P}\right) = 1 \tag{2-18}$$

Therefore, the criterion for this equilibrium is that

$$f_1^s = \bar{f}_1^g \tag{2-19}$$

Equating Equation (2-9) with (2-13) written for solid 1 at constant temperature,

$$dg_1 = RTd\ (\ln f_1^s) = v_1^s dP \tag{2-20}$$

Equation (2-20) is now integrated from the vapor pressure $P_1^\square$ to the pressure of the system, giving

$$RT \ln \frac{f_1^s}{f_1^\square} = \int_{P_1^\square}^{P} v_1^s dP \tag{2-21}$$

But, substitution of Equation (2-19) results in

$$RT \ln \frac{\bar{f}_1^g}{f_1^\square} = \int_{P_1^\square}^{P} v_1^s dP \tag{2-22}$$

which is the equilibrium equation for the system under consideration.

In order to calculate the percent composition of the gas-phase as fixed by (2-22), it will be necessary to determine expressions for $\bar{f}_1^g$ and $f_1^\square$ in terms of the behavior of the gas mixture and pure substance 1, respectively. In both cases, T and V will be selected as independent variables, the reasons for which will become obvious later.

D. Pure Gas Fugacity (component 1)

Taking a cross partial differential in Equation (2-7),

$$\left(\frac{\partial g}{\partial V}\right)_{T,n} = -\left(\frac{\partial P}{\partial n}\right)_{T,V} \tag{2-23}$$

Or, at constant T,n:

$$dg = -\left(\frac{\partial P}{\partial n}\right)_{T,V} dV \tag{2-24}$$

Substituting Equation (2-13) into (2-24),

$$RT\,d\,(\ln f) = -\left(\frac{\partial P}{\partial n}\right)_{T,V} dV \tag{2-25}$$

which may also be written as

$$RT\,d\,(\ln fV) = -\left[\left(\frac{\partial P}{\partial n}\right)_{T,V} - \frac{RT}{V}\right]dV \tag{2-26}$$

Equation (2-26) is to be integrated from an arbitrarily low pressure P * to the vapor pressure $P_1^{\square}$. From this point on, the subscripts 1 will be included to denote that pure substance.

As P* is made to approach zero, note that the lower limit on the left-hand side of (2-26) tends to

$$(f_1 V_1)^* \rightarrow (P_1 V_1)^* = n_1 RT \tag{2-27}$$

and the lower limit on the right-hand side of (2-26) goes to

$$V_1^* \rightarrow \infty \quad \text{as } P^* \rightarrow 0 \tag{2-28}$$

so that

$$RT \ln \frac{f_1^{\square} V_1^{\square}}{n_1 RT} = -\int_{\infty}^{V_1^{\square}} \left[\left(\frac{\partial P}{\partial n}\right)_{T,V} - \frac{RT}{V}\right]dV \tag{2-29}$$

But, since

$$V_1^\square/n_1 = v_1^\square \qquad \text{at } P_1^\square \,, \tag{2-30}$$

$$RT \ln\left(\frac{f_1^\square}{P_1^\square}\right) = \int_{V_1^\square}^{\infty} \left[\left(\frac{\partial P}{\partial n}\right)_{T,V} - \frac{RT}{V}\right] dV - RT \ln \frac{P_1^\square v_1^\square}{RT} \tag{2-31}$$

giving an expression for $f_1^\square$ in terms of the behavior of pure substance 1.

E. Fugacity of a Component in a Gas Mixture

Substituting (2-5) into (2-1),

$$dA = - SdT - PdV + \bar{G}_1 dn_1 + \bar{G}_2 dn_2 \tag{2-32}$$

Taking a cross partial differential,

$$\left(\frac{\partial \bar{G}_1}{\partial V}\right)_{T,n} = - \left(\frac{\partial P}{\partial n_1}\right)_{T,V,n_2} \tag{2-33}$$

Or, at constant T,n:

$$d\bar{G}_1 = - \left(\frac{\partial P}{\partial n_1}\right)_{T,V,n_2} dV \tag{2-34}$$

Substituting Equation (2-17) into (2-34),

$$RTd\ (\ln \bar{f}_1^g) = - \left(\frac{\partial P}{\partial n_1}\right)_{T,V,n_2} dV \tag{2-35}$$

As before, this may be rewritten as

$$RTd\ (\ln \bar{f}_1^g V) = - \left[\left(\frac{\partial P}{\partial n_1}\right)_{T,V,n_2} - \frac{RT}{V}\right] dV \tag{2-36}$$

Equation (2-36) is to be integrated from an arbitrary P* to the pressure of the mixture P. As $P^* \to 0$, the lower left-hand limit of (2-36) is

$$(\bar{f}_1^g V)^* \to (y_1 PV)^* = y_1 nRT \tag{2-37}$$

Integrating,

$$RT \ln \frac{\bar{f}_1^g V}{y_1 nRT} = - \int_{\infty}^{V} \left[\left(\frac{\partial P}{\partial n_1}\right)_{T,V,n_2} - \frac{RT}{V}\right] dV \tag{2-38}$$

But,

$$V/n = v \text{ of the mixture} \tag{2-39}$$

Therefore,

$$RT \ln\left(\frac{\bar{f}_1^g}{y_1 P}\right) = \int_V^\infty \left[\left(\frac{\partial P}{\partial n_1}\right)_{T,V,n_2} - \frac{RT}{V}\right] dV - RT \ln \frac{Pv}{RT} \tag{2-40}$$

relating $\bar{f}_1^g$ to the behavior of the gas mixture.

The reason for selecting volume (rather than pressure) as an independent variable in the derivations of the two preceding sections is now quite apparent. In order to evaluate Equation (2-31) it will be necessary to employ an equation of state for pure 1, and for Equation (2-40), an equation of state for the gas mixture will be required. In both cases, one of the accurate pressure-explicit equations of state can be used. Had pressure been used as an independent variable, the resulting equations analogous to (2-31) and (2-40) would have necessitated the use of volume-explicit equations of state, which are inherently less accurate than the pressure-explicit forms.

F. Enhancement Factor

Before substituting (2-31) and (2-40) into the equilibrium Equation (2-22), it will be convenient to introduce a dimensionless parameter called the enhancement factor ϵ, which is defined by the following conditions:

$$\epsilon = y_1/y_{1(\text{ideal})} \tag{2-41}$$

where, for $y_{1(\text{ideal})}$:

a) the gas mixture behaves ideally, so that

$$\bar{f}_1^g = y_1 P$$

b) increasing pressure from $P_1^{\square}$ to P has no effect on the fugacity of the solid, or

$$f_1^s = f_1^{\square}$$

c) Pure 1 at $P_1^{\square}$ behaves ideally or

$$f_1^{\square} = P_1^{\square}$$

Therefore,

$$y_{1(\text{ideal})} = \frac{P_1^{\square}}{P} \tag{2-42}$$

and

$$\epsilon = y_1 P / P_1^{\square} \tag{2-43}$$

Now, substituting Equation (2-31), (2-40), and (2-43) into (2-22) gives the equilibrium equation, which upon rearrangement may be written

$$RT \ln \epsilon = RT \ln \frac{Pv}{P_1^{\square} v_1^{\square}} + \int_{V_1^{\square}}^{\infty} [(\frac{\partial P}{\partial n})_{T,V} - \frac{RT}{V}]dV$$

$$- \int_{V}^{\infty} [(\frac{\partial P}{\partial n_1})_{T,V,n_2} - \frac{RT}{V}]dV + \int_{P_1^{\square}}^{P} v_1^s dP \tag{2-44}$$

The enhancement factor is a convenient parameter for determining deviation from the ideal behavior given by the assumptions a) - c) above. It should be recalled that in Equation (2-44), the first integral refers to pure substance 1, the second to the gas mixture, and the third to solid 1.

For given values of temperature and pressure, Equation (2-44) specifies one equation in two unknowns, y_1 and v. Note that y_1 is included in ϵ and will also appear upon integration of the integral for the gas mixture. The second relation between y_1 and v comes from the gas mixture equation of state itself, thereby permitting solution of the set for the given T and P.

III. EQUATIONS OF STATE

A. General

In order to be able to obtain solutions of the theoretical Equation (2-44) and thereby predict gas-phase composition for a given temperature and pressure, it will be necessary to use an equation of state to evaluate the integrals. Consequently, an equation will be required for pure carbon dioxide and also one for the gas mixture. The former is not at all a difficult task, as its use lies in an integration from zero to the vapor pressure of carbon dioxide, which is a small number at the temperature of interest. Accurate equations of state for gas mixtures are a different matter, however, and particularly at high densities.

Beattie and Stockmayer[35] have given an excellent review on equation of state development up to 1940, including that from Statistical Mechanics. A great deal of progress has been made since that time, especially in the area of high density equations, mixtures, and theoretical correlations from Statistical Mechanics.

B. Beattie-Bridgeman Equation of State

The Beattie-Bridgeman equation of state (36, 37, 38) is most commonly presented in the form

$$P = \frac{RT}{v^2}(1-c')(v+B') - \frac{A'}{v^2} \qquad (3\text{-}1)$$

where:

$$A' = A(1-a/v) \tag{3-2}$$

$$B' = B(1-b/v) \tag{3-3}$$

$$c' = c/vT^3 \tag{3-4}$$

in which A, B, a, b, c are the five constants evaluated empirically from P-V-T data for a given substance.

While the above form of Equation (3-1) gives some insight into the nature of the Beattie-Bridgeman equation, showing the constants as corrections to the ideal-gas equation, it is perhaps more useful, especially for this study, to present the equation in a virial form,

$$P = \frac{RT}{v} + \frac{\beta}{v^2} + \frac{\gamma}{v^3} + \frac{\delta}{v^4} \tag{3-5}$$

where β, γ, δ can be called the second, third, and fourth virial coefficients, and are given in terms of the Beattie-Bridgeman constants by

$$\beta = BRT - A - cR/T^2 \tag{3-6}$$

$$\gamma = Aa - BbRT - BcR/T^2 \tag{3-7}$$

$$\delta = BbcR/T^2 \tag{3-8}$$

Care must be taken not to confuse these virial coefficients β, γ, δ, with those for an equation of state written in terms of the compressibility factor Pv/RT.

The Beattie-Bridgeman equation of state has been applied to many gases, including all the common ones, with excellent correlation up to approximately 0.8 times the critical density. At densities greater than the critical, however, the equation begins to fail very

badly, since it has been empirically fitted in the lower density region only.

This equation has also been successfully applied to mixtures of gases, through empirical combination of each of the five constants for the pure gases. Although mixture representation has not been found to be as accurate as for pure gases, it is, nevertheless, very good, and comparable to other methods of algebraic representation of similar complexity.

Since the mixture of the present investigation consists of only two components, further discussion will be limited to binary mixtures. Of course, extension of the methods to more complex mixtures follows.

Consider a constant k as part of an equation of state used to represent a given pure gas. If it is assumed that this constant has numerical values k_1 and k_2 for the two gases comprising the mixture, then k for such a mixture can be given by

$$k_M = y_1^2 k_1 + 2y_1 y_2 k_3 + y_2^2 k_2 \qquad (3\text{-}9)$$

Where k_3 is termed the interaction coefficient, the value of which remains to be determined as some function of k_1 and k_2 only.

Three logical combinations of k_1 and k_2 to try in attempting to find a good value for k_3 are the following:

Linear combination (arithmetic mean)

$$k_3 = \frac{1}{2}(k_1 + k_2) \qquad (3\text{-}10)$$

Square-root combination (geometric mean)

$$k_3 = (k_1 k_2)^{1/2} \tag{3-11}$$

Cube-root or Lorentz combination

$$k_3 = \frac{1}{8}(k_1^{1/3} + k_2^{1/3})^3 \tag{3-12}$$

For the linear combination, substitution of (3-10) into (3-9) yields

$$k_M = y_1 k_1 + y_2 k_2 \tag{3-13}$$

or, generalizing,

$$k_M = \sum_i y_i k_i \tag{3-14}$$

For the square-root combination, substituting (3-11) into (3-9) gives:

$$k_M = y_1^2 k_1 + 2y_1 y_2 (k_1 k_2)^{1/2} + y_2^2 k_2 \tag{3-15}$$

or, generalizing,

$$k_M = (\sum_i y_i k_i^{1/2})^2 \tag{3-16}$$

Finally, for the Lorentz combination, substituting (3-12) into (3-9) results in:

$$k_M = y_1^2 k_1 + \frac{1}{4} y_1 y_2 (k_1^{1/3} + k_2^{1/3})^3 + y_2^2 k_2 \tag{3-17}$$

or, generalizing Equation (3-17),

$$k_M = \frac{1}{8} \sum_i \sum_j y_i y_j (k_i^{1/3} + k_j^{1/3})^3 \tag{3-18}$$

A great deal of work has been done in the past in order to determine which combination of the three methods given here should be used for the five constants in the equation of state (39, ..., 42), and others. In particular, those of (15, 41, 42) suggest a square-root combination for the constants A and c, a Lorentz combination for B, and linear combination for both a and b, especially for gaseous equilibrium systems.

In order to test the various methods used previously for mixtures, a computer program was written and executed using the IBM 704 computer facilities of The University of Michigan.(43) The ten most commonly suggested methods of combination were tried, and compared with experimental data for various mixtures of nitrogen and carbon dioxide (44, ..., 47), and also for mixtures of other gases.

The method suggested above gave good correlation, and while it did not show the lowest standard deviation (in pressure) at low densities, it was among the best, and held reasonably well to higher densities than any of the other methods tried, a factor which is of prime importance in this investigation.

There are many references in the literature to the use of the Beattie-Bridgeman equation as applied to gas mixtures. Of these, (15, 41, 48, 49, 50) are of interest in that they dealt with application to high-pressure equilibrium calculations, including mixture fugacity determination. In particular, Reference 49 referred to the prediction of gas-phase composition for the iodine solid-vapor or liquid-vapor equilibrium in the presence of air, carbon dioxide, or

hydrogen. Also, as mentioned in Section I, Reference 15 made use of the Beattie-Bridgeman equation for similar calculations in the systems nitrogen-hydrogen, carbon monoxide-hydrogen, and nitrogen-carbon monoxide-hydrogen.

C. Virial Equation of State

1. Form of Equation and the Lennard-Jones (6-12) Potential

The virial equation of state was used by Kammerlingh Onnes,[51] although simply as a curve-fitting technique. It was not until some time later that much success was achieved in relating the virial coefficients to intermolecular forces and distances using the methods of Statistical Mechanics.

The virial equation is written as a power series in pressure or reciprocal volume, although the latter is more common and generally gives a better correlation with experimental data. The equation is normally written in terms of the compressibility factor, as:

$$\frac{Pv}{RT} = 1 + \frac{B}{v} + \frac{C}{v^2} + \frac{D}{v^3} + \ldots \qquad (3\text{-}19)$$

where B, C, D, the second, third and fourth virial coefficients, respectively, are temperature functions but are not the same as those of the Beattie-Bridgeman Equation (3-5), differing in each case by the factor RT.

Considerable effort has been put forth in the area of determining virial coefficients during the past 25 years, from both the theoretical and empirical standpoints. Almost no success has been realized beyond the third virial coefficient C, and so higher order terms will not be considered further here.

From the methods of Statistical Mechanics, the second and third virial coefficients can be given[52,53] in terms of the intermolecular potential energy $\varphi_{ij}(r)$ of a pair of molecules i and j, of separation r_{ij} by the relations

$$B = -2\pi N \int_0^\infty [\epsilon^{-\varphi(r)/kT} - 1]r^2 dr \qquad (3\text{-}20)$$

$$C = -\frac{8\pi^2 N^2}{3} \iiint f_{12}f_{13}f_{23}\, r_{12}r_{13}r_{23}\, dr_{12}dr_{13}dr_{23} \qquad (3\text{-}21)$$

(Integral over all r_{12}, r_{13}, r_{23}, which form a triangle) where

$$f_{ij}(r_{ij}) = [\epsilon^{-\varphi_{ij}/kT} - 1] \qquad (3\text{-}22)$$

and N is Avogadro's number.

The assumption of additivity of forces has been made here, and also that the molecules have spherically symmetric force fields. Solution of (3-20) and (3-21) for the virial coefficients will, of course, require an expression for the intermolecular potential function $\varphi(r)$.

The Lennard-Jones (6-12) potential, References 53, 54, 55, is such an expression for non-polar molecules, relating the potential energy to the constants E and σ in the form

$$\varphi(r) = 4E[(\sigma/r)^{12} - (\sigma/r)^6] \qquad (3\text{-}23)$$

For a given substance, σ is the separation for which the potential energy is zero, and E is the maximum attractive energy between two molecules, occurring at $r = \sigma(2)^{1/6}$. In (3-23), for large separation of the molecules ($r \gg \sigma$), the inverse sixth-power attractive component dominates. On the other hand, for $r \ll \sigma$, the inverse twelfth-power repulsive term is dominant.

It should be pointed out that the exponents 12, 6 of (3-23) are empirical, and by no means universal. Some calculations have been made using other exponents, particularly for a (6-9) potential, but results seem to correlate better for the (6-12) form, at least for the second virial coefficient.

Integration of (3-20) for the second virial can be performed by substitution of (3-23). In this operation, it will be convenient to incorporate a set of dimensionless parameters, defined as:

$$T^* = kT/E \tag{3-24}$$

$$B^*(T^*) = \frac{B}{\frac{2}{3}\pi N\sigma^3} = \frac{B}{b_o} \tag{3-25}$$

The result of the integration is then

$$B^*(T^*) = \sum_{j=0}^{\infty} b_j \, (T^*)^{-(\frac{2j+1}{4})} \tag{3-26}$$

Where the coefficients b_j are given by

$$b_j = \frac{(2)^{j+\frac{1}{2}}}{4j!}\,\Gamma\left(\frac{2j-1}{4}\right) \tag{3-27}$$

The values for $B^*(T^*)$ have been evaluated and compiled.[56,53]

A similar procedure is followed for the third virial coefficient, by substituting (3-23) into (3-21) and integrating, also making use of (3-24) and the function

$$C^*(T^*) = \frac{C}{b_o^2} \tag{3-28}$$

This integration results in

$$C^*(T^*) = \sum_{j=0}^{\infty} c_j \, (T^*)^{-(\frac{j+1}{2})} \qquad (3\text{-}29)$$

The coefficients c_j of (3-29) are not simple functions, but instead are complex integrals. The values of C* have been evaluated by numerical procedures,(57, 58, 59) and are also compiled in Reference 53.

Some experimental determinations of the virial coefficients and equations for nitrogen and carbon dioxide from P-V-T data are given in References 60, ..., 65. Virial coefficients are determined from the low density compressibility data according to the following procedure:

The equation of state (3-19) is rearranged into the form

$$(\frac{Pv}{RT} - 1)\, v = B + C(\frac{1}{v}) \qquad (3\text{-}30)$$

For a given temperature, a plot of

$$(\frac{Pv}{RT} - 1)\, v \qquad \text{vs. } 1/v$$

will yield B as the intercept at $(1/v) = 0$ and C as the slope at $(1/v) = 0$, both values being for that temperature only. The difficulty with this method of determining virial coefficients is that extremely accurate compressibility data at low densities is required.

Force constants for the Lennard-Jones (6-12) potential may be computed from the second virial coefficient as found from compressibility data, or by a similar procedure using viscosity data.

2. Methods for Gas Mixtures

In the case of gas mixtures, the equation of state has the same form as (3-19), but the virial coefficients must now represent the mixture,

and are therefore functions of mole fractions as well as the temperature. It has been shown[66] by methods similar to those for pure substances that the n-th virial coefficient is a polynomial of n-th degree in the mole fraction. That is,

$$B_{MIX} = \sum_i \sum_j y_i y_j B_{ij} \tag{3-31}$$

$$C_{MIX} = \sum_i \sum_j \sum_k y_i y_j y_k C_{ijk} \tag{3-32}$$

Where the B_{ij}, C_{ijk} in which all subscripts are not the same are termed interaction coefficients. The remaining ones, those for which all subscripts are identical, are simply the coefficients for the pure substances comprising the mixture. The interaction coefficients can be represented by equations analogous to (3-20), (3-21), in which the intermolecular potential function is that between molecules of different species.

In the case of a binary mixture, which is of principal interest here, for components 1 and 2 the Equations (3-31) and (3-32) may be expanded into

$$B_{MIX} = y_1^2 B_{11} + 2y_1 y_2 B_{12} + y_2^2 B_{22} \tag{3-33}$$

$$C_{MIX} = y_1^3 C_{111} + 3y_1^2 y_2 C_{112} + 3y_1 y_2^2 C_{122} + y_2^3 C_{222} \tag{3-34}$$

The problem in representing mixtures now reduces to that of determining the various interaction coefficients appearing in (3-33), (3-34). The B_{11}, C_{111} are those for pure component 1, etc.

The method following (3-30) for experimentally determining virial coefficients cannot readily be followed for mixtures, as sufficiently accurate low-density P-V-T data is lacking. Even in cases for

which this can be done, it must be remembered that virial coefficients so determined are valid for that exact composition only, and are therefore used in turn to calculate the interaction coefficients.

Until such a time when extensive mixture data are available, it seems reasonable to combine the pure substance intermolecular force constants semi-empirically, as suggested in References 16, 53, 62, 67, ..., 70, and the resulting combined constants used with the Lennard-Jones potential to calculate the interaction coefficient B_{12} of Equation (3-33). The most generally accepted method of combination is

$$E_{12} = (E_1 E_2)^{1/2} \tag{3-35}$$

$$\sigma_{12} = \frac{1}{2}(\sigma_1 + \sigma_2) \tag{3-36}$$

From the definition of the parameter b_o in (3-25) Equation (3-36) may be given as

$$b_{o_{12}} = [\tfrac{1}{2}(b_{o_1})^{1/3} + \tfrac{1}{2}(b_{o_2})^{1/3}]^3 \tag{3-37}$$

The interaction coefficient can now be computed by using E_{12} and $b_{o_{12}}$ as for a pure substance in (3-24), (3-25), and tables of the function $B^*(T^*)$.

A similar method is needed to be able to evaluate the two interaction coefficients of (3-34) for the third virial coefficient. Rowlinson, et al.[70] and Ewald[16] have used the following relation for the two third-order interactions,

$$E_{1n2} = E_1^{1-\frac{n}{3}} E_2^{\frac{n}{3}} \tag{3-38}$$

$$b_{o1n2} = [(1 - \tfrac{n}{3})(b_{o1})^{1/3} + (\tfrac{n}{3})(b_{o2})^{1/3}]^3 \tag{3-39}$$

in which n is either 1 or 2. Specification of these parameters now enables calculation of both C_{112} and C_{122} by using the Lennard-Jones potential tabulations for C* (T*) and Equations (3-24), (3-28) as for a pure substance.

It is obvious that the above procedures for computing the interaction coefficients requires a knowledge of the force constants for the pure substances comprising the mixture.

A method similar in nature to that above has been suggested in References 32, 53, 71, and 72, this being particularly useful in cases for which the pure substance force constants are unknown. In this case, empirical relations between the force constants and critical constants are used, assuming the theorem of corresponding states. The relation used by Ewald[32] is

$$kT_c/E = 1.28 \tag{3-40}$$

$$v_c/b_o = 1.46 \tag{3-41}$$

The corresponding numbers given by Hirschfelder[53] for spherical nonpolar substances are 1.30 and 1.33, respectively. Examination of force constants determined from virial coefficient data shows considerable deviation of the values from either of these sets, even for simple molecules. The rule is still useful as an approximation, however, where other data are lacking.

It is apparent that relations of the form (3-40), (3-41) permit calculation of the pure substance virial coefficients, but in order to use these relations to estimate interaction coefficients, it will be necessary to combine the pure gas critical constants in some manner to

give the pseudo-criticals T_{c12}, v_{c12}, etc., which can in turn be used with (3-40), (3-41) to specify $(E/k)_{12}$, b_{o12}, etc.

Guggenheim[71] has shown that, assuming the principle of corresponding states, the relations

$$T_{c_{12}} = (T_{c_1} T_{c_2})^{1/2} \tag{3-42}$$

$$v_{c_{12}} = [\tfrac{1}{2}(v_{c_1})^{1/3} + \tfrac{1}{2}(v_{c_2})^{1/3}]^3 \tag{3-43}$$

are analogous to (3-35), (3-37). Similarly, for the interaction coefficients in the third virial coefficient (3-34), Ewald[32] suggests that, an an approximation

$$T_{c_{1n2}} = T_{c_1}^{1 - \frac{n}{3}} T_{c_2}^{\frac{n}{3}} \tag{3-44}$$

$$v_{c_{1n2}} = [(1 - \tfrac{n}{3})(v_{c_1})^{1/3} + (\tfrac{n}{3})(v_{c_2})^{1/3}]^3 \tag{3-45}$$

where, again, n is either 1 or 2. The relations (3-44), (3-45) are seen to be identical in form to (3-38), (3-39) of the preceding method.

Equations (3-40), ..., (3-45) now permit estimation of all the coefficients appearing in (3-33), (3-34), by using the tabulations for $B^*(T^*)$ and $C^*(T^*)$, as was done previously. As mentioned before, this method will certainly be inferior to the preceding one, but has proved quite useful in calculations involving substances for which the Lennard-Jones intermolecular force constants were not known.

The final method of estimating interaction coefficients to be discussed here is a somewhat different approach to the problem, and is due to Prausnitz.[33] His method has been based on extension of the work of Pitzer, et.al.[73,74] to mixtures of gases.

Pitzer has correlated the properties of non-polar pure gases through a revision of the theory of corresponding states. In doing so, he found it necessary to introduce the acentric factor ω, a third correlating parameter (in addition to reduced temperature and pressure), this being defined by

$$\omega = -\log_{10} P_{R(\text{sat at } T_R = 0.7)} - 1.00 \qquad (3\text{-}46)$$

Since this work dealt with pure gases only, the three interaction coefficients of (3-33), (3-34) cannot be predicted by Pitzer's correlation alone.

Guggenheim and McGlasham,[71] among others, had previously suggested means for predicting the coefficient B_{12}, using only the two-parameter theory of corresponding states and the definitions of (3-42), (3-43). Prausnitz and Gunn[75] later used Pitzer's principles, along with an extension of the acentric factor correlation of Pitzer to determine the critical pressure and temperature for mixtures.

Prausnitz developed these principles to enable prediction of the virial coefficients for mixtures. His procedure can be summarized as follows:

For a pure substance i, the second virial coefficient is correlated in reduced form as

$$\frac{B_i}{v_{c_i}} = \theta_B\left(\frac{T}{T_{c_i}}, \omega_i\right) \qquad (3\text{-}47)$$

where θ_B, a function of the reduced temperature and acentric factor, is tabulated from generalized behavior. For a mixture, the reduced

interaction coefficient of the second virial is given in a similar form,

$$\frac{B_{12}}{v_{c_{12}}} = \theta_B\left(\frac{T}{T_{c_{12}}}, \omega_{12}\right) \tag{3-48}$$

Calculation of the interaction coefficient is now seen to depend on knowledge of the parameters $T_{c_{12}}$, ω_{12}, and $v_{c_{12}}$. From Reference 75, it was decided that the latter two should be combined linearly, so that

$$\omega_{12} = \frac{1}{2}(\omega_1 + \omega_2) \tag{3-49}$$

$$v_{c_{12}} = \frac{1}{2}(v_{c_1} + v_{c_2}) \tag{3-50}$$

It was also found that $T_{c_{12}}$ could not be expressed in the above manner, but could instead be correlated well by a square-root combination with a correction factor, or

$$T_{c_{12}} = k_{12}(T_{c_1}\, T_{c_2})^{1/2} \tag{3-51}$$

where the factor $k_{12} \leq 1$, and is a function of the critical volume ratio. For $(v_{c_1}/v_{c_2}) = 1$, $k_{12} = 1.0$, and it decreases with an increase in the ratio to approximately 0.44 at $(v_{c_1}/v_{c_2}) = 7$.

A similar method is used to estimate the two interaction coefficients appearing in (3-26) for the third virial, the correlation being given as

$$\frac{C_{1n2}}{v_{c_{1n2}}} = \theta_c\left(\frac{T}{T_{c_{1n2}}}, \omega_{1n2}\right) \tag{3-52}$$

where n is either 1 or 2. Approximate values for θ_c are given in the reference as a function of the two parameters, these values being based

on Pitzer's generalized tables and additional volumetric data. Again, it is necessary to empirically combine the parameters for the pure gases to obtain $T_{c_{1n2}}$, ω_{1n2}, and also $v_{c_{1n2}}$. It is suggested that these be given by

$$T_{c_{1n2}} = (T_{c_1} T_{c_n} T_{c_2})^{1/3} \tag{3-53}$$

$$\omega_{1n2} = \frac{1}{3}(\omega_1 + \omega_n + \omega_2) \tag{3-54}$$

$$v_{c_{1n2}} = \frac{1}{3}(v_{c_1} + v_{c_n} + v_{c_2}) \tag{3-55}$$

While the values so obtained for C_{1n2} will certainly be less accurate than those for B_{12}, it should be remembered that in the equation of state the third virial coefficient is of much lesser importance than is the second.

Prausnitz' method for determination of the virial coefficients has been tested in numerous cases, and found to give fairly good correlation for mixtures at moderate densities.

IV. SOLUTION OF THEORETICAL EQUATIONS

A. Beattie-Bridgeman Equation of State

For convenience, the Beattie-Bridgeman Equation (3-5) is repeated here as

$$P = \frac{RT}{v} + \frac{\beta}{v^2} + \frac{\gamma}{v^3} + \frac{\delta}{v^4} \tag{4-1}$$

where

$$\beta = BRT - A - cR/T^2 \tag{4-2}$$

$$\gamma = Aa - BbRT - BcR/T^2 \tag{4-3}$$

$$\delta = Bbc\ R/T^2 \tag{4-4}$$

Using the definition of enhancement factor, (2-43), Equation (2-44) may be written in a convenient form for solution,

$$RT \ln \frac{y_1 v_1^{\square}}{v} - \int_{v_1^{\square}}^{\infty} \left[\left(\frac{\partial P}{\partial n}\right)_{T,V} - \frac{RT}{V}\right] dV - \int_{P_1^{\square}}^{P} v_1^s dP$$

$$+ \int_{V}^{\infty} \left[\left(\frac{\partial P}{\partial n_1}\right)_{T,V,n_2} - \frac{RT}{V}\right] dV = 0 \tag{4-5}$$

Now, writing (4-1) for pure I as

$$P = \frac{nRT}{V} + \frac{n^2\beta_1}{V^2} + \frac{n^3\gamma_1}{V^3} + \frac{n^4\delta_1}{V^4} \tag{4-6}$$

Then,

$$\left(\frac{\partial P}{\partial n}\right)_{T,V} = \frac{RT}{V} + \frac{2n\beta_1}{V^2} + \frac{3n^2\gamma_1}{V^3} + \frac{4n^3\delta_1}{V^4} \tag{4-7}$$

so that the first integral of (4-5) becomes

$$\int_{V_1^{\square}}^{\infty} \left[\left(\frac{\partial P}{\partial n}\right)_{T,V} - \frac{RT}{V}\right] dV = \frac{2\beta_1}{v_1^{\square}} + \frac{3\gamma_1}{2(v_1^{\square})^2} + \frac{4\delta_1}{3(v_1^{\square})^3} \tag{4-8}$$

The second integral of (4-5) involves solid 1, and can be evaluated by use of the relation

$$v_1^s(P,T) = v_1^s(0,T)[1 - k_1 P] \tag{4-9}$$

Where k_1 is the isothermal compressibility of solid 1.

Therefore,

$$\int_{P_1^\circ}^{P} v_1^s dP = v_1^s[(P-P_1^\circ) - \frac{1}{2} k_1(P^2-P_1^{\circ 2})] \tag{4-10}$$

If it can be assumed that k_1 is negligible,

$$\int_{P_1^\circ}^{P} v_1^s dP = v_1^s(P-P_1^\circ) \tag{4-11}$$

In order to evaluate the third integral of (4-5), Equation (4-1) must be written for the gas mixture,

$$P = \frac{nRT}{V} + \frac{n^2\beta_M}{V^2} + \frac{n^3\gamma_M}{V^3} + \frac{n^4\delta_M}{V^4} \tag{4-12}$$

Then,

$$\left(\frac{\partial P}{\partial n_1}\right)_{T,V,n_2} = \frac{RT}{V} + \frac{1}{V^2}\left[\frac{\partial}{\partial n_1}(n^2\beta_M)\right] + \frac{1}{V^3}\left[\frac{\partial}{\partial n_1}(n^3\gamma_M)\right] + \frac{1}{V^4}\left[\frac{\partial}{\partial n_1}(n^4\delta_M)\right] \tag{4-13}$$

and the integral is

$$\int_V^\infty \left[\left(\frac{\partial P}{\partial n_1}\right)_{T,V,n_2} - \frac{RT}{V}\right]dV = \frac{1}{V}\left[\frac{\partial}{\partial n_1}(n^2\beta_M)\right] + \frac{1}{2V^2}\left[\frac{\partial}{\partial n_1}(n^3\gamma_M)\right] + \frac{1}{3V^3}\left[\frac{\partial}{\partial n_1}(n^4\delta_M)\right] \tag{4-14}$$

The first term of (4-14) contains

$$\frac{\partial}{\partial n_1}(n^2\beta_M) = 2n\beta_M + n^2\frac{\partial \beta_M}{\partial n_1} \tag{4-15}$$

But,

$$2n\beta_M = 2n[B_M RT - A_M - c_M R/T^2] \tag{4-16}$$

and

$$n^2\frac{\partial \beta_M}{\partial n_1} = n[RT(n\frac{\partial B_M}{\partial n_1}) - (n\frac{\partial A_M}{\partial n_1}) - \frac{R}{T^2}(n\frac{\partial c_M}{\partial n_1})] \tag{4-17}$$

Substituting (4-16) and (4-17) into (4-15),

$$\frac{\partial}{\partial n_1}(n^2\beta_M) = n[RT(2B_M + n\frac{\partial B_M}{\partial n_1}) - (2A_M + n\frac{\partial A_M}{\partial n_1}) - \frac{R}{T^2}(2c_M + n\frac{\partial c_M}{\partial n_1})] \tag{4-18}$$

Similarly, the second term of (4-14) contains

$$\frac{\partial}{\partial n_1}(n^3\gamma_M) = 3n^2\gamma_M + n^3\frac{\partial \gamma_M}{\partial n_1} \tag{4-19}$$

But,

$$3n^2\gamma_M = 3n^2[A_M a_M - B_M b_M RT - B_M c_M R/T^2] \tag{4-20}$$

and

$$n^3\frac{\partial \gamma_M}{\partial n_1} = n^2[A_M(n\frac{\partial a_M}{\partial n_1}) + a_M(n\frac{\partial A_M}{\partial n_1}) - RT\,B_M(n\frac{\partial b_M}{\partial n_1}) - RTb_M(n\frac{\partial B_M}{\partial n_1}) - \frac{R}{T^2}B_M(n\frac{\partial c_M}{\partial n_1}) - \frac{R}{T^2}c_M(n\frac{\partial B_M}{\partial n_1}) \tag{4-21}$$

Substituting (4-20) and (4-21) into (4-19),

$$\frac{\partial}{\partial n_1}(n^3\gamma_M) = n^2[(3A_M a_M + A_M n\frac{\partial a_M}{\partial n_1} + a_M n\frac{\partial A_M}{\partial n_1}) - RT(3B_M b_M + B_M n\frac{\partial b_M}{\partial n_1} + b_M n\frac{\partial B_M}{\partial n_1}) - \frac{R}{T^2}(3B_M c_M + B_M n\frac{\partial c_M}{\partial n_1} + c_M n\frac{\partial B_M}{\partial n_1})] \tag{4-22}$$

Finally, the third term of (4-14) contains

$$\frac{\partial}{\partial n_1}(n^4\delta_M) = 4n^3\delta_M + n^4 \frac{\partial \delta_M}{\partial n_1} \tag{4-23}$$

But

$$4n^3\delta_M = 4n^3[B_M b_M c_M \, R/T^2] \tag{4-24}$$

and

$$n^4 \frac{\partial \delta_M}{\partial n_1} = n^3 \frac{R}{T^2} [B_M b_M n \frac{\partial c_M}{\partial n_1} + B_M c_M n \frac{\partial b_M}{\partial n_1} + b_M c_M n \frac{\partial B_M}{\partial n_1}] \tag{4-25}$$

Substituting (4-24) and (4-25) into (4-23),

$$\frac{\partial}{\partial n_1}(n^4\delta_M) = n^3 \frac{R}{T^2} \Big[4B_M b_M c_M + B_M b_M n \frac{\partial c_M}{\partial n_1} + B_M c_M n \frac{\partial b_M}{\partial n_1} + b_M c_M n \frac{\partial B_M}{\partial n_1}] \tag{4-26}$$

Now, substituting (4-18), (4-22), and (4-26) into (4-14),

$$\begin{aligned} \int_V^\infty [(\frac{\partial P}{\partial n_1})_{T,V,n_2} - \frac{RT}{V}] dV = \frac{1}{v}[RT(2B_M + n \frac{\partial B_M}{\partial n_1}) - (2A_M + n \frac{\partial A_M}{\partial n_1}) \\ - \frac{R}{T^2}(2c_M + n \frac{\partial c_M}{\partial n_1})] + \frac{1}{2v^2}[3A_M a_M + A_M n \frac{\partial a_M}{\partial n_1} + a_M n \frac{\partial A_M}{\partial n_1}) \\ - RT(3B_M b_M + B_M n \frac{\partial b_M}{\partial n_1} + b_M n \frac{\partial B_M}{\partial n_1}) \\ - \frac{R}{T^2}(3B_M c_M + B_M n \frac{\partial c_M}{\partial n_1} + c_M n \frac{\partial B_M}{\partial n_1})] \\ + \frac{1}{3v^3}[\frac{R}{T^2}][4B_M b_M c_M + B_M b_M n \frac{\partial c_M}{\partial n_1} + B_M c_M n \frac{\partial b_M}{\partial n_1} + b_M c_M n \frac{\partial B_M}{\partial n_1}] \end{aligned} \tag{4-27}$$

In order to solve (4-27), it will be necessary to decide on the methods of pure gas constant combination to be used for the five constants, in order to reduce the terms A_M, B_M, etc., and their derivatives to expressions involving the pure gas constants.

The method of combination to be used here is that discussed in Section III, that being square-root combinations for the constants A and c, cube-root for B, and linear combinations for a and b.

Thus,

$$A_M = (\sum_i y_i A_i^{1/2})^2 = A_2 + 2y_1(A_3-A_2) + y_1^2(A_1+ A_2-2A_3) \quad (4\text{-}28)$$

where, by definition,

$$A_3 = (A_1A_2)^{1/2} \quad (4\text{-}29)$$

Also,

$$B_M = \frac{1}{8} \sum_i \sum_j y_i y_j (B_i^{1/3} + B_j^{1/3})^3$$

$$= B_2 + 2y_1(B_3-B_2) + y_1^2(B_1+B_2-2B_3) \quad (4\text{-}30)$$

Where

$$B_3 = \frac{1}{8} (B_1^{1/3} + B_2^{1/3})^3 \quad (4\text{-}31)$$

As for A_M,

$$c_M = (\sum y_i c_i^{1/2})^2 = c_2 + 2y_1(c_3-c_2) + y_1^2(c_1+c_2-2c_3) \quad (4\text{-}32)$$

where

$$c_3 = (c_1c_2)^{1/2} \quad (4\text{-}33)$$

Finally,

$$a_M = \sum_i y_i a_i = a_2 + 2y_1(a_3-a_2) \quad (4\text{-}34)$$

where

$$a_3 = \frac{1}{2}(a_1+a_2) \quad (4\text{-}35)$$

and

$$b_M = \sum_i y_i b_i = b_2 + 2y_1(b_3-b_2) \tag{4-36}$$

where

$$b_3 = \frac{1}{2}(b_1+b_2) \tag{4-37}$$

Next, taking the partial derivatives required in Equation (4-27),

$$n\frac{\partial A_M}{\partial n_1} = 2[(A_3-A_2) + y_1(A_1+2A_2-3A_3) - y_1^2(A_1+A_2-2A_3)] \tag{4-38}$$

$$n\frac{\partial B_M}{\partial n_1} = 2[(B_3-B_2) + y_1(B_1+2B_2-3B_3) - y_1^2(B_1+B_2-2B_3)] \tag{4-39}$$

$$n\frac{\partial c_M}{\partial n_1} = 2[(c_3-c_2) + y_1(c_1+2c_2-3c_3) - y_1^2(c_1+c_2-2c_3)] \tag{4-40}$$

$$n\frac{\partial a_M}{\partial n_1} = 2[(a_3-a_2) - y_1(a_3-a_2)] \tag{4-41}$$

$$n\frac{\partial b_M}{\partial n_1} = 2[(b_3-b_2) - y_1(b_3-b_2)] \tag{4-42}$$

Substituting Equations (4-28), (4-30), (4-32), (4-34), (4-36), (4-38), ..., (4-42) into (4-27), Equation (4-27) can be reduced, after considerable algebra, to the form

$$\begin{aligned}\int_V^\infty [(\frac{\partial P}{\partial n_1})_{T,V,n_2} - \frac{RT}{V}]dV &= \frac{2}{v}[\beta_3 + y_1(\beta_1 - \beta_3)] \\ &+ \frac{1}{2v^2}\{2\gamma_{23}-\gamma_2+2y_1(2\gamma_{13}-2\gamma_{23}+\gamma_2-\gamma_1) + y_1^2(-4\gamma_{13}+2\gamma_{23}-\gamma_2+5\gamma_1) \\ &\quad - \frac{R}{T^2}y_1[(1-y_1)^2+(1-y_1)^3](B_1+B_2-2B_3)(c_1+c_2-2c_3)\} \\ &+ \frac{2}{3v^3}\{\delta_{223}-\delta_2+y_1(4\delta_{233}-7\delta_{223}+6\delta_2+\delta_{122}) \\ &\quad + y_1^2(4\delta_{133}-12\delta_{233}+15\delta_{223}-\delta_{113}+3\delta_{122}+\delta_{112}-12\delta_2) \\ &\quad + y_1^3(-8\delta_{133}+12\delta_{233}-13\delta_{223}+5\delta_{113}+3\delta_{122}-2\delta_{112}+10\delta_2-\delta_1)\end{aligned} \tag{4-43}$$

$$+ y_1^4(4\delta_{133}-4\delta_{233}+4\delta_{223}-4\delta_{113}-\delta_{122}+\delta_{112}-3\delta_2+3\delta_1)$$

$$+ \frac{R}{T^2}(y_1^2)(1-y_1)^3(b_1-b_3)(B_1+B_2-2B_3)(c_1+c_2-2c_3)\} \quad (4\text{-}43 \text{ Cont'd})$$

Where, for convenience,

$$\beta_1 = B_1 RT - A_1 - c_1 R/T^2 \quad (4\text{-}44)$$

$$\beta_3 = B_3 RT - A_3 - c_3 R/T^2 \quad (4\text{-}45)$$

$$\gamma_1 = A_1 a_1 - RT(B_1 b_1) - \frac{R}{T^2}(B_1 c_1) \quad (4\text{-}46)$$

$$\gamma_2 = A_2 a_2 - RT(B_2 b_2) - \frac{R}{T^2}(B_2 c_2) \quad (4\text{-}47)$$

$$\gamma_{13} = (A_3 a_1 + A_1 a_3) - RT(B_3 b_1 + B_1 b_3) - \frac{R}{T^2}(B_3 c_1 + B_1 c_3) \quad (4\text{-}48)$$

$$\gamma_{23} = (A_3 a_2 + A_2 a_3) - RT(B_3 b_2 + B_2 b_3) - \frac{R}{T^2}(B_3 c_2 + B_2 c_3) \quad (4\text{-}49)$$

$$\delta_1 = B_1 b_1 c_1 R/T^2 \quad (4\text{-}50)$$

$$\delta_2 = B_2 b_2 c_2 R/T^2 \quad (4\text{-}51)$$

$$\delta_{112} = (B_1 b_1 c_2 + B_1 b_2 c_1 + B_2 b_1 c_1) R/T^2 \quad (4\text{-}52)$$

$$\delta_{122} = (B_1 b_2 c_2 + B_2 b_1 c_2 + B_2 b_2 c_1) R/T^2 \quad (4\text{-}53)$$

$$\delta_{113} = (B_1 b_1 c_3 + B_1 b_3 c_1 + B_3 b_1 c_1) R/T^2 \quad (4\text{-}54)$$

$$\delta_{133} = (B_1 b_3 c_3 + B_3 b_1 c_3 + B_3 b_3 c_1) R/T^2 \quad (4\text{-}55)$$

$$\delta_{223} = (B_2 b_2 c_3 + B_2 b_3 c_2 + B_3 b_2 c_2) R/T^2 \quad (4\text{-}56)$$

$$\delta_{233} = (B_2 b_3 c_3 + B_3 b_2 c_3 + B_3 b_3 c_2) R/T^2 \quad (4\text{-}57)$$

The quantities defined above in (4-44) through (4-57) are functions of the gas constants and temperature only.

It should be mentioned at this point that it is possible that Equation (4-43) could be slightly reduced in length, but it was left in this form partly for convenience in attempting certain other combinations

of coefficients. Also, any additional work of reduction did not seem justified, inasmuch as the solution was programmed for the IBM 704, and presented no problem.

The reduction of Equation (4-5) is now completed by the substitution of Equations (4-8), (4-11), and (4-43), resulting in

$$RT \ln \frac{y_1 v_1^{\square}}{v} - (D1) - v_1^s (P-P_1^{\square}) + \frac{2}{v}\{\beta_3 + y_1(D2)\}$$
$$+ \frac{1}{2v^2}\{(D3) + y_1(D4) + y_1^2(D5) - (D21)\frac{y_1}{T^2}[(1-y_1)^2+(1-y_1)^3]\}$$
$$+ \frac{2}{3v^3}\{(D6) + y_1(D7) + y_1^2(D8) + y_1^3(D9) + y_1^4(D10)$$
$$+ (D22)\frac{y_1}{T^2}(1-y_1)^3\} = 0 \qquad (4\text{-}58)$$

where, for further convenience,

$$(D1) = \frac{2\beta_1}{v_1^{\square}} \quad \frac{3\gamma_1}{2(v_1^{\square})^2} \quad \frac{4\delta_1}{3(v_1^{\square})^3} \qquad (4\text{-}59)$$

$$(D2) = \beta_1 - \beta_3 \qquad (4\text{-}60)$$

$$(D3) = 2\gamma_{23} - \gamma_2 \qquad (4\text{-}61)$$

$$(D4) = 2(2\gamma_{13} - 2\gamma_{23} + \gamma_2 - \gamma_1) \qquad (4\text{-}62)$$

$$(D5) = -4\gamma_{13} + 2\gamma_{23} - \gamma_2 + 5\gamma_1 \qquad (4\text{-}63)$$

$$(D6) = \delta_{223} - \delta_2 \qquad (4\text{-}64)$$

$$(D7) = 4\delta_{233} - 7\delta_{223} + 6\delta_2 + \delta_{122} \qquad (4\text{-}65)$$

$$(D8) = 4\delta_{133} - 12\delta_{233} + 15\delta_{223} - \delta_{113} + 3\delta_{122} + \delta_{112} - 12\delta_2 \qquad (4\text{-}66)$$

$$(D9) = -8\delta_{133} + 12\delta_{233} - 13\delta_{223} + 5\delta_{113} + 3\delta_{122} - 2\delta_{112} + 10\delta_2 - \delta_1 \qquad (4\text{-}67)$$

$$(D10) = 4\delta_{133} - 4\delta_{233} + 4\delta_{223} - 4\delta_{113} - \delta_{122} + \delta_{112} - 3\delta_2 + 3\delta_1 \qquad (4\text{-}68)$$

all of which are functions of the various β, γ, δ parameters defined in (4-44), ..., (4-57), that is, functions of the gas constants and temperature only.

Also,

$$(D21) = R\,(B_1 + B_2 - 2B_3)\,(c_1 + c_2 - 2c_3) \tag{4-69}$$

$$(D22) = R\,(b_1 - b_3)\,(B_1 + B_2 - 2B_3)\,(c_1 + c_2 - 2c_3) \tag{4-70}$$

which are functions of only the gas constants, and will be identically zero if either the B's or c's are combined linearly.

Considering T and P as the independent variables, Equation (4-58) gives one equation in two unknowns, y_1 and v. It still remains to reduce Equation (4-1) written for the mixture, so as to obtain a second equation relating v and y_1 for specified values of P and T. To achieve this reduction, Equations (4-28), (4-30), (4-32), (4-34), and (4-36) are substituted into (4-2), (4-3), and (4-4) to find the virial coefficients for the mixture. After considerable reduction, the resulting expressions are

$$\beta_M = \beta_2 + 2y_1\,(\beta_3 - \beta_2) + y_1^2\,(\beta_1 + \beta_2 - 2\beta_3) \tag{4-71}$$

where

$$\beta_2 = B_2RT - A_2 - c_2\,R/T^2 \tag{4-72}$$

Similarly,

$$\begin{aligned}\gamma_M = {} & \gamma_2 + 2y_1\,(\gamma_{23} - 2\,\gamma_2) + y_1^2(2\,\gamma_{13} - 4\,\gamma_{23} + 5\,\gamma_2 - \gamma_1) \\ & + 2y_1^3\,(-\gamma_{13} + \gamma_{23} - \gamma_2 + \gamma_1) \\ & - \frac{R}{T^2}\,(y_1^2)\,(1-y_1)^2\,(B_1+B_2-2B_3)\,(c_1+c_2-2c_3)\end{aligned} \tag{4-73}$$

Finally,

$$\delta_M = \delta_2 + 2y_1(\delta_{223} - 2\,\delta_2) + y_1^2(-10\,\delta_{223} + 4\,\delta_{233} + \delta_{122} + 15\,\delta_2 - 2\,\delta_3) + 2y_1^3(7\,\delta_{223} - 4\,\delta_{233} - \delta_{122} + \delta_{113} - 6\,\delta_2 - \delta_1) + y_1^4(-6\,\delta_{223} + 4\,\delta_{233} + \delta_{122} - 2\delta_{113} + 6\,\delta_2 + 3\,\delta_1) + \frac{2R}{T^2}(y_1^3)(1-y_1)^2 (b_1-b_3)(B_1+B_2-2B_3)(c_1+c_2-2c_3) \quad (4\text{-}74)$$

Where

$$\delta_3 = B_3 b_3 c_3 R/T^2 \quad (4\text{-}75)$$

Substituting (4-71), (4-73), and (4-74) into (4-1) and rearranging,

$$\frac{RT}{v} + \frac{1}{v^2}\{\beta_2 + y_1(D11) + y_1^2(D12)\} + \frac{1}{v^3}\{\gamma_2 + y_1(D13) + y_1^2(D14) + y_1^3(D15) - (D21)\frac{y_1^2}{T^2}(1-y_1)^2\} + \frac{1}{v^4}\{\delta_2 + y_1(D16) + y_1^2(D17) + y_1^3(D18) + y_1^4(D19) + 2(D22)\frac{y_1^3}{T^2}(1-y_1)^2\} - P = 0 \quad (4\text{-}76)$$

Where, again, for convenience,

$$(D11) = 2(\beta_3-\beta_2) \quad (4\text{-}77)$$

$$(D12) = \beta_1 + \beta_2 - 2\beta_3 \quad (4\text{-}78)$$

$$(D13) = 2(\gamma_{23} - 2\,\gamma_2) \quad (4\text{-}79)$$

$$(D14) = 2\,\gamma_{13} - 4\,\gamma_{23} + 5\,\gamma_2 - \gamma_1 \quad (4\text{-}80)$$

$$(D15) = 2(-\gamma_{13} + \gamma_{23} - \gamma_2 + \gamma_1) \quad (4\text{-}81)$$

$$(D16) = 2(\delta_{223} - 2\,\delta_2) \quad (4\text{-}82)$$

$$(D17) = -10\,\delta_{223} + 4\,\delta_{233} + \delta_{122} + 15\,\delta_2 - 2\,\delta_3 \quad (4\text{-}83)$$

$$(D18) = 2(7\,\delta_{223} - 4\,\delta_{233} - \delta_{122} + \delta_{113} - 6\,\delta_2 - \delta_1) \quad (4\text{-}84)$$

$$(D19) = -6\,\delta_{223} + 4\,\delta_{233} + \delta_{122} - 2\,\delta_{113} + 6\,\delta_2 + 3\,\delta_1 \quad (4\text{-}85)$$

Thus, the set of equations to be solved, i.e., (4-5) and (4-1), is now written as Equations (4-58) and (4-76).

For a given P and T, $P_1^{\square}$, $v_1^{\square}$, and v_1^s are known. All the D terms are known in terms of the pure gas coefficients and T, leaving the two equations in the two unknowns y_1 and v. A simultaneous solution of the two will yield the desired values for y_1, the mole fraction of carbon dioxide in the gas phase.

For low temperatures, y_1 and $P_1^{\square}$ will be very small and $v_1^{\square}$ very large. Therefore, terms involving the factors y_1, $P_1^{\square}$, or $1/v_1^{\square}$ can be assumed negligible (with the exception of the first term of Equation (4-58) containing the product $y_1 v_1^{\square}$), so that (4-58) reduces to

$$RT \ln \frac{y_1 v_1^{\square}}{v} - v_1^s P + \frac{2\beta_3}{v} + \frac{\gamma_{23} - 1/2\ \gamma_2}{v^2} + \frac{2(\delta_{223} - \delta_2)}{3\ v^3} = 0 \qquad (4\text{-}86)$$

and (4-76) reduces to

$$\frac{RT}{v} + \frac{\beta_2}{v^2} + \frac{\gamma_2}{v^3} + \frac{\delta_2}{v^4} - P = 0 \qquad (4\text{-}87)$$

It is apparent that this set is a good deal simpler to solve than the general case, since (4-87) is not a function of y_1, so a simultaneous solution is unnecessary.

The simplified solution as given by the set of Equations (4-86), (4-87) is that used by Dokoupil,[15] and others, where the assumption that y_1 is small was made early in the derivations, and no general solution was considered. Comparison of this solution with the general one (4-58), (4-76) will give an indication of the error associated with this assumption.

The procedure for determining the two different solutions will be to first solve the simplified set for a given pressure and temperature by using the Newton iterative method to find v in Equation (4-87). This value is then substituted into (4-86) to find the mole fraction of carbon dioxide. The Newton method is outlined in Appendix A1. The initial guess for v to begin the iteration is generated by converting the Beattie-Bridgeman Equation (4-1) to the approximate volume explicit form, and using the value determined from that. Equation (4-1) is converted by multiplying by the quantity (v/P), giving

$$v = \frac{RT}{P} + \frac{\beta}{Pv} + \frac{\gamma}{Pv^2} + \frac{\delta}{Pv^3} \tag{4-88}$$

In order to make (4-88) explicit in volume, the v's appearing on the right-hand side of the equation are replaced by the ideal-gas law (RT/P), resulting in

$$v = \frac{RT}{P} + \frac{\beta}{RT} + \frac{\gamma P}{(RT)^2} + \frac{\delta P^2}{(RT)^3} \tag{4-89}$$

While (4-89) is not as accurate as the Scatchard volume-explicit form, in which the v's on the right-hand side of (4-88) are replaced by similar equations, it is considerably better than the ideal gas law, and more than sufficient as an initial trial to ensure convergence in the iteration.

For both solutions, values of $P_1^{\square}$, v_1^{S}, and $v_1^{\square}$ are required for each temperature. $P_1^{\square}$ and v_1^{S} were read into the program, having been taken from Reference 24. The values of $P_1^{\square}$ had been calculated from the Plank-Kuprianoff Equation and checked against the data of Reference 76.

At each temperature, $v_1^{\square}$ was calculated from (4-89) using $P_1^{\square}$. This was felt to be sufficiently accurate, inasmuch as the vapor pressure was always very small. The numerical values for $P_1^{\square}$, v_1^{s}, are listed in Table I.

TABLE I

VALUES OF $P_1^{\square}$, v_1^{s}

T (°K)	$P_1^{\square}$ (ATM)	v_1^{s} ($\frac{\text{Lit}}{\text{Mole}}$)
140	0.00184	0.0270
150	0.00841	0.0272
160	0.0314	0.0274
170	0.0993	0.0276
180	0.274	0.0278
190	0.679	0.0280

The pure-gas Beattie-Bridgeman constants used in the calculations are those of Reference 37, and are listed in Table II.

TABLE II

BEATTIE-BRIDGEMAN CONSTANTS

Units: Atm., Lit/Mole, °K

Constant	Comp. 1 (CO_2)	Comp. 2 (N_2)
A	5.0065	1.3445
B	0.10476	0.05046
a	0.07132	0.02617
b	0.07235	-0.00691
c	66.0×10^4	4.2×10^4

Upon completion of the simplified solution, the Newton-Raphson iterative method is used to solve the set of Equations (4-58), (4-76) for the general solution, the principle being outlined in Appendix A2. Inasmuch as this method requires reasonably good initial guesses in order to ensure convergence, the values for y_1 and v determined by the simplified solution are used for the initial trial.

In the program written for the IBM 704 computer to calculate both sets of results, the general solution was not executed in cases for which the simplified one gave a value of y_1 less than 0.001, inasmuch as it was felt that the two solutions would prove to be identical. Examination of the results confirms this opinion.

The flow diagram for the computer program is given in Appendix B, and results are compared with the experimental in Section IX.

B. Virial Equation of State

1. General

For the solution of the theoretical equilibrium Equation (2-44) using the virial equation of state (3-19), the virial equation is rewritten in a pressure-explicit form

$$P = \frac{RT}{v} + \frac{RT\ B}{v^2} + \frac{RT\ C}{v^3} \tag{4-90}$$

As before, Equation (2-44) is put into the form of (4-5). Then to evaluate the first integral of this equation, (4-90) is written for pure substance 1 as

$$P = \frac{nRT}{V} + \frac{n^2RT\ B_1}{V^2} + \frac{n^3RT\ C_1}{V^3} \tag{4-91}$$

Therefore,

$$\left(\frac{\partial P}{\partial n}\right)_{T,V} = \frac{RT}{V} + \frac{2nRTB_1}{V^2} + \frac{3n^2RTC_1}{V^3} \tag{4-92}$$

The first integral of (4-5) is thus found to be

$$\int_{V_1}^{\infty} \left[\left(\frac{\partial P}{\partial n}\right)_{T,V} - \frac{RT}{V}\right]dV = \frac{2RTB_1}{v_1} + \frac{3RTC_1}{2(v_1)^2} \tag{4-93}$$

As for the Beattie-Bridgeman solution, the isothermal compressibility of solid 1 is neglected, so that the second integral of (4-5) results in Equation (4-11).

For the third integral of (4-5), Equation (4-90) is written for the gas mixture as

$$P = \frac{nRT}{V} + \frac{n^2RTB_M}{V^2} + \frac{n^3RTC_M}{V^3} \tag{4-94}$$

where B_M, C_M are given by Equation (3-33), (3-34), respectively. Differentiating (4-94) with respect to n_1,

$$\left(\frac{\partial P}{\partial n_1}\right)_{T,V,n_2} = \frac{RT}{V} + \frac{RT}{V^2}\frac{\partial}{\partial n_1}(n^2B_M) + \frac{RT}{V^3}\frac{\partial}{\partial n_1}(n^3C_M) \tag{4-95}$$

so that the third integral is

$$\int_{V}^{\infty} \left[\left(\frac{\partial P}{\partial n_1}\right)_{T,V,n_2} - \frac{RT}{V}\right]dV = \frac{RT}{V}\left[\frac{\partial}{\partial n_1}(n^2B_M)\right] + \frac{RT}{2V^2}\left[\frac{\partial}{\partial n_1}(n^3C_M)\right] \tag{4-96}$$

From Equation (3-33),

$$n^2B_M = n_1^2B_1 + 2n_1n_2B_{12} + n_2^2B_2 \tag{4-97}$$

Therefore,

$$\frac{\partial}{\partial n_1}(n^2B_M) = 2n_1B_1 + 2n_2B_{12} = 2n[y_1B_1 + y_2B_{12}] \tag{4-98}$$

Similarly, from (3-34)

$$n^3C_M = n_1^3C_1 + 3n_1^2n_2C_{112} + 3n_1n_2^2C_{122} + n_2^3C_2 \qquad (4\text{-}99)$$

and

$$\frac{\partial}{\partial n_1}(n^3C_M) = 3n_1^2C_1 + 6n_1n_2C_{112} + 3n_2^2C_{122}$$

$$= 3n^2[y_1^2C_1 + 2y_1y_2C_{112} + y_2^2C_{122}] \qquad (4\text{-}100)$$

Now, substituting (4-98) and (4-100) into (4-96)

$$\int_V^\infty [(\frac{\partial P}{\partial n1})_{T,V,n_2} - \frac{RT}{V}]dV = \frac{2RT}{v}(y_1B_1 + y_2B_{12})$$

$$+ \frac{3RT}{2v^2}(y_1^2C_1 + 2y_1y_2C_{112} + y_2^2C_{122}) \qquad (4\text{-}101)$$

At this point, Equation (4-5) can be solved by substitution of (4-93), (4-11), and (4-101), giving for the equilibrium equation,

$$\ln\frac{y_1v_1^\square}{v} - \frac{2B_1}{v_1^\square} - \frac{3C_1}{2(v_1^\square)^2} - \frac{v_1^s}{RT}(P-P_1^\square) + \frac{2}{v}(y_1B_1 + y_2B_{12})$$

$$+ \frac{3}{2v^2}(y_1^2C_1 + 2y_1y_2C_{112} + y_2^2C_{122}) = 0 \qquad (4\text{-}102)$$

or, eliminating y_2,

$$\ln\frac{y_1v_1^\square}{v} - \frac{2B_1}{v_1^\square} - \frac{3C_1}{2(v_1^\square)^2} - \frac{v_1^s}{RT}(P-P_1^\square) + \frac{2}{v}[B_{12} + y_1(B_1-B_{12})]$$

$$+ \frac{3}{2v^2}[C_{122} + 2y_1(C_{112}-C_{122}) + y_1^2(C_1+C_{122}-2C_{112})] = 0 \qquad (4\text{-}103)$$

Equation (4-103) gives one equation in the two unknowns y_1, v. The second relation between the two comes from the equation of state for the mixture (4-94) and the coefficient Equations (3-33) and (3-34). The

equation of state becomes;

$$\frac{RT}{v} + \frac{RT}{v^2}\left(y_1^2 B_1 + 2y_1 y_2 B_{12} + y_2^2 B_2\right)$$

$$+ \frac{RT}{v^3}\left(y_1^3 C_1 + 3y_1^2 y_2 C_{112} + 3y_1 y_2^2 C_{122} + y_2^3 C_2\right) - P = 0 \qquad (4\text{-}104)$$

But, y_2 can be eliminated from (4-104), yielding

$$\frac{RT}{v} + \frac{RT}{v^2}\left[B_2 + 2y_1(B_{12}-B_2) + y_1^2(B_1+B_2-2B_{12})\right]$$

$$+ \frac{RT}{v^3}\left[C_2+3y_1(C_{122}-C_2) + 3y_1^2(C_{112}+C_2-2C_{122})\right.$$

$$\left. + y_1^3(C_1-C_2+3C_{122}-3C_{112})\right] - P = 0 \qquad (4\text{-}105)$$

For a given pressure and temperature, solution of the set (4-103), (4-105) for v and the desired y_1 will first necessitate specification of the various pure gas virial coefficients, interaction coefficients and also $v_1^{\square}$ at the temperature under consideration.

As was done with the Beattie-Bridgeman equation of state, a simplification of this general solution can be made at low temperatures, in which case y_1 and $P_1^{\square}$ become very small and $v_1^{\square}$ very large, so that (4-103) reduces to

$$\ln \frac{y_1 v_1^{\square}}{v} - \frac{P v_1^s}{RT} + \frac{2B_{12}}{v} + \frac{3C_{122}}{2v^2} = 0 \qquad (4\text{-}106)$$

and, similarly, (4-105) becomes

$$\frac{RT}{v} + \frac{RTB_2}{v^2} + \frac{RTC_2}{v^3} - P = 0 \qquad (4\text{-}107)$$

Once the four coefficients have been specified, the simplified set (4-106), (4-107) can be solved quite easily, since y_1 does not appear in the latter equation.

2. Numerical Solutions

Two methods of predicting virial coefficients will be considered in the solution of both the simplified set of Equations (4-106), (4-107), and also the general set (4-103), (4-105), these methods having been discussed in some detail in Section III C.

In these calculations, an equation of state is used as the second relation between the dependent variables [in addition to the integrated form of the equilibrium Equation (2-44)]. In the majority of the references cited in Sections I and III, the mole fraction of the condensed component in the gas phase was always very small, and so only the simplified solution was determined. Inspection of the equation of state for this solution (4-107) shows that, as would be expected, the equation reduces to that for pure component 2. Therefore, in many cases those authors simply eliminated the equation of state and substituted experimental specific volumes of component 2 directly into the equilibrium Equation (4-106), to find the gas phase composition. These solutions then reduce to a test only of the assumptions made in integrating the theoretical equations and the methods for predicting interaction coefficients.

For each of the methods to be used here, those of Ewald[16] and Prausnitz,[33] the same pure gas virial coefficients will be used. These were calculated using the Lennard-Jones (6-12) potential with force constants taken from experimentally determined coefficients,[53] these constants being given in Table III.

TABLE III

FORCE CONSTANTS FOR THE LENNARD-JONES (6-12) POTENTIAL

	(E/k) °K	$b_o \frac{lit}{mole}$
CO_2 (1)	189.0	.1139
N_2 (2)	95.05	.06378

These constants were used with the equations of Section III C1 and the tables of Hirschfelder.[53] Values of the virial coefficients so determined are listed in Table IV.

TABLE IV

PURE GAS VIRIAL COEFFICIENTS USING THE LENNARD-JONES (6-12) POTENTIAL

Units: atm, °K, Lit/mole

T	B_1	C_1	B_2	C_2
140	-0.48605	-0.02631	-0.07944	+0.00224
150	-0.43118	-0.01224	-0.06905	+0.00213
160	-0.38571	-0.00399	-0.06019	+0.00203
170	-0.34740	+0.00096	-0.05256	+0.00193
180	-0.31469	+0.00393	-0.04592	+0.00185
190	-0.28667	+0.00578	-0.04009	+0.00178

The first method of determining the three interaction coefficients required in the general solution is that of Ewald, this method making use of the semi-empirical combinations (3-35), (3-37), (3-38), (3-39), and also the Lennard-Jones potential tabulations of $B^*(T^*)$ and $C^*(T^*)$ from Reference 53. The resulting values are given for the six temperatures in Table V.

TABLE V

INTERACTION COEFFICIENTS USING THE METHOD OF EWALD

Units: atm., °K, lit/mole

T	B_{12}	C_{112}	C_{122}
140	-0.20327	+0.00204	+0.00361
150	-0.17989	+0.00384	+0.00364
160	-0.15960	+0.00476	+0.00357
170	-0.14369	+0.00519	+0.00346
180	-0.12877	+0.00535	+0.00333
190	-0.11606	+0.00535	+0.00320

The earlier method of Ewald[32] is not considered in the solutions, inasmuch as it is known to be less accurate than the later method of Reference 16 given above.

The second method of estimating the three interaction coefficients is that of Prausnitz. This procedure requires the acentric factors of Pitzer,[73] and also critical temperatures and volumes of the two pure substances, tabulated in Table VI, according to Reference 77.

TABLE VI

CRITICAL CONSTANTS

	P_c(atm)	T_c(°K)	v_c(lit/mole)
CO_2 (1)	72.9	304.2	0.0942
N_2 (2)	33.5	126.1	0.0901

The coefficients are then computed using Prausnitz' generalized tables.[33] As mentioned in Section III, the values of C_{112}, C_{122}, were difficult to determine accurately, so the values listed in Table VII have been smoothed from the original calculations.

TABLE VII

INTERACTION COEFFICIENTS USING THE METHOD OF PRAUSNITZ

Units: atm., °K, lit/mole

T	B_{12}	C_{112}	C_{122}
140	-0.2315	-0.00172	+0.00376
150	-0.2000	-0.00017	+0.00402
160	-0.1749	+0.00120	+0.00410
170	-0.1540	+0.00240	+0.00400
180	-0.1360	+0.00335	+0.00370
190	-0.1216	+0.00378	+0.00350

For either of the two methods under consideration, the seven coefficients required are now known as functions of temperature, as are $P_1^{\square}$, v_1^s. The only variable remaining to be specified as $v_1^{\square}$, and this may be easily calculated by using an approximation to the equation of state, since $P_1^{\square}$ is very small. Both sides of Equation (4-90) are multiplied by (v/P) and the v's remaining on the right-hand side are approximated by the ideal gas law, leaving

$$v = \frac{RT}{P} + B + \frac{PC}{RT} \tag{4-108}$$

or, for component 1 at pressure $P_1^{\square}$,

$$v_1^{\square} = \frac{RT}{P_1^{\square}} + B_1 + \frac{P_1^{\square} C_1}{RT} \tag{4-109}$$

As was done with the Beattie-Bridgeman equation solutions, Equation (4-107) is solved for v by trial and error using the method of Appendix A1, the initial trial for v being computed from (4-108). The value of v satisfying (4-107) is then substituted into (4-106) to find y_1. The value of v_1^s in this equation is that listed previously in Table I, and v_1^D is determined from (4-109).

As before, in cases for which the simplified solution gives a value of $y_1 > 0.001$, the general set of Equations (4-103), (4-105) is then solved simultaneously for v and y_1, using the method of Appendix A2. The solutions v, y_1 of the simplified equations are used as the initial trials in the iterative procedure for the general solution. The flow diagram for the program written to determine these solutions for either of the mixture methods discussed above is listed in Appendix C. Numerical results for both methods are compared with those of the Beattie-Bridgeman equation and the experimental results in Section IX.

V. EXPERIMENTAL APPARATUS AND INSTRUMENTATION

A. General

In experimental work of this nature, three types of systems have been used successfully in the past, namely the static, flow, and circulation methods. These types and the relative advantages and disadvantages of each are discussed in Reference 15 and 78.

The flow method of achieving equilibrium was selected for this investigation, inasmuch as it is this type of system in which the data should find application, and further to avoid errors introduced in the collecting of samples, as is encountered in a closed system. In addition, the flow-type system allows for continuous gas-phase analysis, a great factor in assuring the achievement of equilibrium, constancy of conditions, and true composition.

In the experimental system (Figure 1), a high-pressure gas mixture consisting of a small percentage of carbon dioxide in nitrogen is cooled down to the desired temperature, during which process most of the carbon dioxide is frozen out of the mixture. Some of the solid will no doubt deposit on the walls of the tubes, and the remainder is trapped in a filter and retained at the equilibrium point. It is necessary that absolutely no solid particles pass through the trap, inasmuch as the solid would sublime on leaving the cryostat and give an erroneously high carbon dioxide concentration in the gas phase, which is to be analyzed after being warmed to ambient temperature.

The heat exchanger serves the dual purpose of cooling the supply gas, so as to avoid large temperature gradients in the cryostat,

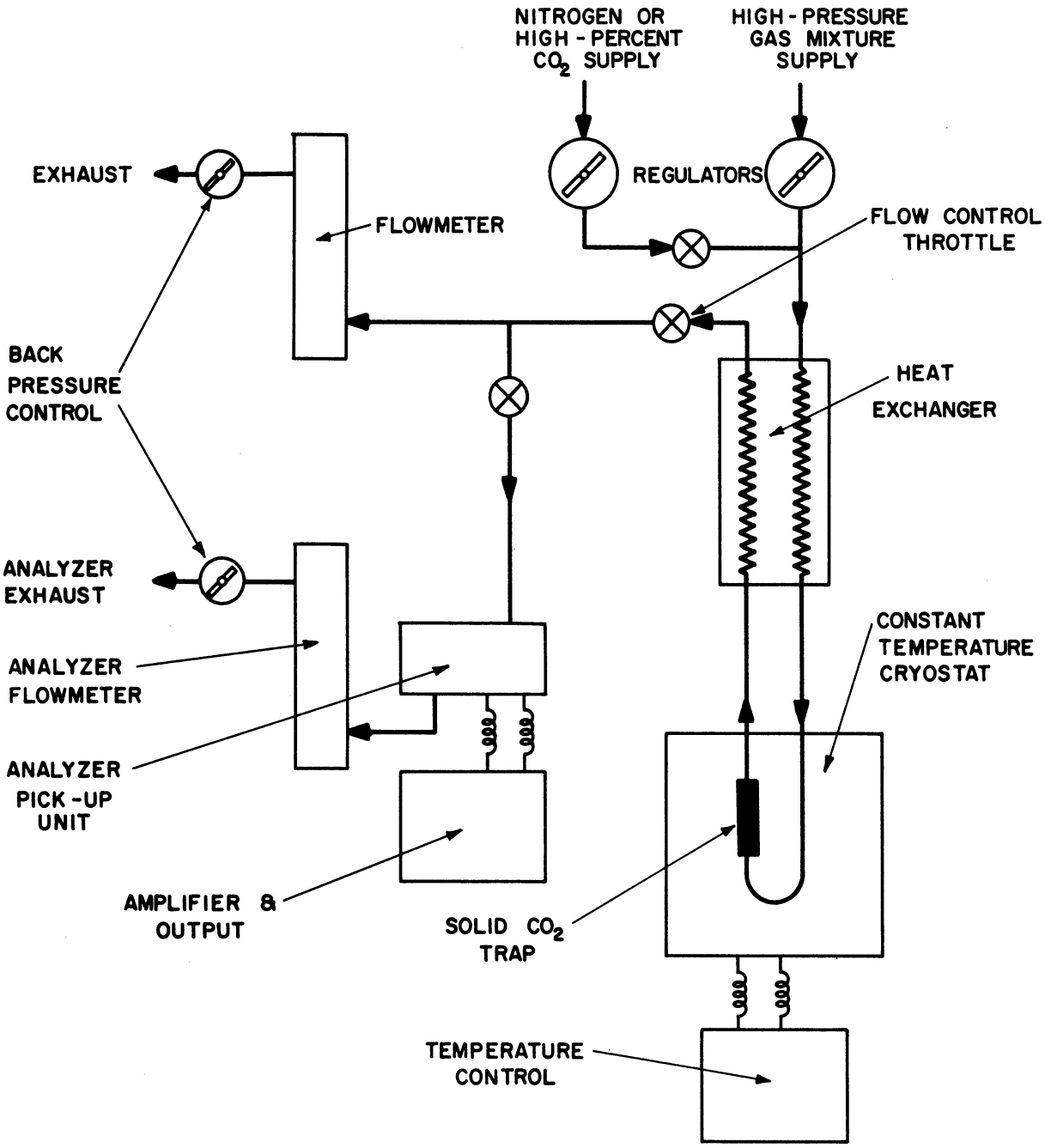

Figure 1. Schematic Diagram of Experimental Equipment

and bringing the cryostat outlet gas up to approximately room temperature. The gas is then throttled to low pressure, analyzed, and exhausted.

Although the flow rate through the system is small, only a small percentage of the total is to be passed through the analyzer, to avoid compression of the gas in the sample cell, which might affect the reading. The needle valve permits accurate regulation of the analyzer flow, to be held constant at the same value at which the analyzer has been calibrated. The analyzer back pressure valve performs a similar function in controlling analyzer pressure. The back pressure valve on the main exhaust line is necessary to enable achievement of the proper analyzer flow at low total flow rates, and also to prevent surging at low flow rates.

The second supply manifold is not used during the data runs, but is instead an auxilliary. The high-concentration carbon dioxide supply may be used as desired prior to the actual run, in order to ensure a good deposit of solid in the cryostat. Pure nitrogen is used to purge the system both during the initial cooling and also after runs in which the system becomes plugged with solid.

B. Construction

1. Cryostat

The cryostat (Figures 2, 3) consists of a solid cylindrical piece of styrofoam 22, 21 inches in diameter and 17 inches high. The inside is hollowed out to a depth of 11 inches and diameter of 9 inches to contain the equilibrium vessel, leaving insulating walls 6 inches thick. The cryostat is also fitted with a styrofoam lid 6 inches thick.

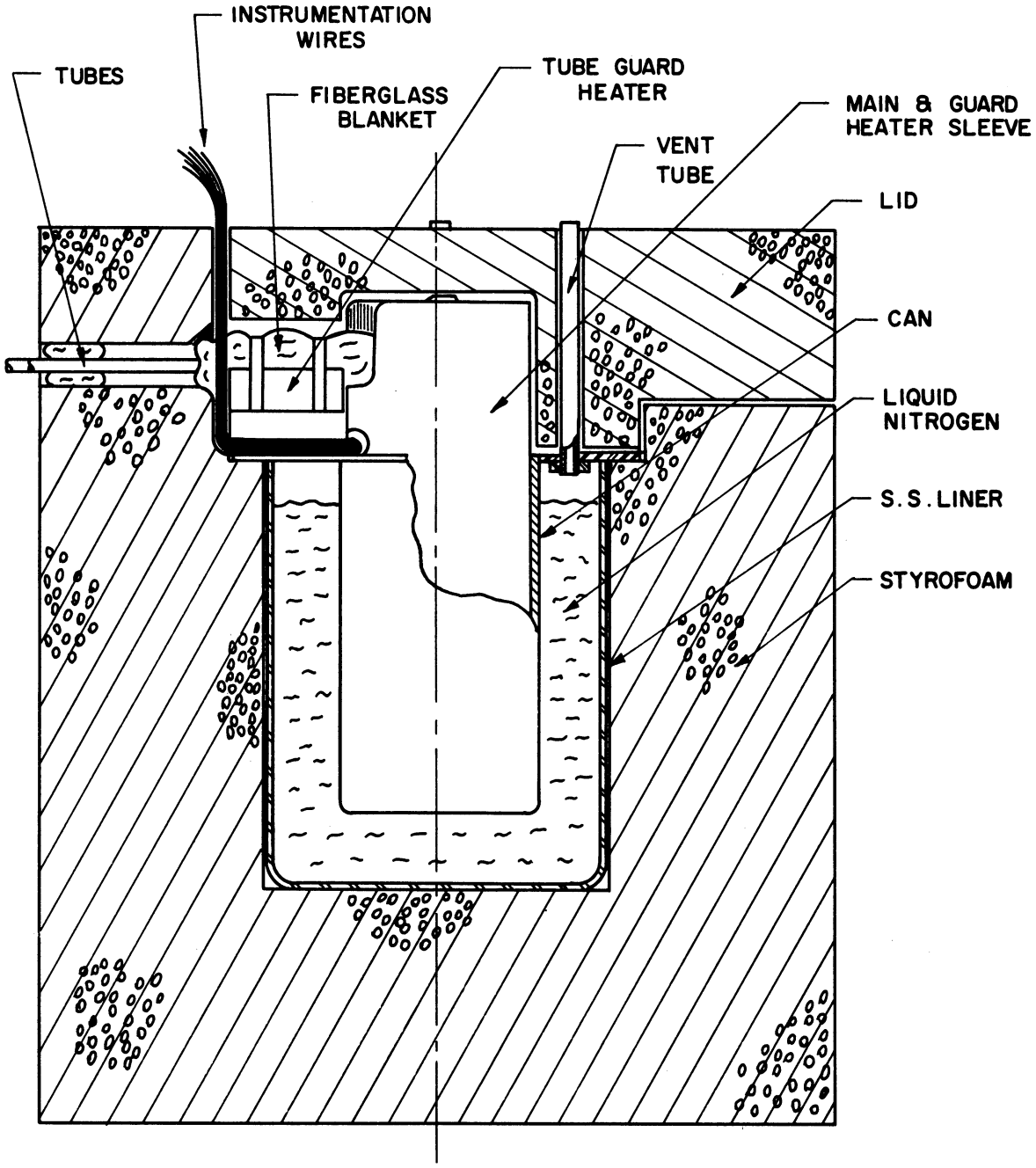

Figure 2. Cryostat Cross-Section

It was originally planned to use the styrofoam cryostat directly as the liquid nitrogen container, as was done in References 79, 80, 81, but when this was attempted the interior walls cracked badly, at some points being as much as 2 inches deep. Therefore, in the final design, a 9-liter stainless steel beaker is used as a liner to hold the liquid nitrogen, which is transferred from a 50-liter storage container at such a rate as required to hold the liquid level constant. The styrofoam now serves only as support and insulation, as discussed in Reference 82. The liquid transfer system is seen in Figure 3. Liquid level is indicated by a styrofoam float fitted inside the beaker, with the float pointer protruding through the top of the cryostat lid. It should be mentioned that little further cracking of the walls was observed after insertion of the liner. It is not known whether the cracks would have become more severe had the liner not been used.

The equilibrium vessel is suspended in the liquid nitrogen inside a brass can supported from the top by a stainless steel ring (Figures 2, 4), and is insulated from the liquid in order to reduce heat transfer rates. This cooling tendency is counter-balanced by three variable-output heaters. Of these, two surround the sides and bottom as an integral part of the insulation between the vessel and liquid nitrogen, their output being individually regulated so as to hold the block temperature uniform and constant. The third heater is a guard to protect the inlet and outlet tubes of the vessel.

The cryostat is located at the end of the long horizontal heat exchanger, the inlet and outlet tubes passing through the side wall of

Figure 3. Outside of Cryostat.

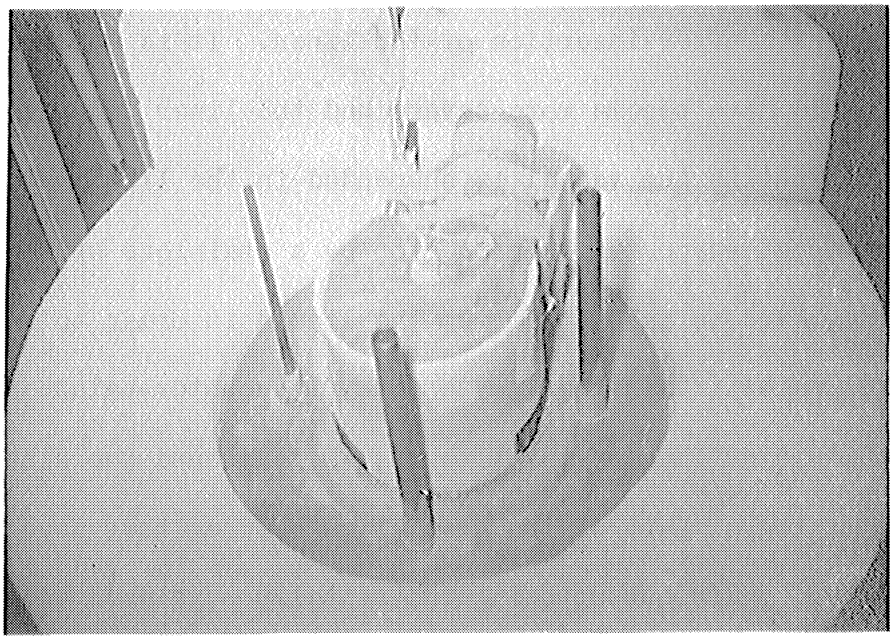

Figure 4. Inside of Cryostat, Assembled.

the cryostat. During operation of the equipment, the cryostat is enclosed in a heavy sheet steel box, shown in Figure 3, as a safety precaution.

2. Equilibrium Vessel

The equilibrium vessel, shown in cross-section in Figure 5, is the heart of the experimental apparatus, and must perform two vital functions. The flowing gas must be brought to the equilibrium temperature, at which point the solid carbon dioxide present in the stream must be trapped and retained, while the gas passes through and leaves the cryostat. It is strictly necessary that no point in the system be allowed to cool below the equilibrium point temperature, and also that no solid particles be permitted to pass through the filter (one of the major difficulties encountered in using the flow system).

The vessel should consist of a long flow path to allow sufficient time for equilibrium to be attained, yet in as compact a volume as possible. It should also have a large mass and high thermal conductivity, so as to minimize temperature gradients, and still have a rapid thermal response to permit accurate temperature control. The flow passages must be of sufficient strength to withstand the high gas pressure.

With these views in mind, the core of the equilibrium vessel is constructed of a cylindrical brass block fitted at the top with a thin stainless steel sleeve, as seen in Figure 6. This central brass block does not extend to the top of the vessel, so as to avoid having the relatively warm inlet gas enter the vessel at a point very close to the equilibrium point. The gas flows through a 3/8" O.D. x .049" wall

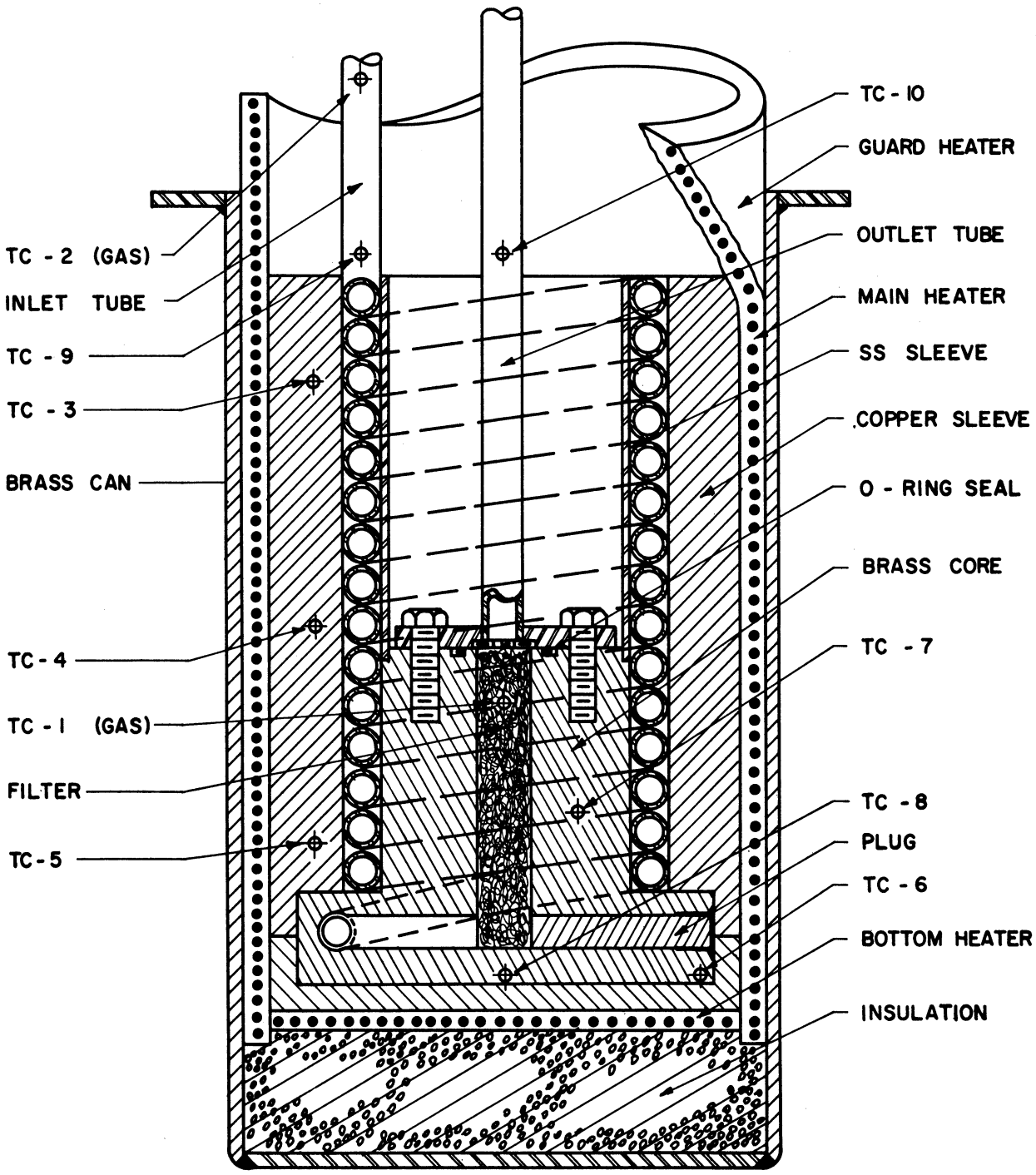

Figure 5. Equilibrium Vessel Cross-Section

Figure 6. Equilibrium Vessel Core.

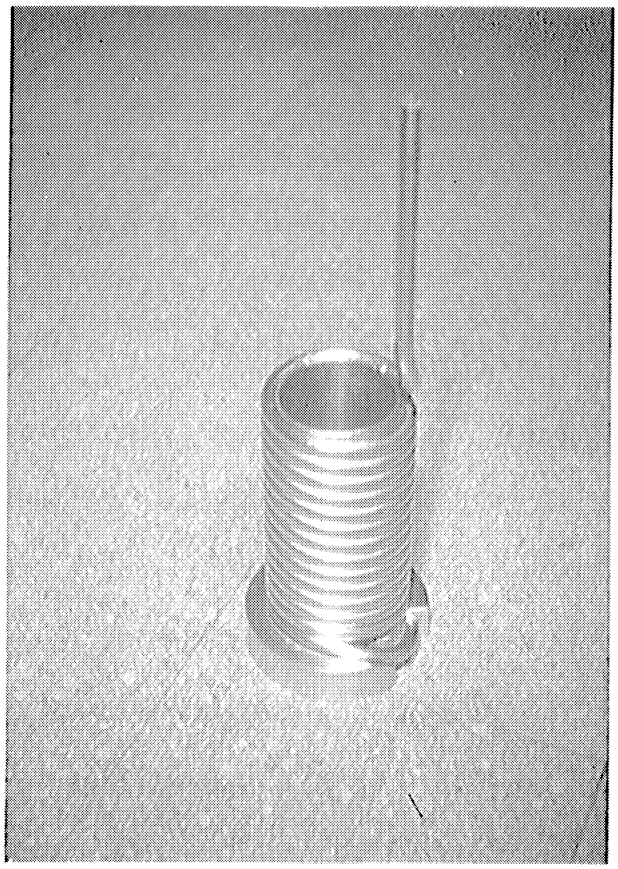

Figure 7. Equilibrium Vessel Tube Coil.

SS tube tightly coiled around the block and sleeve, giving a flow path of approximately twelve feet (see Figure 7). Thermal conductivity has been sacrificed at this point in favor of high strength. The tube is silver soldered to a shoulder at the bottom part of the block, the flow path leading to the center of the block and up vertically through a tightly packed filter of spun glass. The gas leaves the equilibrium vessel through a 3/8" SS tube sealed by a silicone rubber O-Ring seal in combination with a Teflon back-up ring.

A heavy copper sleeve is fitted over the coils and around the bottom of the vessel, so as to minimize any temperature gradients. The completed unit (Figure 8) is 4-1/2 inches in diameter, 6-3/4 inches high, and weighs approximately 25 pounds.

Special fittings are silver-soldered to the inlet and outlet tubes to allow for packing gland connections to the heat exchanger tubes, and also the gas temperature thermocouples and the equilibrium pressure tap. All of these glands are Conax high-pressure packing glands having Lava sealants with the gland pipe threads sealed to the fittings by Permacel tape.

Provision is made for measuring the temperature at twelve points in and around the equilibrium vessel, to assure that no point becomes too cold and to permit minimization of temperature gradients through individual heater control. The equilibrium gas temperature is measured by thermocouple No. 1, which is sealed at the top fitting and hangs down through the vertical outlet tube. It is held in place at the equilibrium point by a special plexiglass ring, to avoid the possibility of having the wires touch the tube, block, or even each other

Figure 8. Equilibrium Vessel, Assembled.

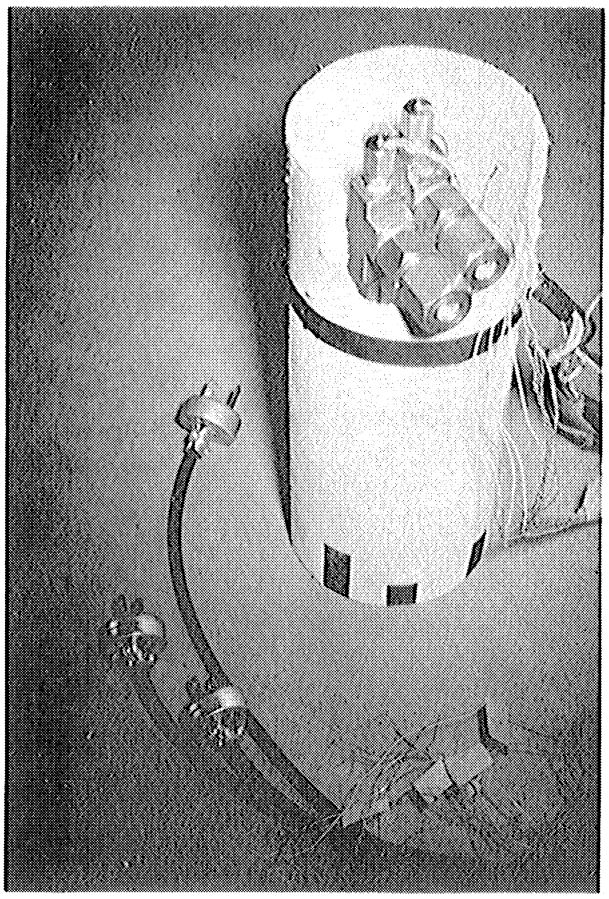

Figure 9. Equilibrium Vessel with Heaters.

somewhere inside the tube. Thus, this thermocouple is directly exposed to approximately the equilibrium temperature for a distance of seven inches, which should assist in giving an accurate reading.

3. Heaters

The main heater used in the regulation of temperature is wound inside a cylindrical sleeve which slides over the equilibrium vessel (Figure 9). The entire unit is 12 inches high and actually contains two separate heater windings. The lower one covers the bottom 7 inches immediately around the vessel, and the upper 5 inches is merely a guard to prevent the inlet and outlet tubes and fittings from possibly being cooled below the equilibrium temperature. The space around the fittings and inside the heater sleeve is packed with fiberglass. This upper assembly is visible in Figure 4.

The construction of this main heater sleeve is as shown in Figure 10. Two layers of asbestos paper are cemented together to form the cylindrical base, with an inside diameter of 4-1/2 inches. Then 42 feet of Chromel A Gage 28 resistance wire are coiled around the lower 7 inches of the sleeve, and cemented in place with Sauerisen porcelain cement. Another layer of asbestos paper is cemented around the assembly, on top of which is coiled a second 42 foot length of wire, to be connected in parallel with the first. Several more layers of asbestos are cemented around the outside to complete the insulation and bring the outside diameter to 5 inches, in order to fit snugly inside the brass can supporting the equilibrium vessel.

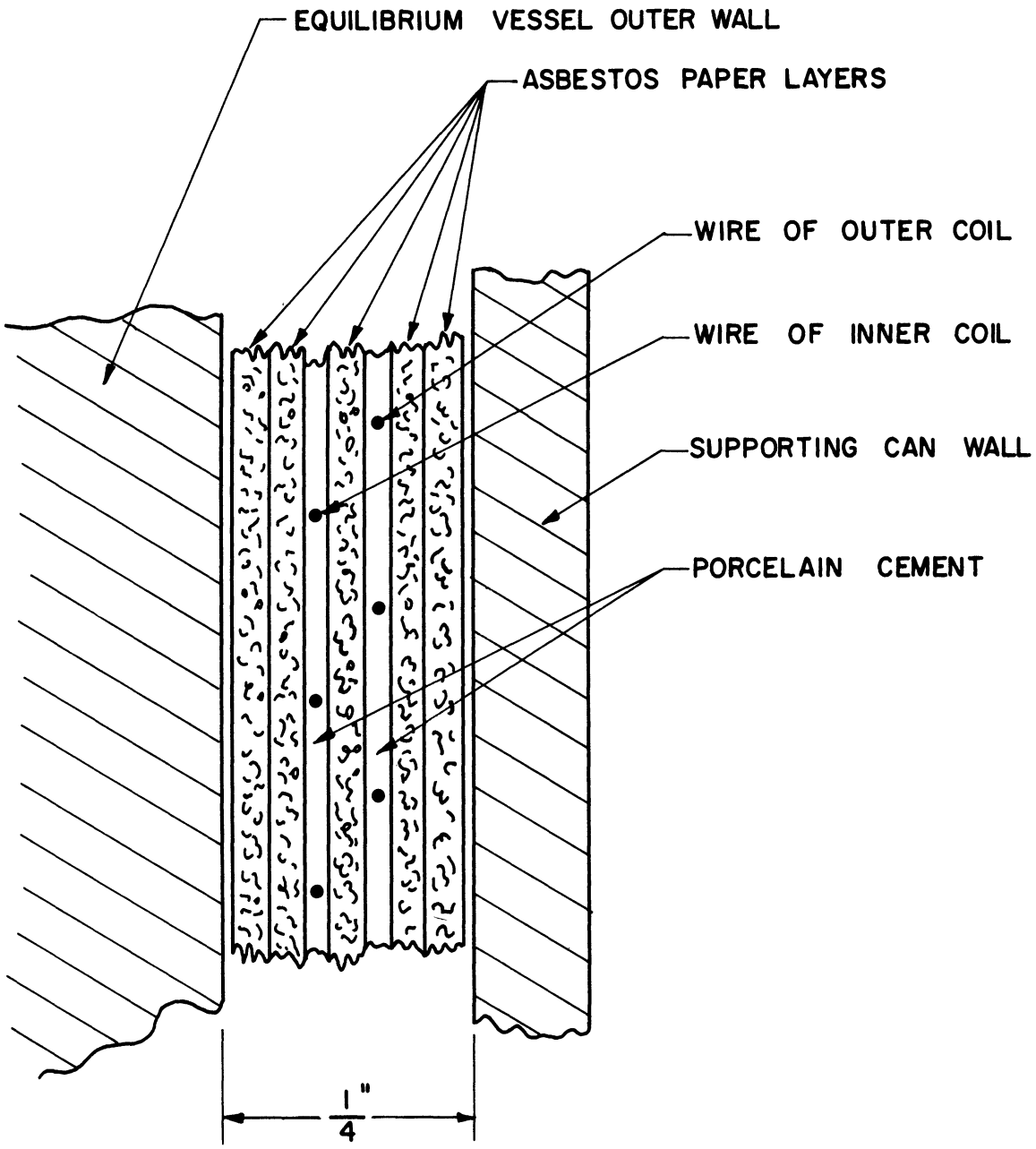

Figure 10. Main Heater Sleeve Construction

The guard heater is wrapped on the upper 5 inches of the sleeve in the same manner, except that only a single layer of resistance wire, 12 feet in length, is used on this portion. There is a second portion of this guard not contained in the sleeve, this part being connected in parallel with the first. It is U-shaped and lies directly beneath the long horizontal tubes connecting the equilibrium vessel to the heat exchanger outside the cryostat. This part is comprised of the same sandwich construction as the other, and also contains 12 feet of heater wire.

In order to prevent a cold spot from developing on the bottom of the vessel, it was found necessary to cover the bottom with a small heater in the shape of a 4-1/2 inch diameter flat disc. This is of a similar construction, consisting of 12 feet of wire coiled back and forth between layers of asbestos. There is also a styrofoam disc, 1-1/4 inches thick, to insulate the vessel bottom from the liquid.

The three heaters are controlled individually by 110-volt variacs, rated at 2 amperes maximum current.

4. Heat Exchanger

The heat exchanger is of the concentric-tube counterflow type construction, and is comprised of 12 sets of tubes 68 inches long, giving a total length of 68 feet. All material in the exchanger is brass, and walls are extra-heavy to withstand the necessary pressures. All connections are silver-soldered.

The principal factor kept in mind in the design of the heat exchanger was that there were to be no soldered joints between the two

passages. All joints are instead between a passage and the atmosphere as shown in Figure 11. This design eliminates the possibility of the equilibrium vessel outlet gas becoming contaminated by the inlet gas because of a tiny internal leak between the two passages. Since pressures are always at least five atmospheres, any pinhole developing would then merely cause a small leak of the gas outward to the atmosphere.

At one end, connections between sets of tubes are relatively simple, as the double-length inside tube is U-shaped and fits into two of the outer tubes, as shown in Figure 11a. A straight tube serves to connect the annular outer-tube passages at this end.

At the opposite end, connections are considerably more difficult, as can be seen in Figure 11b. Since the incoming gas passes through the inside tube, those fittings are rather elongated at one end, in an attempt to induce some of the solid being formed to deposit there instead of blocking the tube passages.

The heat exchanger is heavily insulated with fiberglass blanket and enclosed inside a 10 inch steel pipe closed at both ends, for protection in case of a failure.

C. Accessory Equipment

1. Gas Supply

Gas mixture cylinders at 1600 psig were purchased from the Matheson Company, the concentration of carbon dioxide depending on the range of temperature and pressure to be covered. For most of the temperature range 140-160°K, the supply mixture contains 0.5% carbon dioxide, whereas for most of the range 170-190°K, 2.0% or 4.0% cylinders are used

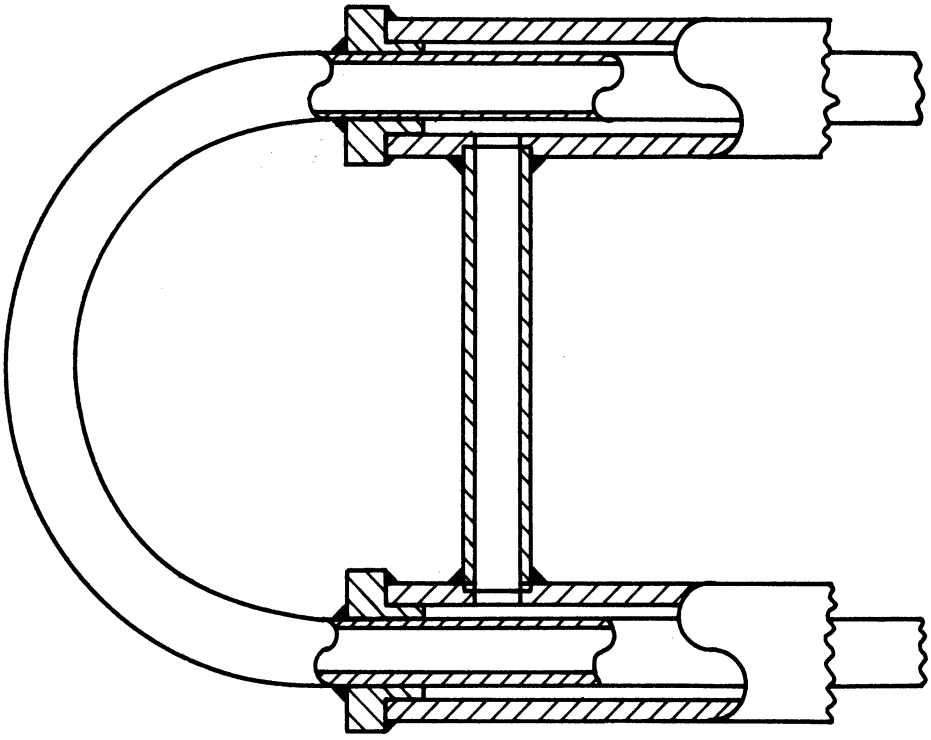

A

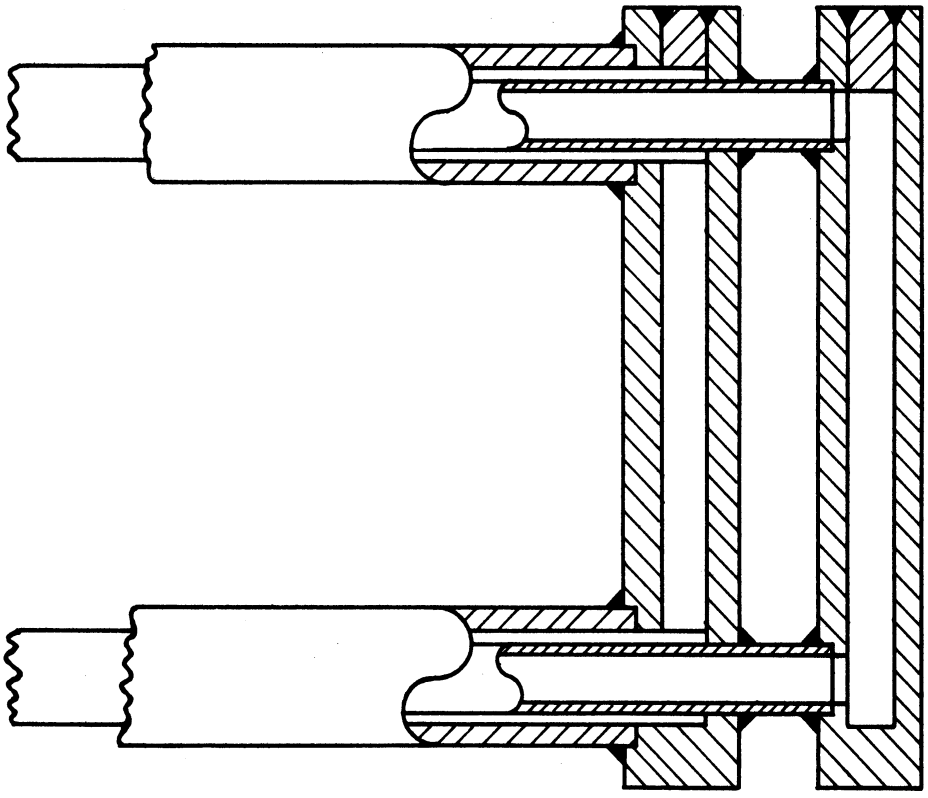

B

Figure 11. Heat Exchanger Fittings

as the running supply. Normally ten such cylinders are manifolded together to prevent the cylinder pressure from dropping excessively during a high-pressure run.

A single cylinder containing from 6-10% carbon dioxide is sometimes used prior to the start of a data run to ensure a good deposit of solid. Caution must be exercised in this matter, however, to prevent the system from becoming plugged with solid.

Nitrogen for purging the system was purchased from the General Stores of The University of Michigan.

2. Pressure Regulators and Valves

A Matheson No. 3-580 high-pressure regulator is installed on the supply manifold to control the equilibrium gas pressure. A No. 1-320 low-pressure regulator is used on the nitrogen manifold for system purging, and also in those cases where the initial high-concentration supply is to be used.

Two Hoke needle valves in series are used in the exhaust line to control the flow rate and throttle the gas to just above atmospheric pressure. A Matheson needle valve controls the analyzer flow rate, and two Fisher type 289U relief valves, 1/2 to 1-1/2 psig range, are used to regulate the back pressure on the two branches of the exhaust line.

D. Instrumentation

1. Temperature Measurement

All temperatures are measured relative to the ice point using 30-gage copper-constantan thermocouples. References (82, 83, 84) and others were consulted in the design and installation. EMF's from the

ten important equilibrium vessel thermocouples designated in Figure 5 are measured by a Leeds and Northrup type K3 potentiometer, in conjunction with a type 2285 reflecting galvanometer, which is hung from the ceiling by a Julius suspension as shown in Figures 12 and 13. EMF's from the remaining six thermocouples are read on a Leeds and Northrup type 8662 potentiometer. These six temperatures are as follows: equilibrium vessel outlet fitting; cryostat gas outlet tube; equilibrium pressure gage (gas); exhaust line downstream of flow control valves; main stream flowmeter; and gas analyzer exit.

The thermocouples were calibrated with a specially built vapor-pressure thermometer patterned after that of Scott.[82,85] The pure vapor used was nitrogen or carbon dioxide, depending upon the temperature range. In addition, the thermocouples were also calibrated at the freezing point of mercury. Deviations from standard EMF were then plotted against EMF, and tables of observed EMF versus temperature prepared.

2. Pressure Measurement

Equilibrium pressures greater than 50 atmospheres are read on a calibrated 6 inch Marsh bourdon gage reading to 3000 psig. Those of 50 atmospheres and less are measured on a calibrated 6 inch Ashcroft gage reading to 800 psig. Other pressures measured are read on stock bourdon gages of various ranges. The other pressures read are downstream side of flow control throttle, main stream flowmeter, gas analyzer exhaust, liquid nitrogen storage container, and of course, upstream and downstream sides of the manifold regulator.

Figure 12. Galvanometer Julius Suspension.

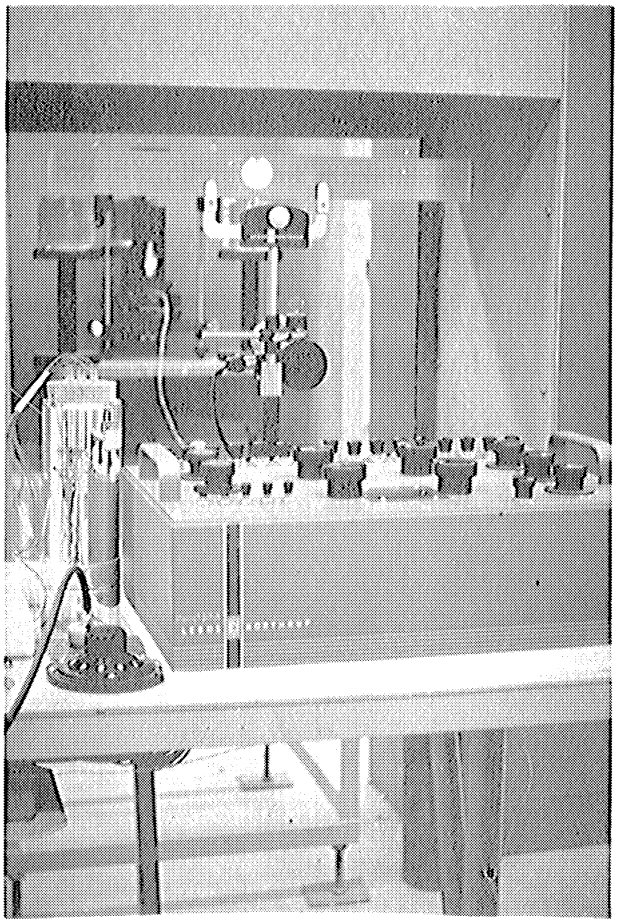

Figure 13. Potentiometer-Galvanometer Installation.

3. Gas Analysis

The equilibrium gas mixture is analyzed in a continuous-flow Beckman L/B Model 15A non-dispersive infrared analyzer, sensitized to detect for carbon dioxide. A schematic diagram of the pick-up section is given in Figure 14. Three sets of cells, of 3/16", 3/4", and 5-1/4" length are used, depending on the percentage of carbon dioxide expected. Cell windows are sapphire, and the detector is charged with carbon dioxide to 50 mm. pressure. The output signal from the detector is fed to the amplifier unit, and eventually read on a calibrated meter.

The gas analyzer is connected in the exhaust line with a needle valve in order to be able to control the flow rate through the analyzer pick-up section. The exhaust line from the analyzer contains a flowmeter and a back pressure regulator to control the analyzer gas pressure. The unit as installed is shown in Figure 15.

4. Flowmeters

A Matheson No. 206 tapered-tube flowmeter with a glass float, 0 - 1.2 Standard CFM, is used to measure the flow in the main exhaust line. Either a No. 201A, 0.1 - 2.0 Standard CFH, or a No. 201, 0.01 - 0.08 SCFH, tapered-tube flowmeter measures the analyzer flow rates.

The overall set-up of the experimental apparatus and instrumentation is shown in Figure 16.

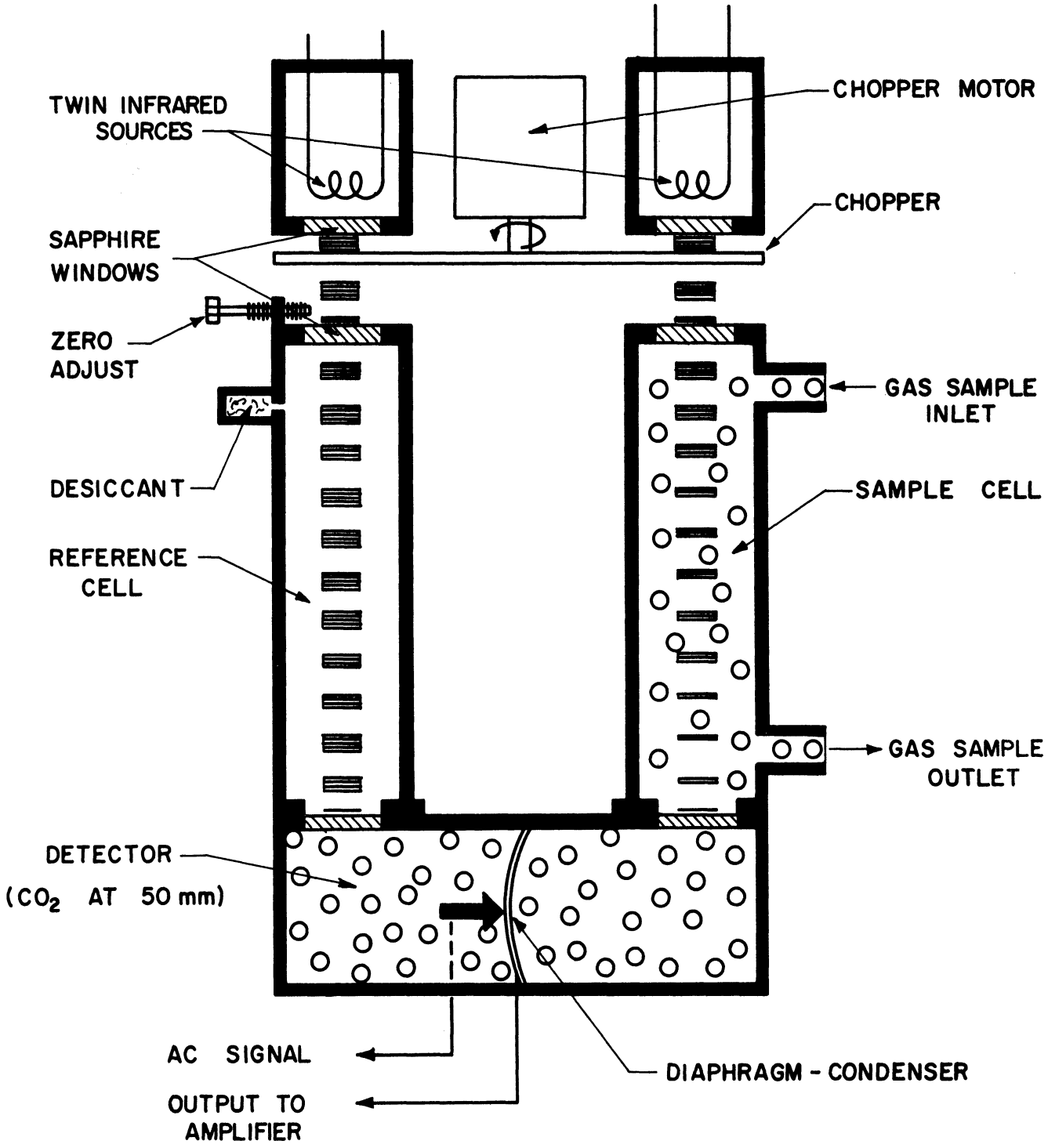

Figure 14. Schematic Diagram of Gas Analyzer

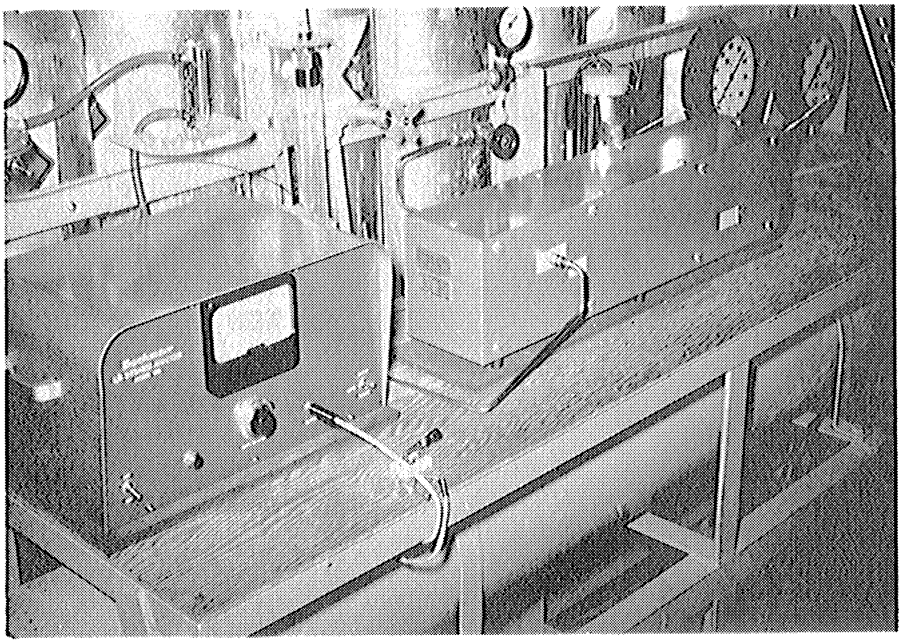

Figure 15. Gas Analyzer Installation.

Figure 16. Experimental Apparatus Overall Views.

VI. EXPERIMENTAL ERRORS

A. Temperature Measurement

1. Potentiometer-Galvanometer

Leeds and Northrup Company specify a maximum error for the K3 potentiometer of ± (0.015% + 0.5μv) in the range used. In tests run at the liquid nitrogen point over a period of several weeks, the maximum deviation from the mean in ten separate readings was found to be 0.5μv, well within the limits given above.

The potentiometer case is grounded through a 0.01μf capacitor, in order to guard against electrostatic disturbances.

The potentiometer is balanced against an Eppley unsaturated type cadmium standard cell, certified to be accurate to 0.01%. Regular checks showed the standardization of the potentiometer to remain quite constant over a period of time. The sensitivity of a change in standardization on an EMF measurement was also made, a galvanometer scale deflection of ± 8 mm on the standard cell circuit being required to give an error of 1μv in the unknown EMF measurement, for the temperature range of interest. The standard cell balance was always held within ± 2mm deflection during operation of the equipment.

The reverse key on the potentiometer was also used periodically, to assure that no errors were introduced in the thermocouple-potentiometer circuitry.

The Leeds and Northrup No. 2285 reflecting-type galvanometer used in conjunction with the potentiometer has a sensitivity of 0.0003μ amp/mm at a distance of 1 meter. During the operation the galvanometer

was checked regularly for zero-drift. The galvanometer hangs from the ceiling by three cables, each connected to the Julius suspension by a short spring to damp out any vibrations in the vertical direction. Rotation about the vertical axis is completely eliminated by the three dashpots filled with a heavy mineral oil, and any tendency for the light spot to move is further reduced by the design of the suspension system, which is counterbalanced to put the center of gravity of the suspended mass at the galvanometer mirror.

2. Thermocouples

All thermocouples were constructed of 30 gage copper-constantan wire, the ten used to indicate the block and tube temperatures being made from the same spools. The two thermocouples used in the Conax glands to indicate gas temperature were from different spools.

The thermocouples were calibrated using the vapor-pressure thermometer discussed in V D1, along with carbon dioxide or nitrogen. The manometer used to read vapor pressure was considered accurate to 0.1 inch of water, and vapor pressures were taken from References 24, 76, 82, 86. Calibrations were also made at the freezing point of mercury.

Curves of deviation versus EMF were slightly parabolic in shape and very smooth, indicating that the thermocouples are reliable to better than 0.1°C in the range covered. According to Wiebe,[87] they should be accurate to approximately $\pm$ 0.05°C. Scott[85] was somewhat more conservative, but as he pointed out, his experience was based on thermocouples of widely differing origins. The only differences of

more than 1μv (~.04°) observed in calibration were between the two sets of thermocouples, where deviations were quite different. The curve for the two gas thermocouples, (Nos. 1,2) had smaller deviations from the standard than did the block and tube temperature thermocouples (Nos. 3, ..., 10) at any given temperature, this difference reaching 14μv at the boiling point of nitrogen.

B. Temperature Control

Manual control of the equilibrium vessel temperature proved to be very precise, well within the ± 0.1°C limits desired. The block temperature uniformity was always more than adequate, the side temperatures being held either at the equilibrium value or 0.1°C high to preclude any possibility of a cold point. The center of the block bottom was held at the desired value by manipulation of the small heater covering the bottom. This often resulted in a temperature 0.1 to 0.2° high at the bottom corner, due to the junction of the side and bottom heaters there. This could probably have been partially eliminated by respacing the heater coils in the bottom heater, but this was not deemed necessary. The top part of the block normally ran 0.1 to 0.2° high also, due to the warm gas entering there, but this was expected. This temperature also proved to be a function of the liquid nitrogen level in the cryostat, the top temperature increasing slightly if the level were permitted to fall.

It was found that the block temperature distribution is a function of both the gas velocity and the supply gas carbon dioxide concentration. The reason for the first is obvious; the other is due to

the fact that freezing more carbon dioxide out of the mixture tends to warm the central block slightly. With respect to this latter point, perhaps the more conventional equilibrium vessel comprised of a tube coil in a stirred liquid would be superior to the type used in this investigation. In other respects, the type used here seems to be better.

The top heater was installed to assure that the inlet and outlet gas temperature was always greater than that at the equilibrium point. The amount of difference is unimportant, except that if it becomes too large, the temperature distribution in the block will be affected.

C. Pressure

For equilibrium pressures of 50 atmospheres and less, the accuracy of the pressure reading and control is of the order of $\pm$ 0.1 atmosphere, as read on the calibrated Ashcroft gage. The manifold pressure regulator was certainly not this steady, but any differences were apparently damped out in the 35 feet of flow path between the regulator and equilibrium vessel. In a few runs at low pressures the regulator apparently hunted to the extent that equilibrium pressure varied as much as $\pm$ 5 psig. In these cases, the run was not started until the pressure settled down to a stable value.

For pressures greater than fifty atmospheres, the accuracy of the Marsh gage is considered to be approximately $\pm$ 0.5 atmospheres. At five of the six isotherms studied, the fifty atmosphere point was run twice, once with each gage. In every case, the resulting equilibrium compositions were identical, or at least within the limit of experimental accuracy.

The remaining pressures measured were read on bourdon gages accurate to approximately ± 1% full scale, which is satisfactory.

D. Gas Analysis

The Beckman L/B Model 15A infrared analyzer is specified to have a maximum error of ± 1% full scale, with a sensitivity of one-half that value.

The particular instrument used in this study was tested, with results as follows:

Zero drift in 8 hrs.	± 0.1% full scale
Span drift in 24 hrs.	± 0.3% full scale
Max. noise level	± 0.05% full scale

Calibrating cylinders were purchased from the Matheson Company. The zero-point was set with pre-purified nitrogen, and tests showed that small differences in the zero setting had no effect on the upscale readings. The calibrations were made at the temperature, pressure, and flow rate to be encountered in the experimental runs.

On several occasions, extensive tests and recalibrations of the unit were made continuously for as long as ten hours, with the resulting output meter readings being in every case constant within ± 0.5% of full scale.

It was found early in the testing that the analyzer could not be run with the cover plates removed from the pick-up section (as has been done in some installations), inasmuch as the resulting air movement between the sources and cells tended to cause a drift of as much as 1% in some instances. The readings were also found to be extremely sensitive

to the gain control setting, so the dial was locked prior to calibration and subsequent operation of the unit.

Tests were also performed to determine the effects of varying analyzer pressure and flow rate. During actual data runs, the pressure was always held at 0.6 psig, but no difference in analyzer reading could be detected by varying the pressure ± 0.05 psig from this value. Similarly, the analyzer flow rate ranged from 0.5 to 1.0 SCFH, depending on cell length used, but no difference in reading was observed due to varying the flow from 0.2 to 1.5 SCFH. These tests were carried out with all three lengths of cells. Some tests were also run at much lower flow rates, down to 0.02 SCFH, but the readings were found to be more unstable and sensitive to changes in this region.

Prior to starting the equipment, the analyzer was calibrated using four or more points. As mentioned before, the gain control dial was locked and never touched once the calibration had been started.

Recalibrations were made regularly at the conclusion of a set of runs, and also periodically during a lengthy set. No recalibration ever showed a change of as much as ± 0.5% full scale. The consistency of these recalibrations also shows that the tendency for the analyzer exit temperature to increase by approximately a degree during a series of runs has no effect on the calibration curve or accuracy of the readings.

Twenty-five percent of the points were checked by rerunning at different flow rates. In every case, the analysis was either identical or at least within the ± 0.5% full scale considered to be the accuracy

of this instrument. Among these tests were check runs made at certain points using different cell lengths, in order to assure that two different cells would give the same analysis of the gas phase. These checks were also run at different flow rates in order to test the attainment of equilibrium and effectiveness of the filter. It was at one of these different-cell checks that the largest deviation of any of the checks was found, that of 160°K, 70 atm. pressure. The 5-1/4 inch cells showed a carbon dioxide mole fraction of 0.00334 $\pm$ 0.00002, while 3/4 inch cells gave a reading of 0.00330 $\pm$ 0.00003. It is noted that the limits of these readings do overlap, and the test was therefore considered successful.

E. Throttling Valves

There was some question as to whether severe throttling of the gas mixture across the flow control valves could possibly cause a change in composition across those valves. Therefore, using a mixture of known composition, a thorough test was run, completely covering the entire range of flow rates and equilibrium pressures. In no case could a difference in analyzer reading of even $\pm$ 0.5% be detected.

F. Flow Rates

The tests were normally run at such a flow rate as to give a gas velocity in the equilibrium vessel of approximately 0.1 ft/sec ($3 \frac{cm}{sec}$). As long as the velocity was of this order of magnitude, the results were not affected by changes in flow, so a precise measurement of flow was not required. The tapered tube flowmeter used can certainly be relied on to $\pm$ 10% of the reading, which is sufficient.

The analyzer flow, as discussed in VI-D, is not critical in the range used, so the same accuracy as with the large flowmeter is again acceptable.

G. Attainment of Equilibrium

In work of this type, the important question of whether or not a true equilibrium is achieved in a run can only be answered by inspection of the behavior of the system during the run, and by resorting to indirect tests.

The most important factor in determining the attainment of equilibrium was having the continuous reading gas analyzer directly in the system. At the beginning of operation, the analyzer would read some value greater than that to be expected in the experimental point, because the initial high-concentration mixture was always run at a very low pressure. When the running mixture was turned on (at the higher operating pressure), the analyzer output reading began to drop within a very few minutes and would steadily fall to the equilibrium reading, at which point it would remain for however long the test was run. The same points were run without the initial mixture, in which case the analyzer reading steadily rose from zero to above the equilibrium reading, and then fell slowly to the same value. It is felt that the ability to continually watch the analysis results during the test run was of immeasurable benefit in obtaining good experimental data.

The flow rates used were such as to give a particle an average time of over two minutes spent in the equilibrium vessel, which should be much more than a minimum time to come to equilibrium, especially in view of the relatively small change of temperature in the equilibrium vessel.

The rerunning of 25% of the experimental points at different flow rates, ranging in equilibrium vessel gas velocities of from 0.04 to 0.2 ft/sec, is again a strong argument for the attainment of equilibrium in the vessel, in view of the consistency of the results.

H. Solid Carbon Dioxide Filter

The tests run at different flow rates, discussed in the preceding sections, give a strong indication that little or no solid passed the filter. If this were not the case, it would be certain that higher flow rates would result in greater percentages of carbon dioxide in the exhaust gas.

Of the 16 points checked at different flows, the lower velocity gave identically the same reading 6 times, a lower reading 6 times, and a higher reading 4 times. Of the 10 that were not identical, the difference was always within the limits considered as the gas analyzer accuracy. It should also be mentioned that for many of these, the check point was run at a later time on a different calibration curve, so that a reading identical to the original was often impossible due to limitations in the preciseness to which the analyzer scale could be read.

I. Gas Purity

The gas mixtures were made up of 99.7% minimum purity extra-dry nitrogen (impurities principally argon) and 99.8% minimum carbon dioxide (impurities principally nitrogen and carbon monoxide). Before running, the system was purged for at least 30 minutes with nitrogen.

Calibrating gas mixtures for the gas analyzer were mixed of gases of the same purity as given above. The analyzer zero setting was always made with nitrogen of 99.996% minimum purity, with most of the remaining impurities substances that would not affect this reading. Moreover, as mentioned in VI-D, a small error in the zero setting will only affect the lower portion of the calibration curve, which was not encountered in the experimental work.

VII. TEST PROCEDURES

A. Temperature-Pressure Range

Six isotherms were studied, ranging from 140 to 190°K in ten degree intervals. The minimum pressure was five atmospheres absolute, and was incremented from ten to 100 atmospheres in ten atmosphere intervals.

The five atmosphere point at 190°K was not taken because the gas-phase carbon dioxide concentration exceeded the range of the analyzer. This was not considered of prime importance, as the experimental and predicted results should conform closely at this low pressure. At 140°K, the 100 atmosphere point was not studied, inasmuch as densities greater than 1.5 times the critical were not of interest in this investigation.

B. Run Procedure

The cryostat required a cooling-down time of from three to four hours, due to the fact that the equilibrium vessel is insulated from the liquid nitrogen to reduce heat transfer rates. While the cryostat was being cooled, the gas analyzer was carefully calibrated at four or more points and rechecked. During the last half-hour of cooling, nitrogen was passed through the system in order to purge the lines and also cool down the heat exchanger.

Once the desired block temperature was reached, the main heater was turned on and set to hold that value. This setting varied from approximately 10 watts at 140° to 120 watts at 190°K. The small bottom

heater was then adjusted to prevent a cold spot on the bottom of the block, the power drawn by this heater varying up to two watts.

When the temperatures were stable and quite uniform, the gas mixture was turned on. In some runs, the initial high-carbon dioxide concentration mixture was used first to give a good deposit of solid, but at the higher pressure points, where the mass flow rates are larger, this initial mixture was not used, in order that the system could be run for longer periods of time without plugging. The test results were found to be independent of whether or not the initial mixture was used.

The running mixture was turned on, and the desired pressure and flow rates set. The heater settings often had to be readjusted at this time, because of the carbon dioxide freezing out of the mixture. The top guard heater was adjusted periodically to ensure that the inlet and outlet tubes and fittings did not approach the equilibrium temperature, the maximum output of this heater running approximately ten watts.

After the temperature, pressure and flow had been stabilized, the analyzer valve was opened and the analyzer flow and pressure were set to the values at which the unit had been calibrated. Depending on the flow rate through the system, the analyzer lagged from four to ten minutes behind the equilibrium point. The output reading was observed over a period of time, while the temperature, pressure and flow were held constant. When the equilibrium condition had been reached, the system was run for at least thirty minutes to ensure that no further change would take place, after which the readings were taken.

Inasmuch as the gas phase was not analyzed by collecting a sample over an interval of time as was done by Webster,[13,14] Dokoupil,[15]

etc., or by periodic sampling, as by Ewald[16] and others, it was not deemed necessary to run each point a number of times and take the average of the readings. Since the gas phase was analyzed continuously during a run, it was possible to observe the manner in which the carbon dioxide percentage changed as the system approached equilibrium, at which point it remained constant for as long as desired. This was felt to be a very reliable test of the concentration, as well as of the equilibrium itself. In order to check this equilibrium, and particularly the solid carbon dioxide filter, 25% of the data points were repeated at different flow rates.

Three different sets of sample and reference cells were used in the analyzer, depending upon the concentration expected. The 5-1/4" cells were used for carbon dioxide mole fractions less than 0.004, the 3/4" cells from 0.004 to 0.020, and the 3/16" cells from 0.02 to 0.10.

Inasmuch as the gas analyzer accuracy is considered to be a fixed percentage of full-scale deflection, it would be desirable to have the experimental readings fall on the upper portion of the calibration curve, so as to minimize the percent error in the reading itself. Consequently, the runs were grouped according to the carbon dioxide mole fraction expected, and the analyzer calibrated with the maximum in carbon dioxide percentage as small as possible. The portion over 90% full-scale deflection was not used, however, because the output becomes quite non-linear in this region. This procedure worked quite well, especially since the observed concentrations were at least fairly close to those expected, and were generally smaller. Some points that fell particularly low on the calibration curve were rerun later using different analyzer calibration.

C. Criteria for an Acceptable Run

The following conditions must all be met, in order for a run to be considered successful:

1) The temperature, pressure, flow rate, and analyzer readings must all be constant for thirty minutes.

2) There should be no temperature in the block more than 0.3°C above the equilibrium temperature TC-1, and none less than TC-1.

3) Inlet and outlet tube temperatures TC-9 and TC-10 must be at least 0.5° greater than temperature TC-1.

4) The outlet fitting and upper tube temperatures TC-11 and TC-12 must be at least 5° greater than TC-1.

5) The analyzer output should read at least 0.001 less carbon dioxide than the supply mixture.

Once the system was checked out and the difficulties eliminated, the only runs discarded were those in which the system plugged with solid before condition 1 above could be fulfilled. This occurred possibly ten or twelve times during the course of the experimental work.

VIII. EXPERIMENTAL RESULTS

A. General

Considerable difficulty was experienced during the initial running of the equipment. The gas-phase carbon dioxide mole fractions were found to be even lower than that predicted for ideal behavior, which seemed very unreasonable, and were strongly dependent upon flow rate through the system.

At this time, the apparatus was being run with only the side and bottom heaters, and it was discovered that the equilibrium vessel upper tubes and fittings were being cooled below the equilibrium temperature by the cold cryostat vent gas. This resulted, in effect, in an equilibrium temperature lower than what was being held and measured in the vessel itself, with a correspondingly smaller percentage of carbon dioxide remaining in the gas phase for a given pressure.

These troubles necessitated the addition of sealed pipes on the cryostat vent, filler, and float pointer, in order to carry the cold nitrogen vapor completely out of the cryostat, these pipes being visible in Figure 4. In addition, the fittings were heavily packed with fiberglas, and a new heater sleeve designed to completely surround the fittings and tubes, as shown in Figures 4 and 9. A second portion of the heater, part of which can also be seen in Figure 4, was placed horizontally beneath the tubes leading out of the cryostat, to guard those from possibly being overcooled. In order to regulate this new guard heater properly, the four thermocouples designated TC-9 to TC-12 were

added, and read regularly. These precautions completely eliminated the cooling difficulties, and no further troubles were experienced.

The ten equilibrium vessel temperatures designated TC-1 to TC-10 in the data (locations shown on Figure 5) are considered reliable to better than 0.1°C, and the upper cryostat temperatures TC-11 and TC-12 to 0.25°. Temperatures TC-13 to TC-16, at the equilibrium pressure gage (gas), line downstream of the throttle, and the two flowmeters, were checks only, and are listed to 0.5°. Equilibrium pressures of 60 atmospheres and above are accurate to roughly 0.5 atmospheres, and those less than 60 atmospheres to approximately 0.1 atmosphere.

Accuracy of the gas-phase analysis is based upon the extensive testing of the analyzer carried on through the entire course of the experimental work, and is considered to be $\pm$ 0.5% of full-scale deflection. The operating procedure of attempting to keep the experimental results reasonably high on the calibration curve results in a variation in accuracy from point to point depending on the calibration curve used in the run. These error limits are listed with the experimental data in Appendix D, and are seen to be roughly $\pm$ 1% of the reading in most cases although for some of the extremely small concentrations at 140°K, they reach $\pm$ 5%.

In the data of Appendix D, the run designations are as follows: the letters A, B, C refer to the three sets of analyzer cells used, and the following numbers denote the calibration curve under which the point was run. For example, all points listed under run A1 were made with the 5-1/4" cells and calibration curve number 1 for those cells. Each

of these calibration curves was checked periodically during the course of taking a set of points, and was found to be reproducible in every case.

In the presentation of the experimental data, after some deliberation it was decided to use the metric system for any measurements made in the cryostat, because of its more frequent use in work involving equations of state, cryogenics, and phase equilibria. The remaining readings, those checks at approximately room temperature and pressure, are given in the English system, largely because of its familiarity in this country and also because the instruments used were calibrated in those units. It is sincerely hoped that no one will be confused or offended by this mixing of systems of units.

B. Results and Discussion

The Series A points, designating 5-1/4" analyzer cells, included points in which a gas-phase carbon dioxide mole fraction of less than 0.004 was expected. Most of the pressures at temperatures of 140, 150, and 160°K were covered in this series.

At 140°K, points were run from 5 through 90 atmospheres. The 100 atmosphere point was not included because the gas density would be greater than 1.5 times the critical, which was not of particular interest in this study. Since it should be possible to predict the carbon dioxide concentrations quite accurately at low pressures, it would be expected that the mole fraction of carbon dioxide would fall quite rapidly from unity at the vapor pressure, 0.00184 atmospheres, as the total pressure is increased. As seen in Figure 17, there is a minimum

at about 25 atmospheres, after which the concentration begins to increase with pressure. This minimal pressure, as it is often termed, is of particular interest in the purification of gases by selective freezing. If the behavior were ideal, and all three assumptions discussed in Section II-F were valid, then the mole fraction y_1 would be given by the ratio $P_1^{\square}/P$ and would show no such minimum point, but would continue to decrease with increasing pressure. The assumption of ideal behavior will hold reasonably well for low pressures, but is seen to be completely out of the question here. At about 60 atmospheres, there is an inflection in the isotherm, above which pressure the slope of the curve begins to decrease, this effect being much more apparent on a large scale plot. This behavior is consistent with that observed by Webster[14] and others with this type of system. It is only reasonable to expect a limit to the increase of solubility of the condensed phase in the gas. At this temperature, check points were run at 70 and 10 atmospheres, with excellent agreement. The experimental accuracy of the carbon dioxide mole fraction is given as $\pm$ 0.00001, except for the 10 atmosphere check, which was run on a calibration curve at lower gain, with a corresponding estimated accuracy of $\pm$ 0.00002.

At 150°K, similar behavior of the isotherm is observed. At the lower end, the carbon dioxide mole fraction would go to unity at 0.00841 atmospheres, the vapor pressure of pure carbon dioxide. The minimal pressure at this temperature occurs at 30 atmospheres having increased from 25 atmospheres at 140°. Again, an inflection is observed at higher pressure, this time around 75 atmospheres, as compared with

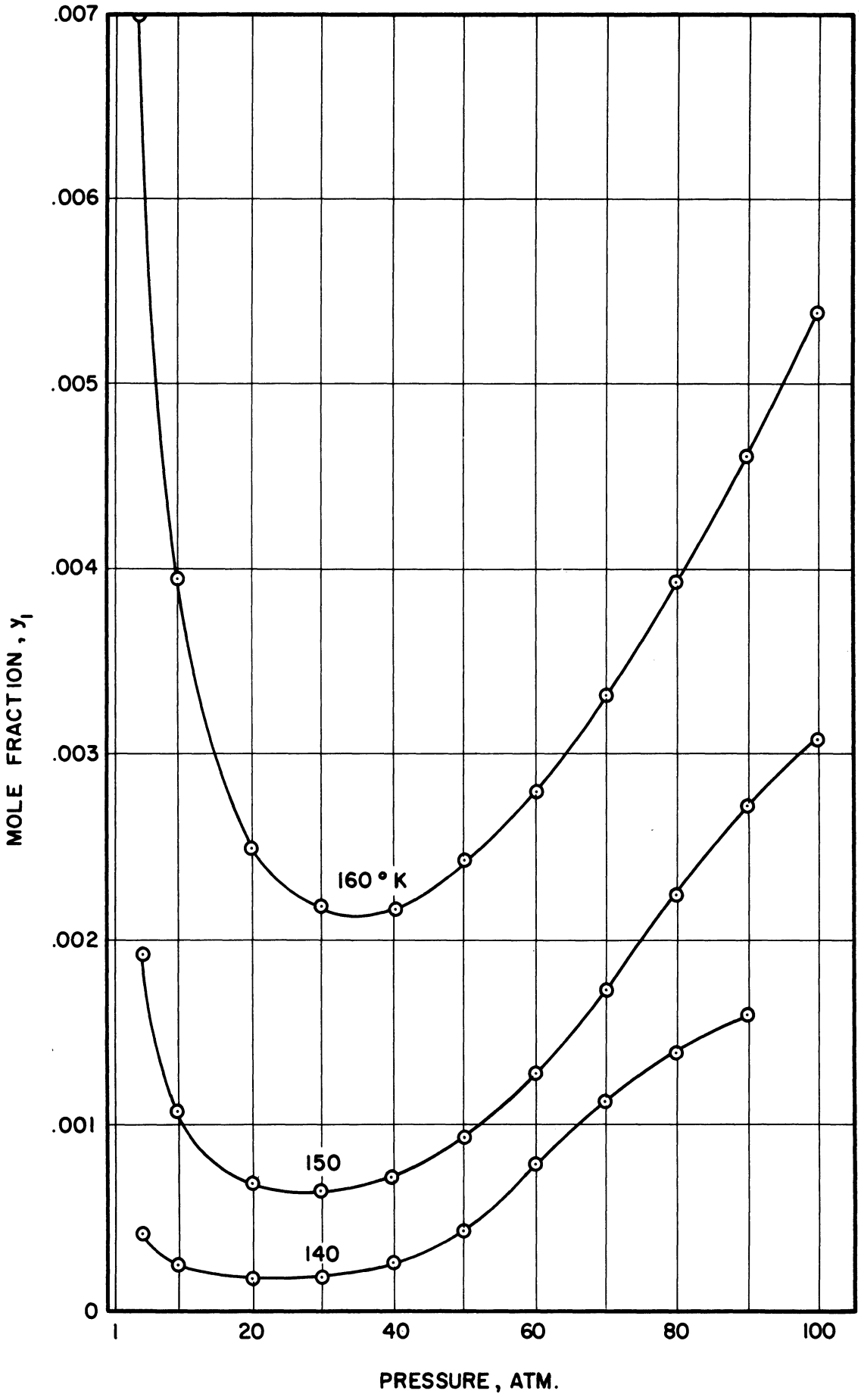

Figure 17. Mole Fraction y_1 vs. Pressure at 140°, 150°, 160°K

60 atmospheres at the lower temperature. For this isotherm, check points were run at 80, 50, and 10 atmospheres, the 50 atmosphere point being run with a different pressure gage and calibration curve, as well as at a different flow rate. As before, there were no discrepancies between the check points and the originals. The gas-phase analysis was accurate to ± 0.00002 at 60 atmospheres and above, and ± 0.00001 at the lower pressures.

The final isotherm of Series A is 160°K, also plotted in Figure 17, although the points at 5, 80-100 atmospheres were actually run in Series B because of higher carbon dioxide concentration. At this temperature, the mole fraction can be extrapolated to unity at 0.0314 atmospheres, and the minimal pressure has now increased to 35 atmospheres. At higher pressure, no inflection is observed for 160°K, although it appears that such a point may occur very close to 100 atmospheres, the maximum pressure studied. Four check runs were made at this temperature at 90, 70, 50 and 10 atmospheres. The 70 atmosphere point was run in both Series A and B, i.e., with the 3/4" as well as the 5-1/4" cells, as a special check of the correlation between results obtained with different cell lengths. The agreement is not exact, but the average, lying within the limits of error of both points, gives a very smooth curve. The other three check runs showed closer agreement. Accuracy of the mole fraction determination is ± 0.00003 from 80-100 atmospheres, ± 0.00002 from 10-70 atmospheres, and ± 0.00005 at 5 atmospheres, due to the different ranges in calibration.

Series B, using the 3/4" analyzer cells, includes all of 170 and 180°K, with the exception of the lowest pressures, as well as the four points at 160°K discussed above.

At 170°K, Figure 18, the mole fraction of carbon dioxide would tend toward unity at 0.0993 atmospheres. The minimum point at this temperature is seen to occur at about 43 atmospheres, and although no inflection is observed at higher pressure, the isotherm becomes nearly linear around 100 atmospheres. The points at 50 and 10 atmospheres were rerun, and agreed very well. The accuracy is considered to be ± 0.00007 at 90 and 100 atmospheres, ± 0.00005 from 20-80 atmospheres, ± 0.0001 at 10 atmospheres, and ± 0.0002 at 5 atmospheres. The 5 atmosphere point was actually run in Series C, due to the relatively higher mole fraction of carbon dioxide.

Experimental results for 180°K are also shown in Figure 18. At the low pressure end, the carbon dioxide mole fraction could be extrapolated to unity at 0.274 atmospheres. The pressure at which the minimum mole fraction occurs has now increased to just over 50 atmospheres, and the slope of the isotherm is still increasing at the maximum pressure covered, 100 atmospheres. The check runs, at 50 and 20 atmospheres, showed excellent correlation with the original points, the latter one being checked in Series C with the 3/16" cells, which makes the agreement particularly satisfactory. The estimated gas-phase accuracy is ± 0.0001 at pressures from 20-100 atmospheres, ± 0.0002 at 10 atmospheres and ± 0.0004 at 5 atmospheres, these latter two points actually being run in Series C.

Series C, run with the set of 3/16" analyzer cells, included all the 190°K points, and also the three at 170 and 180° mentioned previously. The vapor pressure at 190° is 0.679 atmospheres, and the mole

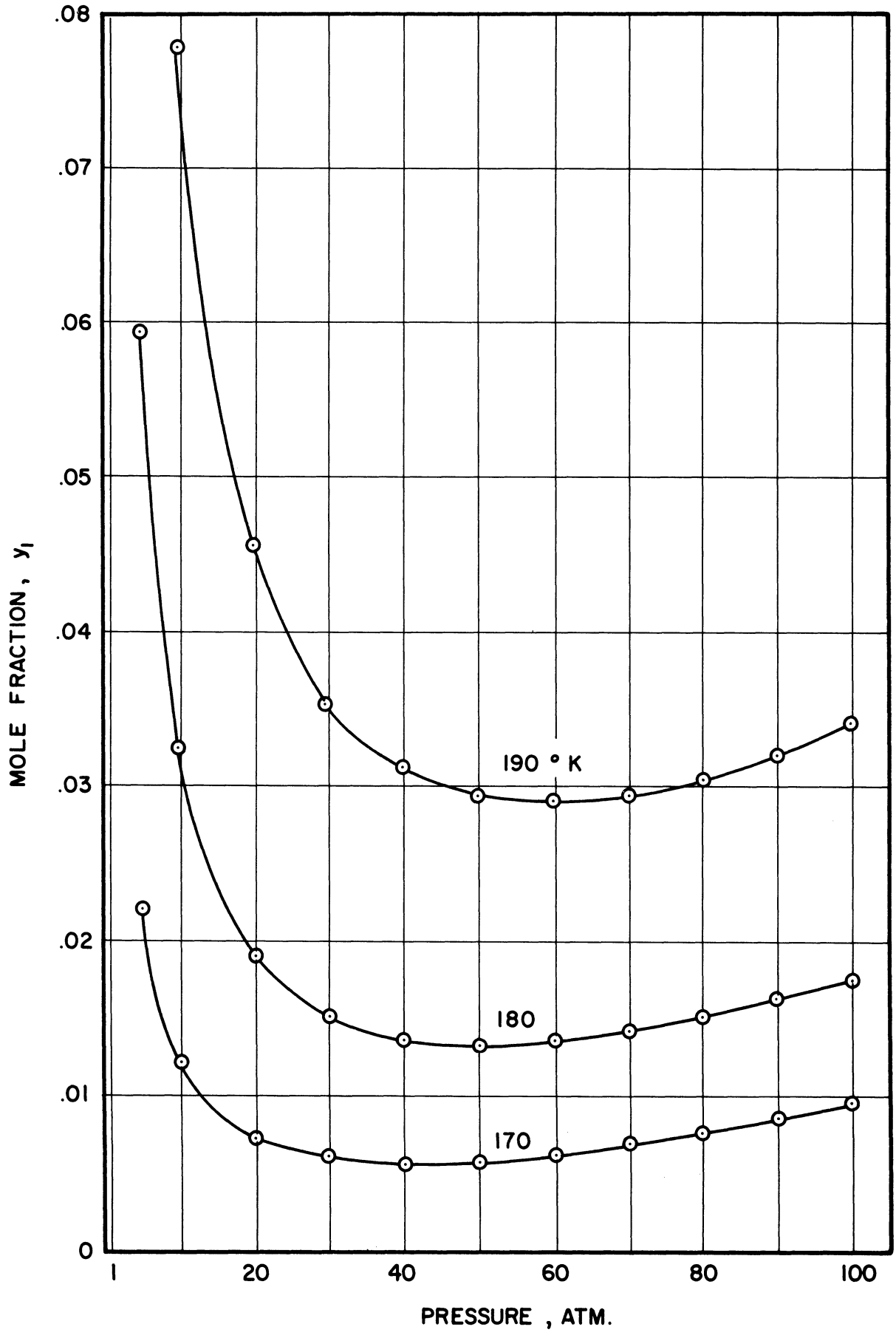

Figure 18. Mole Fraction y_1 vs. Pressure at 170°, 180°, 190°K

fraction falls to a minimum at 60 atmospheres. As at 180°, no tendency for an inflection to occur is observed at up to 100 atmospheres pressure. The 5 atmosphere point was not run at this temperature, due to the limiations in the range of the analyzer cells. The runs checked at 190° were at 90, 50, and 30 atmospheres. There was some difference at 90 atmospheres, but the original and check points were each within the other's specified limits of error. The accuracy of the points at this temperature is considered to be $\pm$ 0.0002, except for 10 and 20 atmospheres, which is $\pm$ 0.0004.

The six isotherms have been plotted on two separate graphs because of the wide variance in mole fraction over the temperature range covered. The check points have also been included in these plots, but in all but a few cases appear identical to the original, especially on the scale used in Figures 17 and 18. From larger scale graphs, the best values have been determined, and these are tabulated in Table VIII. The only alterations made to the original data were to average the original and check point values at 160°K, 70 atmospheres, giving 0.00332 (from 0.00334 $\pm$ 0.00002 and 0.00330 $\pm$ 0.00003), and also to average those at 150°K, 80 atmospheres, to give 0.00222 (from 0.00223 $\pm$ 0.00002 and 0.00221 $\pm$ 0.00002). The only other point and check which could have been averaged without overspecification in the number of significant figures was that at 190°K, 90 atmospheres, and this was not done because the original point gave a smoother curve.

TABLE VIII

MOLE FRACTION OF CARBON DIOXIDE AS A FUNCTION OF TEMPERATURE AND PRESSURE

Pressure, atm.	Temperature, °K 140	150	160	170	180	190
5	.00042	.00192	.00699	.0220	.0595	. --
10	.00024	.00107	.00395	.0121	.0325	.0778
20	.00018	.00069	.00251	.00735	.0190	.0455
30	.00019	.00064	.00217	.00608	.0151	.0354
40	.00025	.00071	.00217	.00572	.0137	.0311
50	.00043	.00094	.00243	.00580	.0133	.0293
60	.00078	.00128	.00280	.00618	.0135	.0290
70	.00112	.00172	.00332*	.00685	.0141	.0293
80	.00139	.00222**	.00393	.00760	.0150	.0303
90	.00158	.00270	.00461	.00860	.0161	.0320
100	. --	.00304	.00536	.00968	.0176	.0340

*Average of .00334 ± .00002 and .00330 ± .00003

**Average of .00223 ± .00002 and .00221 ± .00002

As a point of particular interest, the 16 points that were checked are listed below in Table IX, along with their respective limits of error based on the gas analyzer tests. Values of the gas velocity in the equilibrium vessel for each of these runs are also given, these being important in evaluating the effectiveness of the solid trap.

Examination of Table IX with regard to accuracy of gas-phase analysis shows that for fifteen of the sixteen points, both the original and check fall inside each other's limits of errors. The only exception is the point at 160°K, 70 atmospheres, for which a mole fraction 0.00332 seems to be the best value, this lying within the limits of both the experimental readings. With respect to effectiveness of the solid

TABLE IX

COMPARISON OF THE ORIGINAL AND CHECK RUNS

T(°K)	P(atm)	$\bar{V}$(cm/sec)	y_1
140	70	2.08	0.00112 ± 0.00001
		0.98	0.00112 ± 0.00001
140	10	3.20	0.00024 ± 0.00001
		4.56	0.00023 ± 0.00002
150	80	1.98	0.00223 ± 0.00002
		2.20	0.00221 ± 0.00002
150	50	1.13	0.00094 ± 0.00001
		3.17	0.00094 ± 0.00002
150	10	3.20	0.00107 ± 0.00001
		4.56	0.00107 ± 0.00002
160	90	2.26	0.00461 ± 0.00003
		1.34	0.00460 ± 0.00007
160	70	2.75	0.00334 ± 0.00002
		1.74	0.00330 ± 0.00003
160	50	2.66	0.00243 ± 0.00002
		3.75	0.00243 ± 0.00002
160	10	6.40	0.00395 ± 0.00002
		3.29	0.00394 ± 0.00002
170	50	3.11	0.00580 ± 0.00005
		2.07	0.00580 ± 0.00005
170	10	3.08	0.0121 ± 0.0001
		6.10	0.0120 ± 0.0001
180	50	2.86	0.0133 ± 0.0001
		1.16	0.0132 ± 0.0001
180	20	3.07	0.0190 ± 0.0001
		2.20	0.0189 ± 0.0002
190	90	3.44	0.0320 ± 0.0002
		2.75	0.0322 ± 0.0002
190	50	3.07	0.0293 ± 0.0002
		2.53	0.0292 ± 0.0002
190	30	3.29	0.0354 ± 0.0002
		4.30	0.0354 ± 0.0002

trap, it is seen from the table that the lower flow rate resulted in a lower mole fraction six times, a higher mole fraction four times, and the identical value the other six times. These random differences certainly do not give any indication that solid carbon dioxide passed through the filter and sublimed as the outlet gas was warmed to room temperature.

The experimental mole fractions have previously been plotted as functions of pressure at constant temperature in Figure 17 and 18. It is also of interest to present these results as functions of temperature at constant pressure, this being given in Figure 19. In this graph the 30, 50, 70, and 90 atmosphere isobars have been omitted for the sake of clarity. Designation of the experimental points has also been neglected, for the same reason.

As defined and discussed in Section II-F, the enhancement factor ϵ is a dimensionless parameter equal to the ratio of the carbon dioxide mole fraction in the gas phase to that which would exist for ideal behavior of the system. In this sense, the parameter ϵ gives an indication of the departure of the system from the ideal behavior defined in II-F. The values for ϵ tabulated in Table X have been computed from the experimental mole fractions given in Table VIII and the vapor pressures listed in Table I. The enhancement factor is also plotted in Figure 20 as a function of pressure at constant temperature.

Examination of the enhancement factors of Table X shows several apparent discrepancies at low pressure, since plots of enchancement factor vs. temperature at constant pressure should yield smooth curves. From such plots, it appears that the 5 atmosphere points at

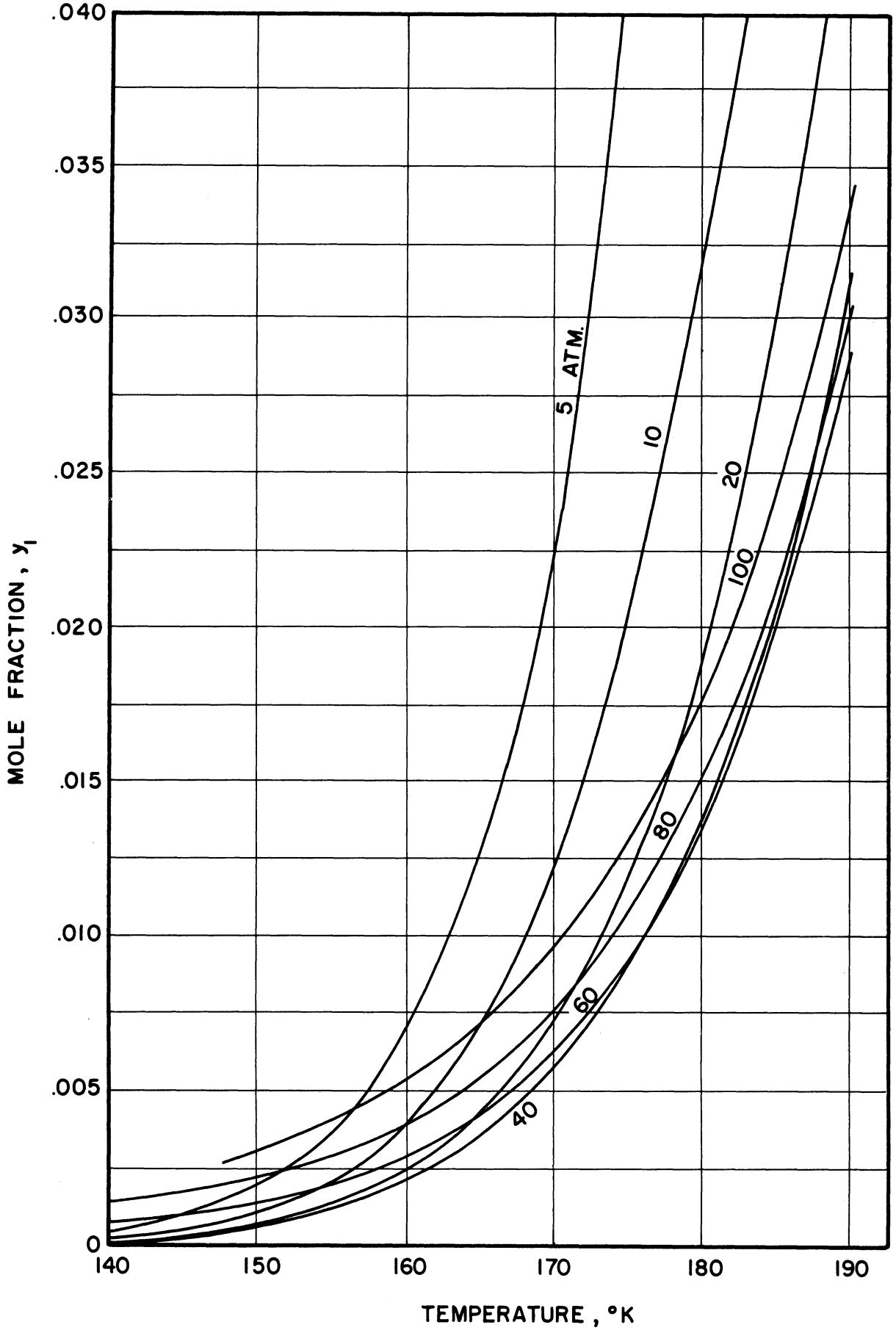

Figure 19. Mole Fraction y_1 vs. Temperature at Constant Pressure

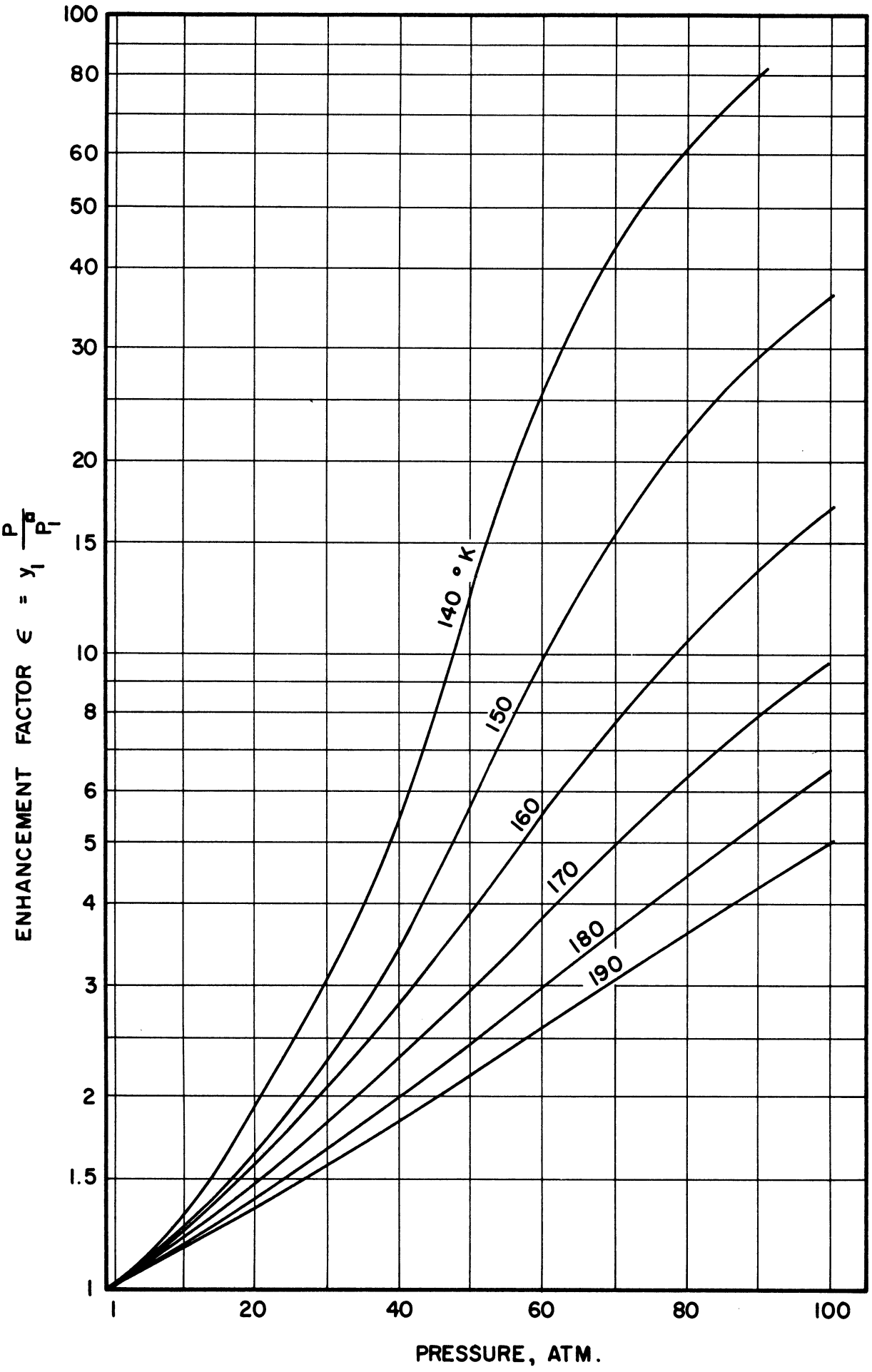

Figure 20. Enhancement Factor ϵ vs. Pressure at Constant Temperature

140 and 160° should be at or near their upper limits, respectively, in order to give a smooth curve. It also seems that the 10 atmosphere points at 140 and 150° should be somewhat larger than the values given in Table VIII, although still within the limits given in the data. The computed values of enhancement factor are very sensitive to small changes in the mole fraction and/or the vapor pressure of carbon dioxide, and the scatter may be due in part to the values used here for the latter.

TABLE X

ENHANCEMENT FACTOR AS A FUNCTION OF TEMPERATURE AND PRESSURE

$$\epsilon = y_1 \frac{P}{P_1^{\square}}$$

Pressure atm	Temperature, °K 140	150	160	170	180	190
5	1.1414	1.1415	1.1131	1.1078	1.0858	-
10	1.3043	1.2723	1.2580	1.2185	1.1861	1.1458
20	1.9565	1.6409	1.5987	1.4804	1.3869	1.3402
30	3.0978	2.2830	2.0732	1.8369	1.6533	1.5641
40	5.4348	3.3769	2.7643	2.3041	2.0000	1.8321
50	11.685	5.5886	3.8694	2.9204	2.4270	2.1576
60	25.435	9.1320	5.3503	3.7341	2.9562	2.5626
70	42.609	14.316	7.4013	4.8288	3.6022	3.0206
80	60.435	21.118	10.013	6.1229	4.3796	3.5700
90	77.283	28.894	13.213	7.7946	5.2883	4.2415
100	-	36.147	17.070	9.7482	6.4234	5.0074

As mentioned earlier in presenting the results, the minimal pressure, that at which the mole fraction of carbon dioxide is a minimum for the given isotherm, is of particular use in the purification of a gas mixture by selective freezing. It is of interest to note

that a plot of this minimal pressure as a function of temperature (Figure 21) shows a fairly smooth curve. The minimal pressure can itself be construed as some function of non-ideal behavior, as no such minimum would exist for ideal behavior. This statement is not meant to imply that the minimal pressure is that at which the system departs from ideal behavior; in fact, it occurs at a much lower pressure. The point to be made is that above the minimal pressure the system is behaving non-ideally to such an extreme degree that the carbon dioxide concentration actually changes in the opposite direction to that predicted for ideal behavior. The term function is referred to above only in the sense that it would be expected that the system should behave more ideally as the temperature increases and becomes progressively farther removed from the critical point of nitrogen. The regular behavior of minimal pressure with temperature confirms this expectation.

The matter of phase determination should also be discussed during the presentation and discussion of the experimental results of this investigation. Inasmuch as it was not possible to view the mixture at the equilibrium point, there may be some conjecture as to a possible phase transformation, especially at high pressure. It would be expected that, for reasonably large initial percentages of carbon dioxide, there would be some pressure at which a transformation from the carbon dioxide solid-gas equilibrium in the presence of gaseous nitrogen would occur, resulting in the introduction of a liquid phase, as mentioned particularly in References 14, 21.

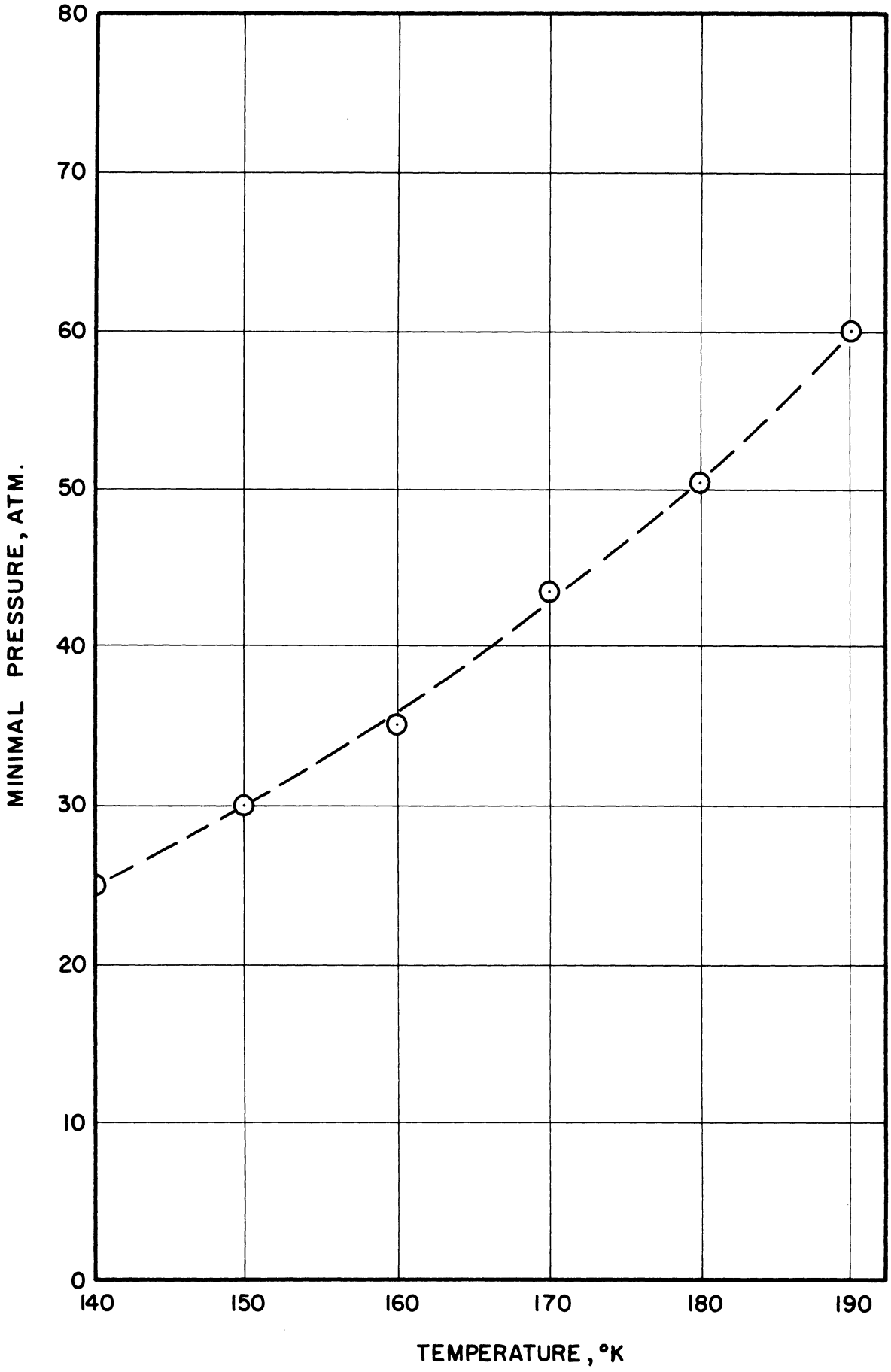

Figure 21. Minimal Pressure vs. Temperature

This transformation never occurred in the present tests, because of the very low initial concentrations of carbon dioxide, which should result in mixture critical temperatures below the range of this investigation. Further, there were no discontinuities of the concentrations as functions of pressure, as might be expected as a result of a change in solubility occurring with such a phase transformation. Finally, there was no indication in the operating characteristics of the system to indicate in any way the presence of liquid in the equilibrium vessel. A further investigation might be worthwhile, in order to determine a more complete phase diagram for different initial concentrations of these components.

As a final point to be made, the data in Appendix D shows that the heat exchanger performance was very disappointing, the equilibrium vessel gas inlet temperature running much higher than had been the intention when the heat exchanger was designed. This can be readily explained in that the flow rates used in the experimental runs were smaller than originally planned by a factor of 5, so that gas Reynolds numbers in the heat exchanger sometimes were as low as 2000. In addition, latent heat from the condensing carbon dioxide also caused performance to deteriorate.

If the heat exchanger had been more effective in cooling the incoming gas, the temperature gradients in the block would have been almost nonexistent, but since these were sufficiently small even with the relatively warm gas, it was not found necessary to redesign this part of the apparatus.

IX. COMPARISON OF PREDICTED AND EXPERIMENTAL RESULTS

A. Numerical Comparisons

In this final section, the experimental results given in Section VIII will be compared with those predicted by the three methods used to solve the theoretical equilibrium equation. As discussed previously in Section IV, there will be two sets of solutions for each of these methods, one arising from the assumptions made to simplify solution of the equations, and the other from solution of the general equations. It is recalled, however, that both solutions are made under the assumption that the solid is pure carbon dioxide and is incompressible.

The first method of solution is that making use of the Beattie-Bridgeman equation of state, an equation fitted empirically to a large set of P-V-T data for a pure substance. The combinations of coefficients to represent a mixture are also empirical, and have been decided upon by comparison with mixture P-V-T data. In applying this equation of state to the system under investigation, there is naturally some question as to how accurately the equation can be expected to represent the mixture, inasmuch as the pure gas constants and mixture combinations have been fitted at much higher temperatures. A more severe problem is that the equation is intended for application below 0.8 times critical density, and the maximum densities reached at 140 and 150°K are of the order of 1.5 times critical, well beyond the range of the equation.

The second method, using a virial equation of state with the Lennard-Jones (6-12) potential and Ewald's revised method of force constant combination for interaction coefficients, is commonly termed theoretical, although the Lennard-Jones potential is itself an empirical representation of the intermolecular force, and the pure-gas force constants have been found from experimental virial coefficients. Some inaccuracy is being introduced in using the Lennard-Jones potential, as carbon dioxide molecules are non-spherical. Also, the force constants have been evaluated from data at temperatures greater than the range being studied here. As before, the most severe problem will be that of the failure of the equation of state at high density, inasmuch as virial coefficients beyond the third could not be included.

The third method of solution, that of Prausnitz, can be classed as that of generalized behavior in that it incorporates the three-parameter theory of corresponding states to predict interaction coefficients. The pure-gas virial constants necessary for solution are those used with the preceding method, having been calculated from the Lennard-Jones potential. In this respect, this method will suffer the same equation of state failure as Ewald's method, since the equation for the mixture reduces to that for pure nitrogen in the case of the simplified solution.

Thus, the three methods of solving the theoretical equations to be compared with the experimental results might properly be termed empirical, theoretical, and generalized behavior, respectively, even

though all are empirical in part. In the discussion to follow, all three will be referred to as predicted, simply as a distinction from results determined directly by experiment.

The results and comparisons are presented in this section in the form of enhancement factors, in order to show a greater numerical contrast between different methods than is seen in the mole fractions. For example, at 140°K and 30 atmospheres:

	y_1	ϵ
Experimental	0.00019	3.0978
General Beattie-Bridgeman	0.00020	3.3284
General Ewald	0.00019	3.1032
General Prausnitz	0.00023	3.7663

Since the simplified and general solutions for each method are very close at the lower temperatures, it has been decided to plot only the three general solutions, and present both the simplified and general solutions in tabular form. The results listed in Table XI and plotted in Figures 22-27 have been calculated on the IBM 704 computer using the procedures given in Appendices B and C. The same program was used for the Ewald and Prausnitz solutions, since the equations to be solved are identical. The differences between the two lie in numerical values of the interaction coefficients, which were read as input data to the machine.

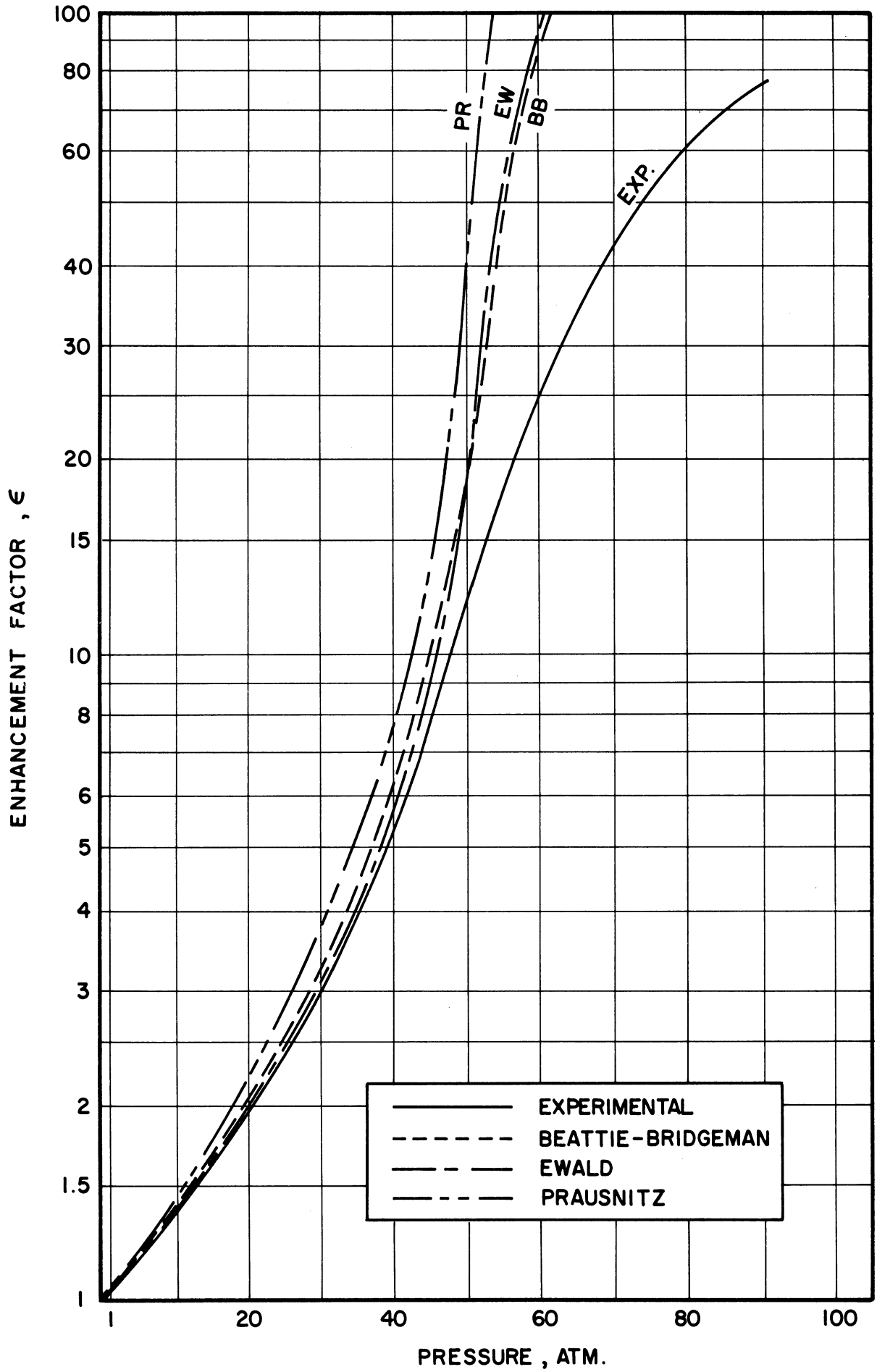

Figure 22. General Solutions at 140°K

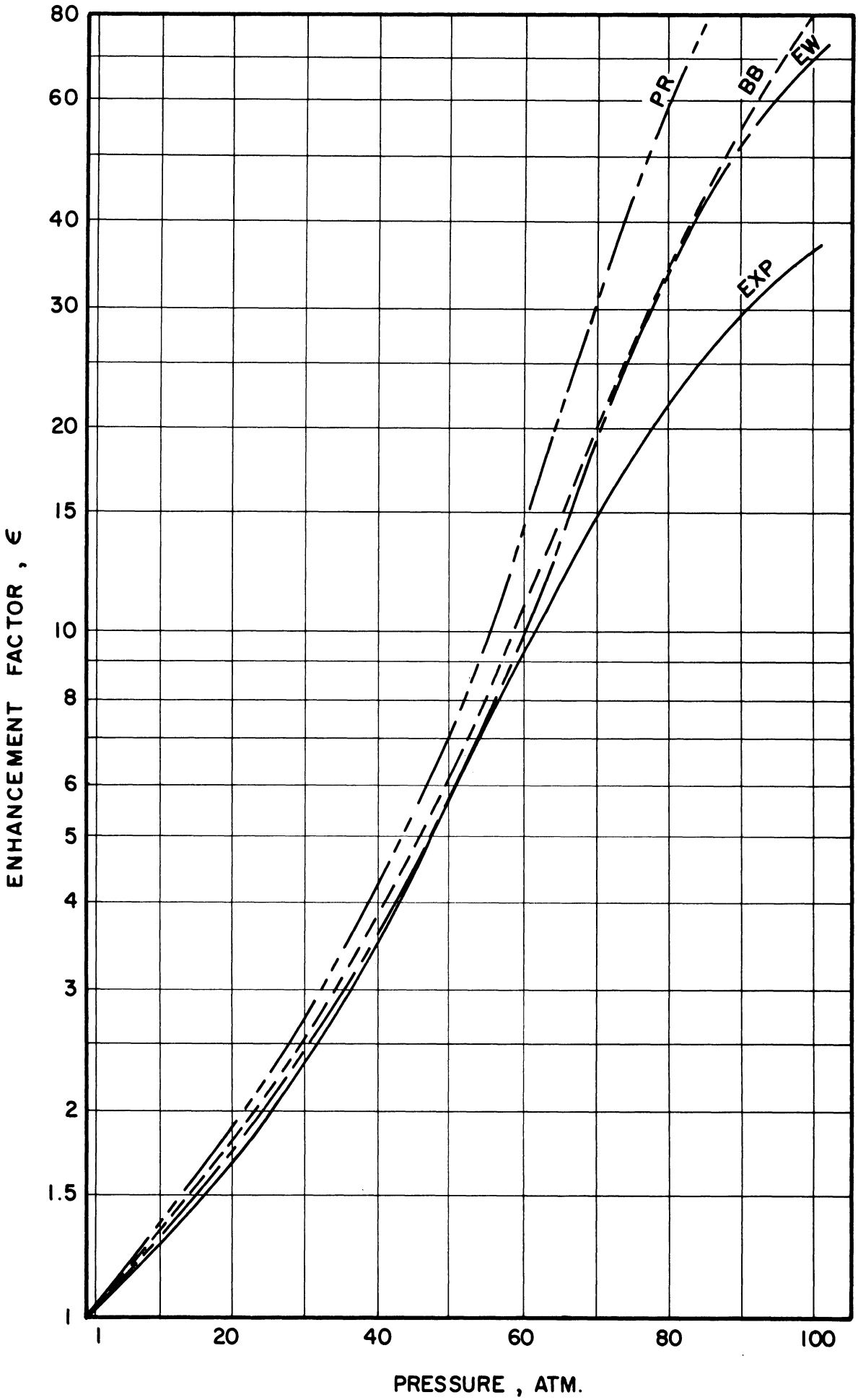

Figure 23. General Solutions at 150°K

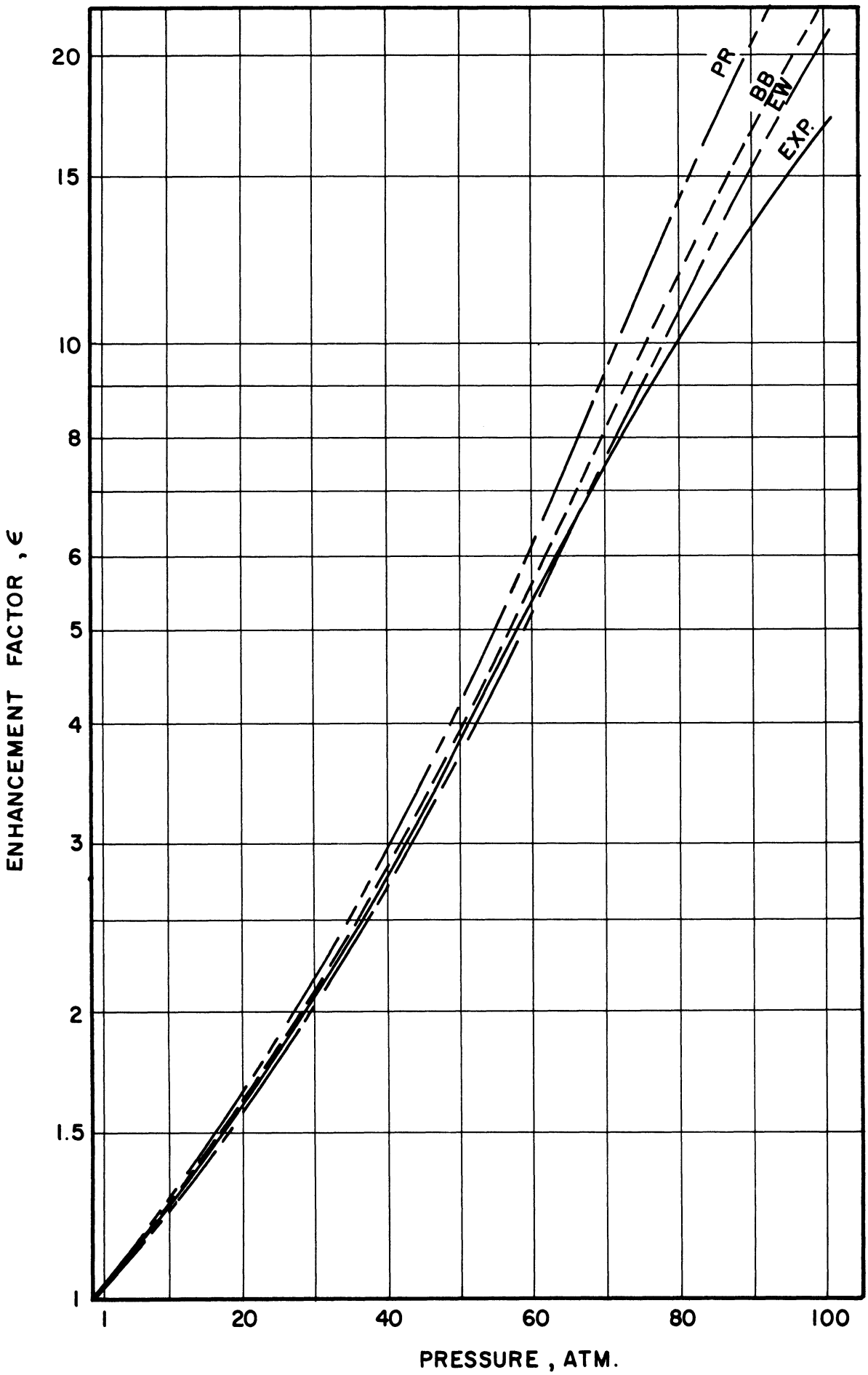

Figure 24. General Solutions at 160°K

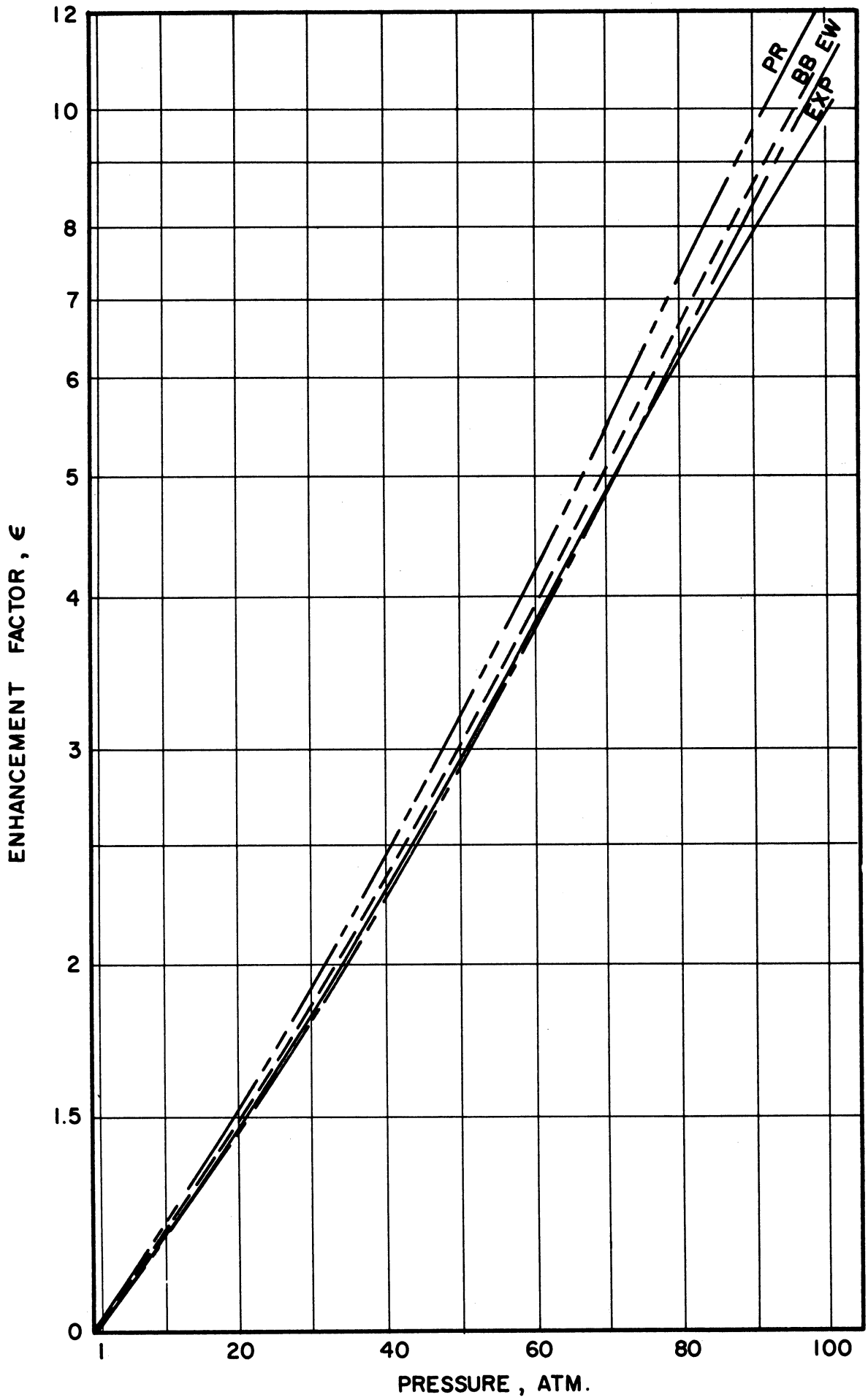

Figure 25. General Solutions at 170°K

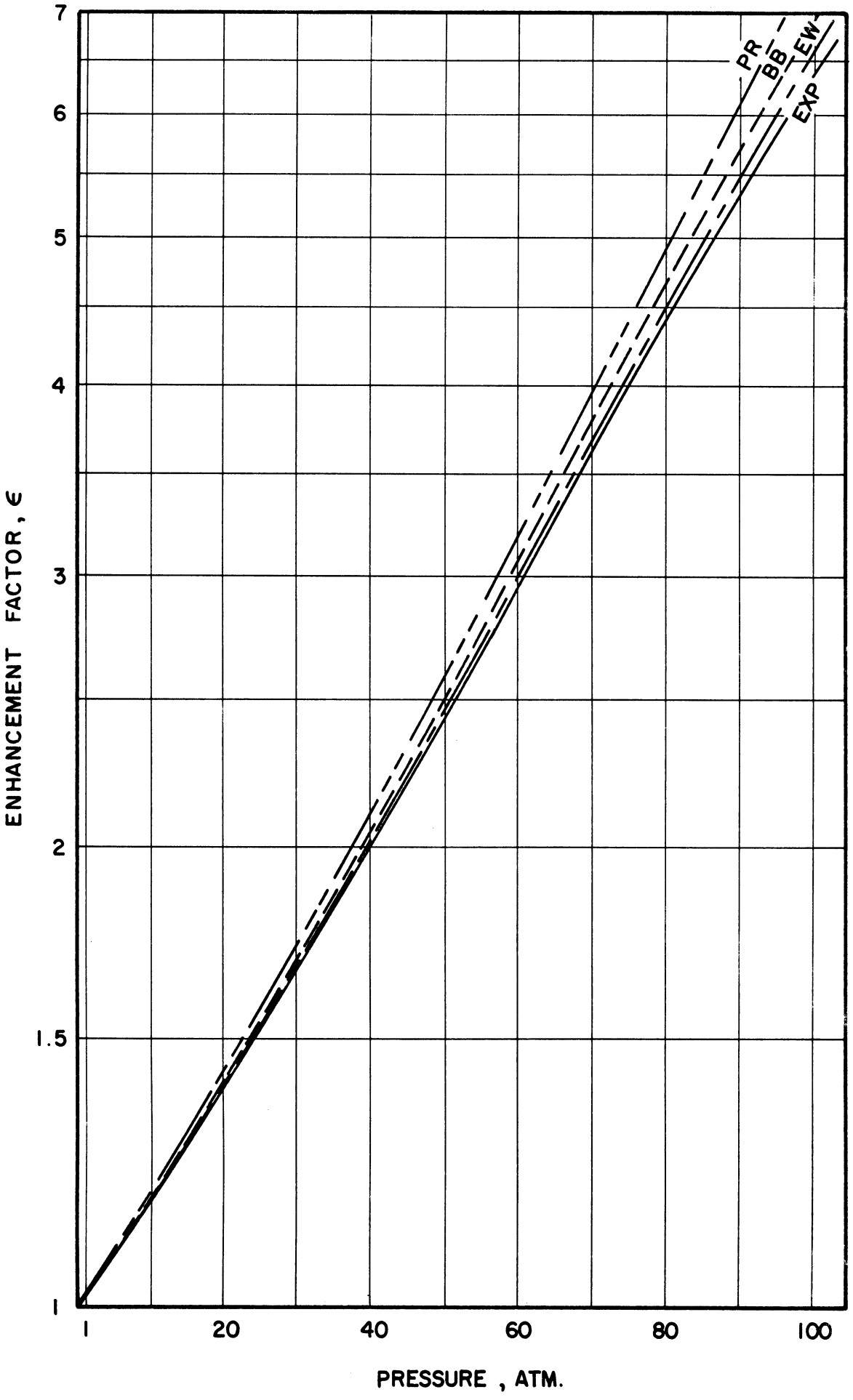

Figure 26. General solutions at 180°K

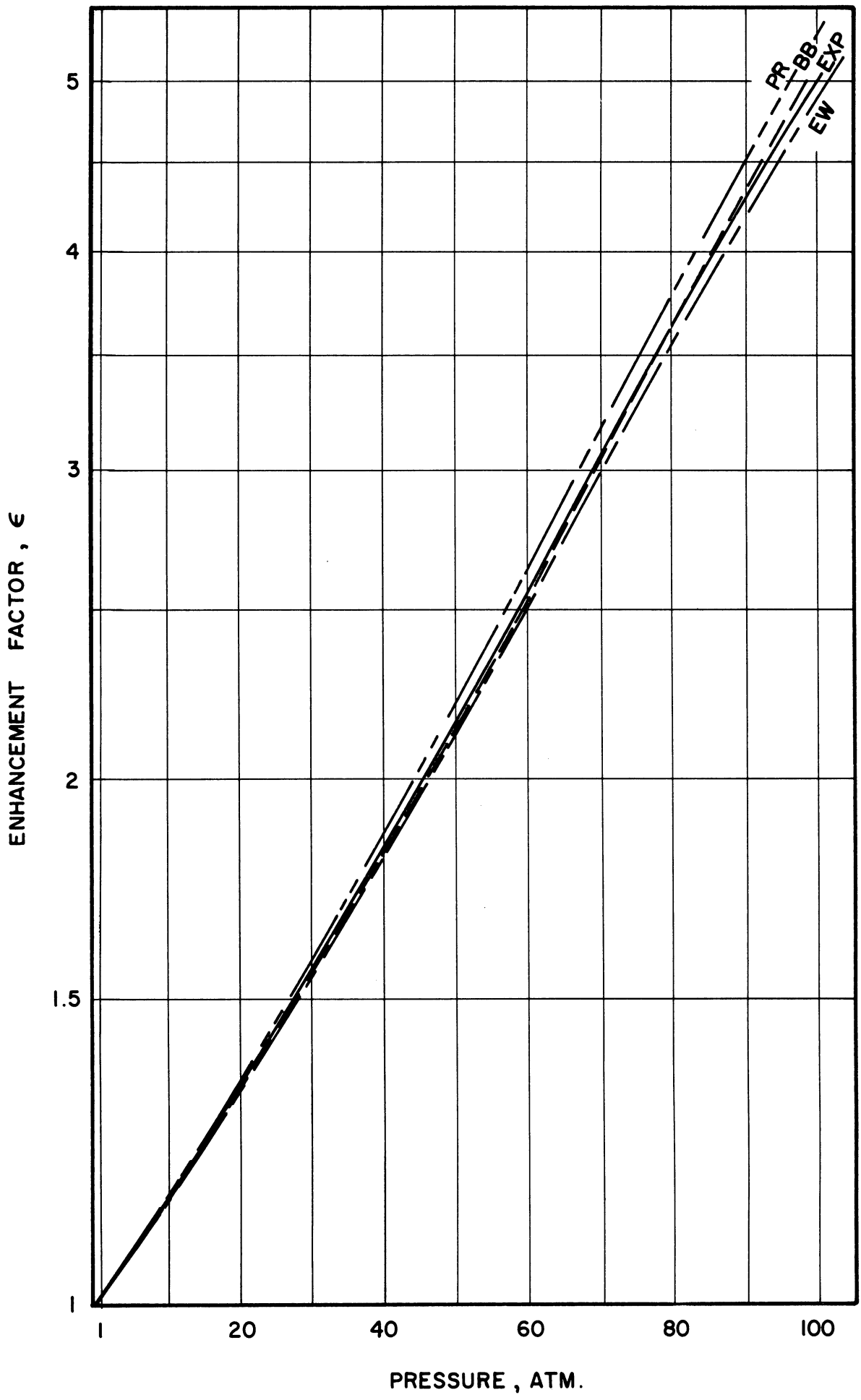

Figure 27. General Solutions at 190°K

TABLE XI

COMPARISON OF PREDICTED AND EXPERIMENTAL RESULTS

Notation:

Experimental Results	EXP
Simplified Beattie-Bridgeman	SBB
Simplified Ewald	SEW
Simplified Prausntiz	SPR
General Beattie-Bridgeman	GBB
General Ewald	GEW
General Prausnitz	GPR

A. Enhancement Factor at 140°K

P(atm)	EXP	SBB	SEW	SPR	GBB	GEW	GPR
5	1.1414	1.1798	1.1713	1.2015	1.1798	1.1713	1.2015
10	1.3043	1.4060	1.3841	1.4591	1.4060	1.3841	1.4591
20	1.9565	2.0777	2.0007	2.2450	2.0777	2.0007	2.2450
30	3.0978	3.3284	3.1032	3.7663	3.3284	3.1032	3.7663
40	5.4348	6.2615	5.5577	7.5452	6.2615	5.5580	7.5452
50	11.685	19.223	19.244	34.397	19.223	19.244	42.730
60	25.435	76.621	82.591	208.71	88.209	92.737	-
70	42.609	151.72	- *	- *	184.73	- *	-
80	60.435	240.78	-	-	310.02	-	-
90	77.283	345.41	-	-	472.83	-	-

*Solution Failed to Converge

B. Enhancement Factor at 150°K

P(atm)	EXP	SBB	SEW	SPR	GBB	GEW	GPR
5	1.1415	1.1459	1.1410	1.1602	1.1455	1.1406	1.1598
10	1.2723	1.3208	1.3085	1.3541	1.3204	1.3081	1.3537
20	1.6409	1.7940	1.7546	1.8862	1.7940	1.7546	1.8862
30	2.2830	2.5310	2.4328	2.7309	2.5310	2.4328	2.7309
40	3.3769	3.7643	3.5388	4.1789	3.7643	3.5388	4.1789
50	5.5886	6.0254	5.5379	6.9574	6.0628	5.5379	7.0120
60	9.1320	10.512	9.6743	13.145	10.703	9.8270	13.532
70	14.316	18.985	18.379	27.292	19.831	19.211	29.996
80	21.118	31.940	31.581	50.275	34.447	33.914	59.724
90	28.894	48.541	46.806	77.976	53.967	51.120	98.856
100	36.147	68.186	63.194	108.63	78.009	69.924	146.99

C. Enhancement Factor at 160°K

P(atm)	EXP	SBB	SEW	SPR	GBB	GEW	GPR
5	1.1131	1.1213	1.1180	1.1313	1.1199	1.1167	1.1298
10	1.2580	1.2607	1.2529	1.2833	1.2595	1.2517	1.2819
20	1.5987	1.6148	1.5914	1.6718	1.6142	1.5906	1.6709
30	2.0732	2.1102	2.0570	2.2199	2.1118	2.0576	2.2212
40	2.7643	2.8235	2.7160	3.0166	2.8311	2.7209	3.0246
50	3.8694	3.8787	3.6780	4.2120	3.9032	3.6950	4.2408
60	5.3503	5.4647	5.1226	6.0578	5.5362	5.1742	6.1504
70	7.4013	7.8216	7.3107	8.9286	8.0162	7.4587	9.2140
80	10.013	11.156	10.503	13.211	11.629	10.884	14.006
90	13.213	15.536	14.755	19.005	16.535	15.576	20.846
100	17.070	20.902	19.870	26.026	22.744	21.333	29.548

D. Enhancement Factor at 170°K

P(atm)	EXP	SBB	SEW	SPR	GBB	GEW	GPR
5	1.1078	1.1037	1.1025	1.1107	1.1001	1.0988	1.1068
10	1.2185	1.2177	1.2149	1.2332	1.2143	1.2114	1.2294
20	1.4804	1.4939	1.4856	1.5309	1.4916	1.4827	1.5279
30	1.8369	1.8536	1.8344	1.9196	1.8541	1.8335	1.9193
40	2.3041	2.3275	2.2896	2.4329	2.3347	2.2937	2.4395
50	2.9204	2.9569	2.8899	3.1175	2.9791	2.9053	3.1405
60	3.7341	3.7938	3.6867	4.0350	3.8480	3.7267	4.0948
70	4.8288	4.8956	4.7422	5.2592	5.0146	4.8336	5.3984
80	6.1229	6.3134	6.1190	6.8626	6.5540	6.3108	7.1615
90	7.7946	8.0778	7.8593	8.8896	8.5266	8.2282	9.4789
100	9.7482	10.193	9.9654	11.333	10.966	10.611	12.390

E. Enhancement Factor at 180°K

P(atm)	EXP	SBB	SEW	SPR	GBB	GEW	GPR
5	1.0858	1.0924	1.0915	1.0969	1.0838	1.0828	1.0876
10	1.1861	1.1875	1.1859	1.1976	1.1792	1.1774	1.1885
20	1.3869	1.4101	1.4057	1.4337	1.4033	1.3980	1.4257
30	1.6533	1.6853	1.6754	1.7257	1.6822	1.6703	1.7210
40	2.0000	2.0270	2.0078	2.0885	2.0318	2.0085	2.0914
50	2.4270	2.4516	2.4187	2.5401	2.4720	2.4310	2.5585
60	2.9562	2.9776	2.9260	3.1012	3.0266	2.9601	3.1496
70	3.6022	3.6232	3.5493	3.7941	3.7226	3.6224	3.8974
80	4.3796	4.4042	4.3067	4.6392	4.5875	4.4457	4.8380
90	5.2883	5.3305	5.2114	5.6505	5.6453	5.4552	6.0058
100	6.4234	6.4050	6.2679	6.8320	6.9142	6.6671	7.4265

F. Enhancement Factor at 190°K

P(atm)	EXP	SBB	SEW	SPR	GBB	GEW	GPR
10	1.1458	1.1688	1.1680	1.1763	1.1504	1.14 1	1.1564
20	1.3402	1.3529	1.3514	1.3707	1.3367	1.3337	1.3522
30	1.5641	1.5719	1.5685	1.6019	1.5605	1.5540	1.5875
40	1.8321	1.8325	1.8254	1.8771	1.8307	1.8178	1.8714
50	2.1576	2.1421	2.1293	2.2040	2.1575	2.1346	2.2150
60	2.5626	2.5080	2.4875	2.5909	2.5527	2.5150	2.6312
70	3.0206	2.9371	2.9075	3.0459	3.0293	2.9712	3.1350
80	3.5700	3.4350	3.3954	3.5758	3.6004	3.5156	3.7429
90	4.2415	4.0049	3.9557	4.1850	4.2788	4.1598	4.4710
100	5.0074	4.6477	4.5900	4.8749	5.0751	4.9126	5.3341

Upon examination of the results, some general trends are observed. Of the three methods used, Ewald's is generally the best, closely followed by that using the Beattie-Bridgeman equation. Values predicted by the Prausnitz method are nearly always high, and not nearly as good as the other two. The simplified solutions are seen to give as good or better results over much of the temperature range below 190°K. For each of the methods, the general solutions lie somewhat below the simplified (in enhancement factor) at low pressures, and then become higher at pressures above the minimal pressure. The equations of state tend to fail at high density in the direction of predicting volumes too small, and the simplifying assumptions seem to exert a damping tendency on the equation, causing predicted mole fractions to be lower for those solutions than for the general case.

In general, at low pressure the Beattie-Bridgeman equation predicts high and the Ewald either between the Beattie-Bridgeman and the experimental or else slightly low. At high pressure, the curves normally line up downward from highest predicted ϵ in the order GPR, SPR, GBB, SBB, GEW, SEW, although sometimes the GEW value is above that of the SBB. The notation used here is that of Table XI. At the lower temperatures, the entire set is above the experimental at high pressure so that for each method the simplified solution is better, since its prediction of ϵ lies below that of the corresponding general solution in every case. As the temperature is increased, the entire set of curves decreases relative to the experimental, and the curves for the different solutions also become closer together. Throughout nearly all of the temperature range, the GEW

or SEW prediction is the closest to the experimental, followed by the SBB and SEW or GEW. At 190°, however, the predicted set has fallen relative to the experimental to such a degree that the GBB gives the best correlation with all other curves except the GPR lying below the experimental. At this temperature, even the SPR, which has always been high, crosses over at 90 atmospheres and dips below the experimental results.

The correlation is in general very good except at 140°, this isotherm meriting special discussion. At this temperature, the Ewald and Beattie-Bridgeman equations prove to be very accurate at up to forty atmospheres, with the former being better throughout. However, the equations of state were not intended for densities greater than this, and consequently the solutions begin to show considerable deviations at fifty atmospheres. At seventy atmospheres, the Beattie-Bridgeman equation fails very badly, and the other two will not even converge to a solution.

This presents the problem as to how much of this gross failure can be attributed to the high-density inaccuracy of the equations of state used, as opposed to failure of the interaction coefficient prediction and assumptions that the solid is pure carbon dioxide and also incompressible. This question can be resolved by eliminating the equation of state entirely as the second relation between the dependent variables y_1 and v, as was done in the majority of the references cited earlier regarding this type of work. It is recalled that at low temperature the mixture equation of state reduces to essentially that for pure nitrogen, so it is possible to simply substitute experimental volumes directly into the integrated form of the equilibrium equation, and make a direct calculation of the

carbon dioxide mole fraction. This has been done with both the form derived using the Beattie-Bridgeman constants (4-86) and also that using the Ewald interaction coefficients (4-106). The resulting empirically calculated enhancement factors at 140°K are

P(atm)	Eq.(4-86)	Eq.(4-106)
60	23.8	19.4
70	45	34.7
80	87	62
90	172	117.5

and the principal failure here is seen to be that due to the equation of state. This is not at all unexpected; in fact, the experimental range was chosen particularly to overextend the equations of state regarding density. It was hoped, however, that these equations would not fail as badly as they did at 140°. The results at 150°, for example, are still reasonable at pressures considerably beyond the range for which the equations are considered accurate, that being roughly fifty atmospheres.

Another prime interest, that of comparing simplified and general solutions, has led to the rather interesting conclusion that the simplifying assumptions do not impair the accuracy of the predictions until the carbon dioxide concentration reaches approximately 2 or 3 percent, which is somewhat higher than might be expected.

The preceding discussion gives some insight into the problems associated with the predictions being made in this investigation. Of the two principal factors, namely the inert-gas equation of state and the method of estimating virial-interaction coefficients, the former seems to be predominant. The Ewald and Prausnitz methods give a direct comparison of the latter, inasmuch as the same virial coefficients were used

for pure nitrogen and carbon dioxide in both cases. While the Prausnitz method is not of the caliber of the others as far as this system is concerned, it must be remembered that this procedure is an attempt to generalize gas mixture behavior, which in addition to being very convenient in calculations, can prove valuable in cases for which the fairly extensive information required by other methods is not known.

The inaccuracies mentioned earlier in this section, such as those resulting from extrapolating the Beattie-Bridgeman constants range, considering carbon dioxide molecules to be spherical, etc., apparently had little effect on the overall accuracy of the results.

B. Concluding Remarks

The correlation of the theoretical results with those determined experimentally was, for the most part, very satisfactory except for 140°, which indicates that a more accurate high-density equation of state will be required to give accurate results in this density range. The author is presently conducting an investigation intended to apply the very accurate Martin-Hou equation to gas mixtures. Once a satisfactory means of coefficient combination has been determined, it is expected that this equation will enable accurate predication of composition over the entire pressure-temperature range of this investigation, including the 140° isotherm.

APPENDIX A

ITERATIVE METHOD

1. Newton Method for One Equation in One Unknown

Consider a function of one variable,

$$F(v) = 0 \tag{A1-1}$$

In order to find the value of v satisfying (A1-1), assume some initial value, say v_1. In general, $F_1(v)$ will be unequal to zero, since v_1 is not the true solution. Then it will be necessary to correct $F_1(v)$ by some amount $\Delta F_1(v)$, in order to equate it to zero. That is,

$$F_1(v) + \Delta F_1(v) = 0 \tag{A1-2}$$

The problem now reduces to that of specifying $\Delta F_1(v)$ in terms of a correction Δv_1 in v which will give a closer approximation to the solution of (A1-1) than did the first trial v_1. This relation can be given by

$$\Delta F_1(v) \approx \left[\frac{dF(v)}{dv}\right]_1 \Delta v_1 = F_1'(v) \cdot \Delta v_1 \tag{A1-3}$$

Now, equating (A1-2) and (A1-3),

$$\Delta v_1 = \frac{-F_1(v)}{F_1'(v)} \tag{A1-4}$$

or, the value v_2 for the next trial is given by

$$v_2 = v_1 - \frac{F_1(v)}{F_1'(v)} \tag{A1-5}$$

In general, for the i-th trial,

$$v_{i+1} = v_i - \frac{F_i(v)}{F'_i(v)} \tag{A1-6}$$

The iterative process is repeated until the error Δv_i is less than the desired amount.

2. The Newton-Raphson Method for Two Equations in Two Unknowns

Consider two non-linear functions in two variables,

$$F_A(y, v) = 0 \tag{A2-1}$$

$$F_B(y, v) = 0 \tag{A2-2}$$

In order to simultaneously solve the above set for y, v, assume some initial values y_1, v_1. Since these values will, in general not satisfy (A2-1), (A2-2), the functions $F_{A_1}(y,v)$ and $F_{B_1}(y,v)$ must be corrected by some amounts to equal zero, or

$$F_{A_1}(y,v) + \Delta F_{A_1}(y,v) = 0 \tag{A2-3}$$

$$F_{B_1}(y,v) + \Delta F_{B_1}(y,v) = 0 \tag{A2-4}$$

Corrections to y_1 and v_1 to give improved values can be related to the function corrections in a manner analogous to that for one equation in one unknown, since the corrections can be expressed as:

$$\Delta F_{A_1}(y,v) \approx \left[\frac{\partial F_A(y,v)}{\partial y}\right]_1 \Delta y_1 + \left[\frac{\partial F_A(y,v)}{\partial v}\right]_1 \Delta v_1 \tag{A2-5}$$

$$\Delta F_{B_1}(y,v) \approx \left[\frac{\partial F_B(y,v)}{\partial y}\right]_1 \Delta y_1 + \left[\frac{\partial F_B(y,v)}{\partial v}\right]_1 \Delta v_1 \tag{A2-6}$$

Substituting (A2-3) into (A2-5) and (A2-4) into (A2-6) results in

$$\left[\frac{\partial F_A(y,v)}{\partial y}\right]_1 \Delta y_1 + \left[\frac{\partial F_A(y,v)}{\partial v}\right]_1 \Delta v_1 = - F_{A_1}(y,v) \tag{A2-7}$$

$$\left[\frac{\partial F_B(y,v)}{\partial y}\right]_1 \Delta y_1 + \left[\frac{\partial F_B(y,v)}{\partial v}\right]_1 \Delta v_1 = - F_{B_1}(y,v) \tag{A2-8}$$

The resulting set of linear correction Equations (A2-7), (A2-8), can be solved simultaneously for the corrections Δy_1, Δv_1, by matrix inversion. Therefore,

$$\Delta y_1 = \frac{Dy_1}{D_1}, \qquad \Delta v_1 = \frac{Dv_1}{D_1} \tag{A2-9}$$

where

$$D_1 = \begin{vmatrix} \left[\frac{\partial F_A(y,v)}{\partial y}\right]_1 & \left[\frac{\partial F_A(y,v)}{\partial v}\right]_1 \\ \left[\frac{\partial F_B(y,v)}{\partial y}\right]_1 & \left[\frac{\partial F_B(y,v)}{\partial v}\right]_1 \end{vmatrix}$$

$$Dy_1 = \begin{vmatrix} - F_{A_1}(y,v) & \left[\frac{\partial F_A(y,v)}{\partial v}\right]_1 \\ - F_{B_1}(y,v) & \left[\frac{\partial F_B(y,v)}{\partial v}\right]_1 \end{vmatrix} \tag{A2-10}$$

$$Dv_1 = \begin{vmatrix} \left[\frac{\partial F_A(y,v)}{\partial y}\right]_1 & - F_{A_1}(y,v) \\ \left[\frac{\partial F_B(y,v)}{\partial y}\right]_1 & - F_{B_1}(y,v) \end{vmatrix}$$

the values y_2, v_2 for the second trial are thus given by

$$\begin{aligned} y_2 &= y_1 + Dy_1/D_1 \\ v_2 &= v_1 + Dv_1/D_1 \end{aligned} \tag{A2-11}$$

In general, for the i-th trial

$$y_{i+1} = y_i + Dy_i/D_i$$
$$v_{i+1} = v_i + Dv_i/D_i \qquad \text{(A2-12)}$$

in which the D's represent the determinants of the i-th trial, as in (A2-10). The iterative procedure is repeated until both of the errors Δy_i, Δv_i, are as small as desired.

This method can be converted quite easily to a logarithmic form if it is found necessary to improve the convergence or preclude the possibility of y or v becoming negative during the course of the solution.

APPENDIX B

FLOW DIAGRAM FOR BEATTIE-BRIDGEMAN EQUATION SOLUTIONS

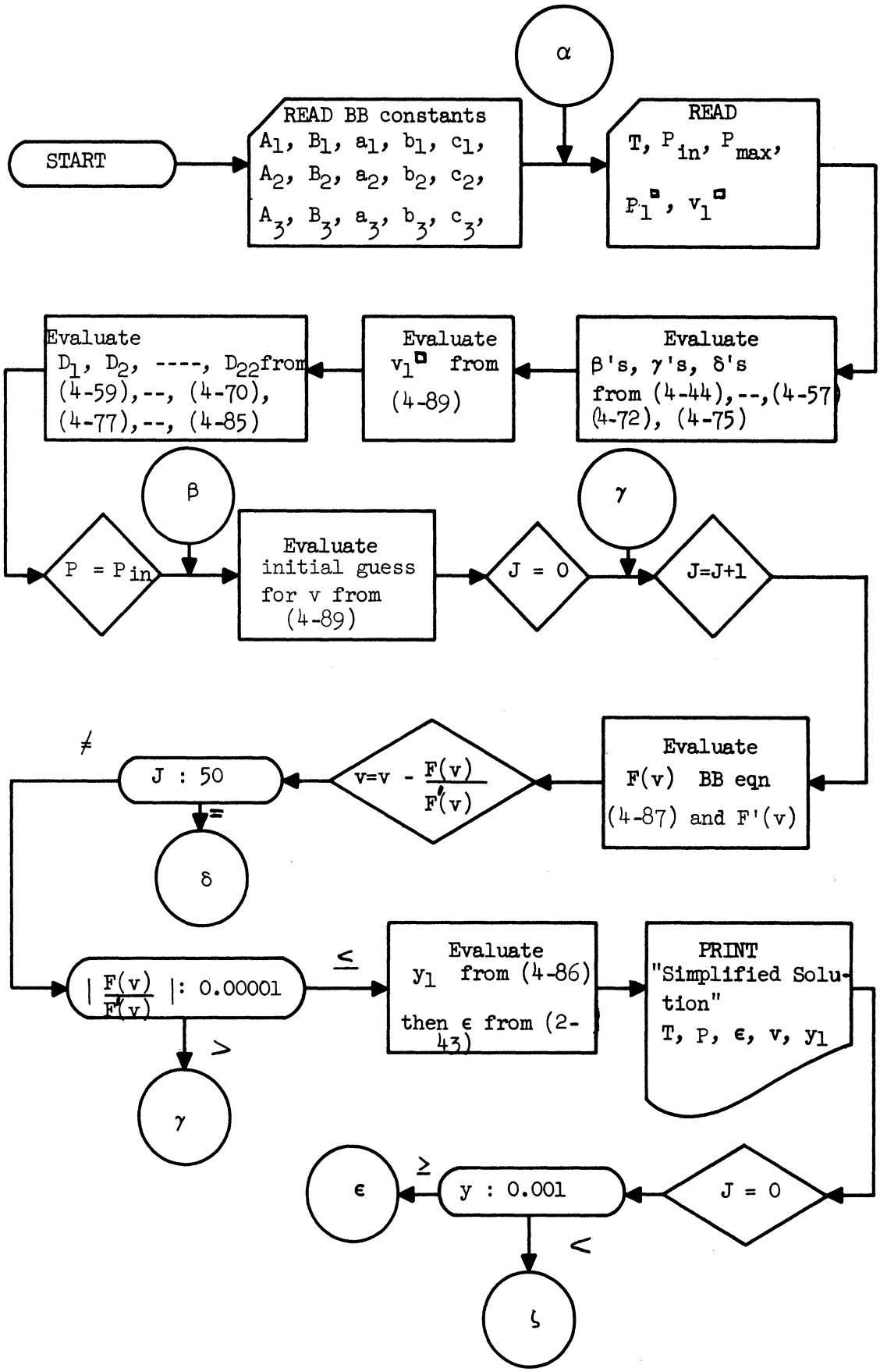

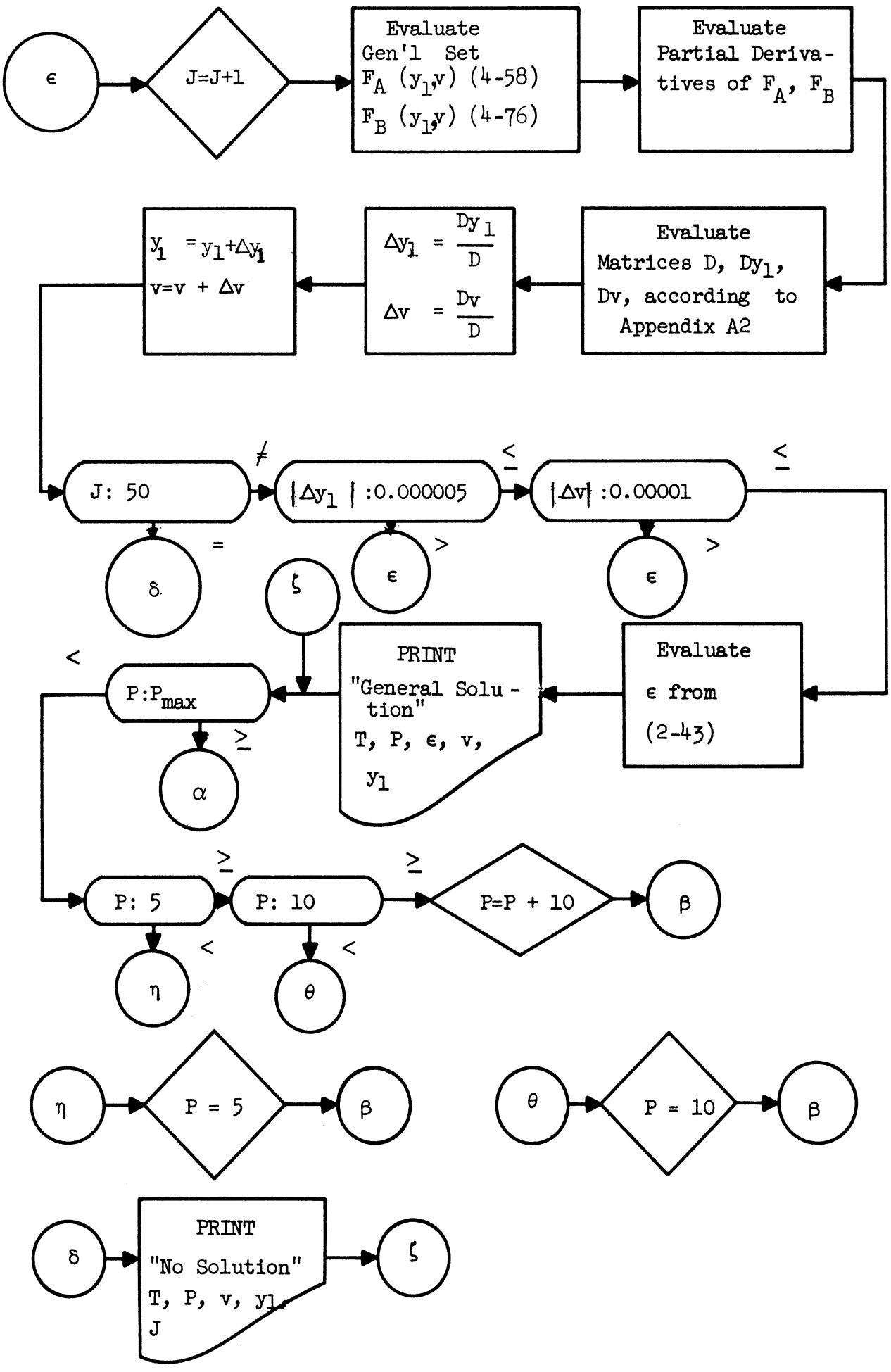
ε
J=J+1
Evaluate Gen'l Set F_A (y_1,v) (4-58) F_B (y_1,v) (4-76)
Evaluate Partial Derivatives of F_A, F_B
Evaluate Matrices D, Dy_1, Dv, according to Appendix A2
$\Delta y_1 = \frac{Dy_1}{D}$
$\Delta v = \frac{Dv}{D}$
$y_1 = y_1 + \Delta y_1$
$v = v + \Delta v$
J: 50
$|\Delta y_1|$:0.000005
$|\Delta v|$:0.00001
≠
≤
≤
=
>
>
δ
ε
ε
ζ
<
P:P_{max}
≥
α
PRINT "General Solution" T, P, ε, v, y_1
Evaluate ε from (2-43)
≥
≥
P: 5
P: 10
P=P + 10
β
<
<
η
θ
η
P = 5
β
θ
P = 10
β
δ
PRINT "No Solution" T, P, v, y_1, J
ζ

APPENDIX C

FLOW DIAGRAM FOR VIRIAL EQUATION SOLUTIONS

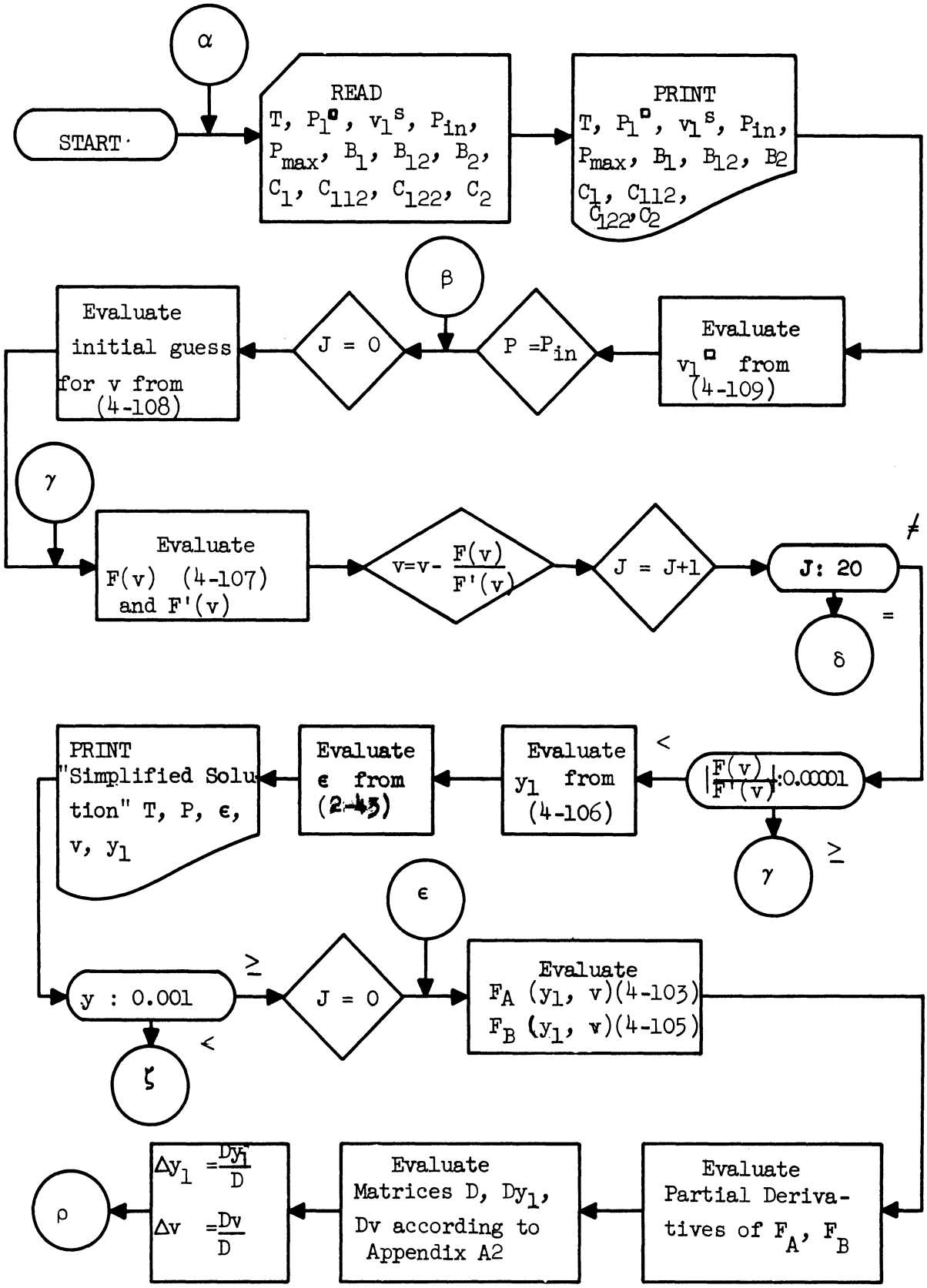

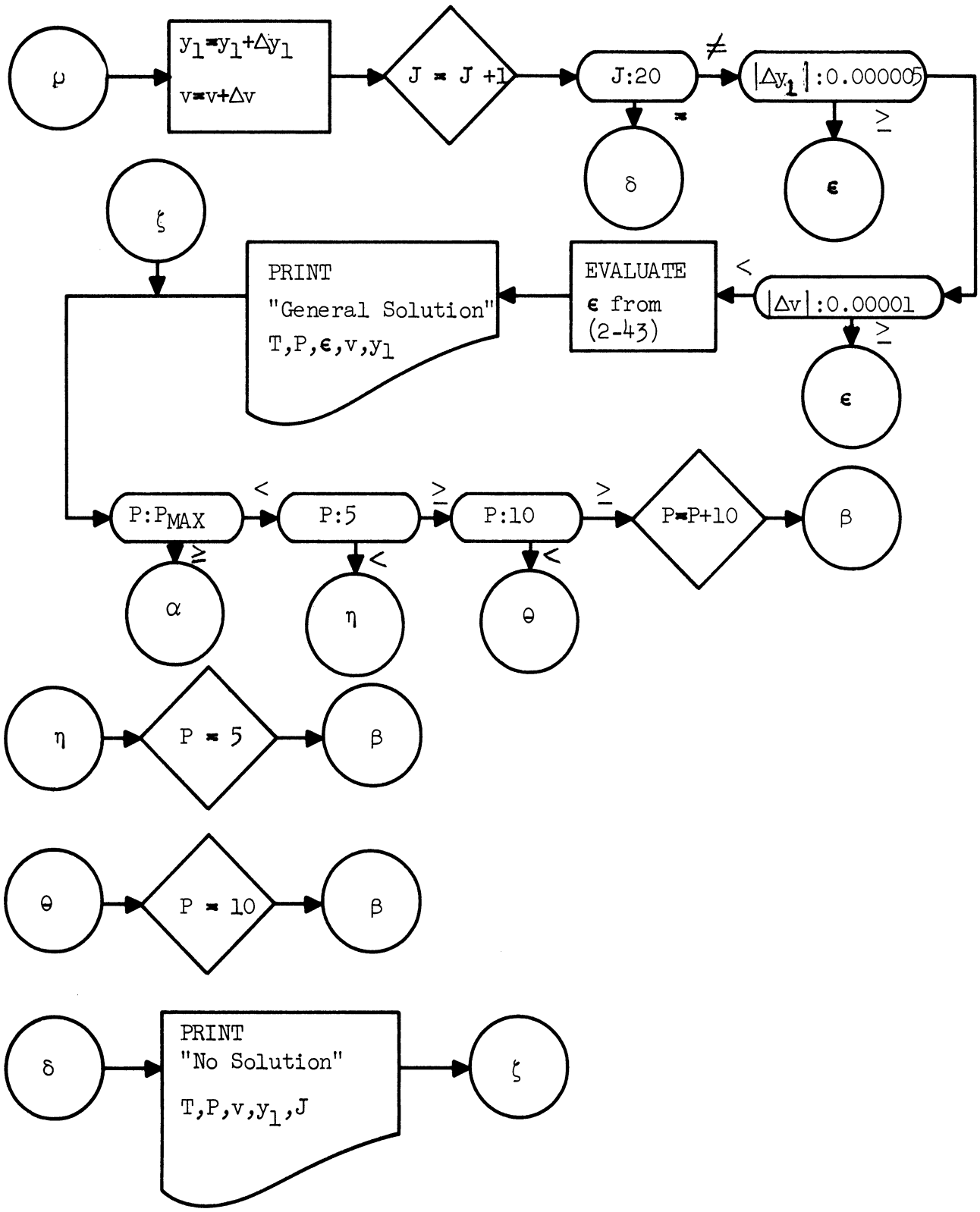
μ
$y_1 = y_1 + \Delta y_1$
$v = v + \Delta v$
J = J + 1
J:20
≠
=
$|\Delta y_1|$:0.000005
≥
δ
ε
ζ
PRINT
"General Solution"
T,P,ε,v,y_1
EVALUATE
ε from
(2-43)
<
$|\Delta v|$:0.00001
≥
ε
P:P_{MAX}
<
P:5
≥
P:10
≥
P=P+10
β
≥
<
<
α
η
θ
η
P = 5
β
θ
P = 10
β
δ
PRINT
"No Solution"
T,P,v,y_1,J
ζ

APPENDIX D

EXPERIMENTAL DATA

The data following is given in the following notation and units:

TIME:	Minutes
NOMT:	Nominal Equilibrium Temperature, °K
NOMP:	Nominal Equilibrium Pressure, ATM
AMBT:	Ambient Temperature, °F
AMBP:	Ambient Pressure, in. HG.
ANAL:	Gas Analyzer Reading, Percent CO_2
ANACC:	Analyzer error Limits, + Percent CO_2
M1:	System Flow Rate, LBM/HR
M2:	Analyzer Flow Rate, SCFH
P1:	Equilibrium Pressure, PSIG
P2:	Pressure Downstream of Throttle, PSIG
P3:	Main Stream Flowmeter Pressure, PSIG
P4:	Analyzer Exit Pressure, PSIG
TC-1:	Equilibrium Gas Temperature, °K
TC-2:	Vessel Inlet Gas Temperature, °K
TC-3:	Block Side Top Temperature, °K
TC-4:	Block Side Middle Temperature, °K
TC-5:	Block Side Bottom Temperature, °K
TC-6:	Block Bottom Corner Temperature, °K
TC-7:	Block Core Temperature, °K
TC-8:	Block Bottom Center Temperature, °K
TC-9:	Inlet Tube Temperature, °K
TC-10:	Outlet Tube Temperature, °K
TC-11:	Outlet Upper Fitting Temperature, °K
TC-12:	Outlet Upper Tube Temperature, °K
TC-13:	Equilibrium Pressure Gage Temperature, °F
TC-14:	Temperature Downstream of Throttle, °F
TC-15:	Main Flowmeter Temperature, °F
TC-16:	Analyzer Exit Temperature, °F

Run	A1	A1	A1	A1	A1	A1	A1	A2
TIME	30	30	30	30	30	30	30	40
NOMT	150	150	150	150	160	160	160	140
NOMP	80	70	60	50	50	60	70	70
AMBT	80	80	80	80	80	80	81	78
AMBP	29.03	29.03	29.03	29.03	29.03	29.03	29.03	28.89
ANAL	0.223	0.172	0.128	0.094	0.243	0.280	0.334	0.112
ANACC	0.002	0.002	0.002	0.002	0.002	0.002	0.002	0.001
M1	0.95	0.900	0.85	0.85	0.85	0.85	0.95	1.05
M2	1.0	1.0	1.0	1.0	1.0	1.0	1.0	1.0
P1	1160	1015	870	720	720	865	1015	1015
P2	1	1	1	1	1	1	1	1
P3	1	1	1	1	1	1	1	1
P4	0.6	0.6	0.6	0.6	0.6	0.6	0.6	0.6
TC-1	150.0	150.0	150.0	150.1	160.0	160.0	160.0	140.1
TC-2	212.1	214.7	216.1	220.2	220.5	222.9	226.0	211.1
TC-3	150.2	150.2	150.1	150.2	160.1	160.2	160.2	140.1
TC-4	150.1	150.1	150.1	150.1	160.1	160.2	160.2	140.1
TC-5	150.1	150.1	150.1	150.1	160.0	160.1	160.0	140.0
TC-6	150.2	150.2	150.1	150.2	160.1	160.2	160.2	140.2
TC-7	150.1	150.1	150.1	150.1	160.1	160.1	160.1	140.2
TC-8	150.0	150.0	150.0	150.0	160.0	160.0	160.0	140.0
TC-9	202.6	203.3	204.3	207.6	208.9	212.3	215.0	198.3
TC-10	151.2	151.0	151.1	151.4	160.9	161.2	161.5	141.0
TC-11	162.2	163.0	160.8	163.3	168.5	171.6	171.6	161.5
TC-12	168.0	169.1	166.2	167.8	171.6	176.3	176.0	171.2
TC-13	81.5	81.5	81.0	81.5	81.5	82.0	82.0	77.5
TC-14	81.5	81.5	82.0	82.0	82.0	82.0	82.0	79.0
TC-15	82.0	82.0	82.0	82.5	82.5	82.5	82.5	81.0
TC-16	81.5	81.5	82.0	82.0	82.0	82.0	82.0	79.0

RUN	A2	A2	A2	A2	A2	A2	A2	A2
TIME	30	30	30	30	30	30	30	30
NOMT	140	140	140	140	140	140	140	140
NOMP	70	60	50	40	30	20	10	5
AMBT	78	78	78	79	79	79	79	79
AMBP	28.89	28.89	28.89	28.89	28.89	28.89	28.89	28.89
ANAL	0.112	0.078	0.043	0.025	0.019	0.018	0.024	0.042
ANACC	0.001	0.001	0.001	0.001	0.001	0.001	0.001	0.001
M1	0.50	0.80	0.72	0.5	0.4	0.2	0.14	0.14
M2	1.0	1.0	1.0	1.0	1.0	1.0	1.0	1.0
P1	1015	870	720	572	426	280	132	59
P2	1	1	1	1	1	1	1	1
P3	1	1	1	1	1	1	1	1
P4	0.6	0.6	0.6	0.6	0.6	0.6	0.6	0.6
TC-1	140.0	140.1	140.0	140.0	140.0	140.0	140.0	140.0
TC-2	215.0	211.3	208.7	209.8	214.0	213.4	215.2	215.7
TC-3	140.1	140.2	140.1	140.1	140.0	140.1	140.0	140.0
TC-4	140.0	140.1	140.1	140.1	140.0	140.0	140.0	140.0
TC-5	140.0	140.0	140.0	140.0	140.0	140.0	140.0	140.0
TC-6	140.2	140.3	140.2	140.2	140.1	140.1	140.1	140.1
TC-7	140.1	140.2	140.1	140.1	140.0	140.1	140.0	140.0
TC-8	140.0	140.0	140.0	140.0	140.0	140.0	140.0	140.0
TC-9	196.8	200.6	195.8	192.6	194.0	186.3	183.9	179.4
TC-10	141.1	141.4	141.0	140.8	141.3	143.3	146.4	150.6
TC-11	159.9	155.2	153.8	156.0	159.4	168.8	177.8	184.8
TC-12	170.0	164.5	157.3	163.0	164.8	177.0	185.5	193.8
TC-13	78.0	78.0	78.5	78.5	78.5	79.0	79.0	79.0
TC-14	79.0	79.0	79.5	79.5	79.5	80.0	80.0	80.0
TC-15	81.0	81.0	81.5	82.0	82.0	82.0	82.0	82.0
TC-16	79.0	79.5	80.0	80.5	80.5	80.5	80.5	80.5

RUN	A3	A3	A3	A3	A3	A3	A4	A4
TIME	35	40	30	30	30	35	30	30
NOMT	150	150	150	150	150	150	160	160
NOMP	40	30	20	10	5	50	40	30
AMBT	78	78	78	78	78	78	80	80
AMBP	28.95	28.95	28.95	28.95	28.95	28.95	28.95	28.95
ANAL	0.071	0.064	0.069	0.107	0.192	0.094	0.217	0.217
ANACC	0.001	0.001	0.001	0.001	0.001	0.001	0.002	0.002
M1	0.4	0.4	0.2	0.14	0.1	0.3	0.5	0.3
M2	1.0	1.0	1.0	1.0	1.0	1.0	1.0	1.0
P1	573	426	280	132	59	720	572	426
P2	1	1	1	1	1	1	1	1
P3	1	1	1	1	1	1	1	1
P4	0.6	0.6	0.6	0.6	0.6	0.6	0.6	0.6
TC-1	150.0	150.0	150.0	150.1	150.0	150.1	160.0	160.0
TC-2	219.7	220.2	215.6	211.5	208.1	220.4	223.5	223.7
TC-3	150.2	150.0	150.0	150.0	150.0	150.0	160.0	160.0
TC-4	150.1	150.0	150.0	150.0	150.0	150.0	160.0	160.0
TC-5	150.0	150.0	150.0	150.0	150.0	150.0	160.0	160.0
TC-6	150.1	150.1	150.1	150.2	150.1	150.2	160.1	160.1
TC-7	150.1	150.1	150.1	150.1	150.0	150.1	160.1	160.1
TC-8	150.0	150.0	150.0	150.0	150.0	150.0	160.0	160.0
TC-9	212.1	203.9	187.3	182.1	177.9	201.2	204.0	204.3
TC-10	151.8	151.2	151.3	152.0	152.5	150.5	160.3	161.4
TC-11	179.6	172.7	176.5	177.0	177.7	170.0	170.2	175.1
TC-12	187.3	176.5	183.3	182.5	183.3	178.7	179.3	179.1
TC-13	78.0	78.5	78.5	78.5	79.0	79.0	80.0	80.0
TC-14	79.0	79.5	79.5	79.5	80.0	80.0	81.0	81.0
TC-15	81.5	82.0	82.0	82.0	82.0	82.0	82.0	82.0
TC-16	79.0	79.5	79.5	79.5	79.5	79.5	81.0	81.0

RUN	A4	A4	A4	A5	A5	A5	B1	B1
TIME	30	30	30	40	70	50	30	35
NOMT	160	160	160	160	150	140	180	180
NOMP	20	10	50	10	10	10	80	70
AMBT	80	80	80	78	78	78	78	78
AMBP	28.95	28.95	28.95	29.01	29.01	29.01	29.31	29.31
ANAL	0.251	0.394	0.243	0.395	0.107	0.023	1.50	1.41
ANACC	0.002	0.002	0.002	0.002	0.002	0.002	0.01	0.01
M1	0.2	0.1	0.6	0.2	0.2	0.2	0.83	0.6
M2	1.0	1.0	1.0	0.5	0.5	0.5	0.75	0.75
P1	279	132	720	132	132	132	1160	1015
P2	1	1	1	1	1	1	1	1
P3	1	1	1	1	1	1	1	1
P4	0.6	0.6	0.6	0.6	0.6	0.6	0.6	0.6
TC-1	160.0	160.1	160.0	160.0	150.0	140.0	180.0	180.0
TC-2	222.8	220.0	222.5	205.7	212.0	210.5	229.9	229.4
TC-3	160.0	160.0	160.1	160.1	150.1	140.1	180.1	180.1
TC-4	160.0	160.0	160.0	160.0	150.0	140.0	180.1	180.1
TC-5	160.0	160.0	160.0	160.0	150.0	140.0	180.0	180.0
TC-6	160.1	160.2	160.1	160.1	150.1	140.1	180.1	180.1
TC-7	160.0	160.1	160.1	160.1	150.0	140.0	180.1	180.1
TC-8	160.0	160.0	160.0	160.0	150.0	140.0	180.0	180.0
TC-9	199.4	191.7	215.2	192.5	196.1	196.8	225.1	224.1
TC-10	162.0	164.4	161.7	168.7	159.0	146.8	181.6	181.2
TC-11	181.6	188.7	179.3	185.8	178.0	177.3	194.6	189.3
TC-12	186.3	194.1	180.6	182.5	177.3	176.6	202.9	196.6
TC-13	80.0	80.0	80.0	77.5	77.5	77.5	77.0	77.0
TC-14	81.0	81.0	81.5	78.0	78.0	78.5	78.0	78.0
TC-15	82.5	82.5	82.5	80.0	80.0	80.5	79.0	79.0
TC-16	81.0	81.0	81.0	78.0	78.5	79.0	79.0	79.0

RUN	B1	B2	B2	B2	B3	B3	B3	B3
TIME	30	30	30	30	35	30	30	30
NOMT	180	160	160	160	170	170	170	170
NOMP	60	90	80	70	80	70	60	50
AMBT	78	79	79	79	79	79	79	79
AMBP	29.31	29.31	29.31	29.31	29.31	29.31	29.31	29.31
ANAL	1.35	0.461	0.393	0.330	0 760	0.685	0.618	0.580
ANACC	0.01	0.003	0.003	0.003	0.005	0.005	0.005	0.005
M1	0.6	1.05	0.95	0.6	0.83	0.83	0.6	0.6
M2	0.75	0.75	0.75	0.75	0.75	0.75	0.75	0.75
P1	865	1310	1160	1015	1160	1015	870	720
P2	1	1	1	1	1	1	1	1
P3	1	1	1	1	1	1	1	1
P4	0.6	0.6	0.6	0.6	0.6	0.6	0.6	0.6
TC-1	180.0	160.0	160.1	160.0	170.0	170.0	170.0	170.0
TC-2	229.2	211.3	221.2	212.8	221.0	223.6	223.7	225.0
TC-3	180.1	160.1	160.1	160.1	170.1	170.1	170.2	170.2
TC-4	180.1	160.1	160.1	160.1	170.1	170.1	170.2	170.1
TC-5	180.0	160.0	160.0	160.0	170.0	170.0	170.0	170.0
TC-6	180.1	160.2	160.2	160.2	170.2	170.1	170.2	170.1
TC-7	180.1	160.1	160.2	160.1	170.1	170.1	170.1	170.1
TC-8	180.0	160.0	160.0	160.0	170.0	170.0	170.0	170.0
TC-9	221.4	203.6	212.9	202.9	212.0	213.3	214.2	215.5
TC-10	181.3	161.3	161.6	160.8	170.7	171.0	171.1	171.4
TC-11	188.4	166.3	172.3	168.6	176.5	177.5	177.7	178.2
TC-12	194.3	173.0	181.2	175.8	182.3	187.7	184.7	184.3
TC-13	77.0	77.0	77.5	79.0	78.0	78.0	78.0	78.0
TC-14	78.5	78.5	78.5	79.0	79.5	79.5	79.5	79.5
TC-15	79.5	79.0	79.5	80.0	80.0	80.0	80.0	80.0
TC-16	79.0	79.0	79.5	79.5	79.5	79.5	80.0	80.0

RUN	B3	B3	B3	B3	B3	B4	B4	B4
TIME	30	30	30	30	40	40	30	35
NOMT	170	170	170	170	160	170	170	180
NOMP	50	40	30	20	5	10	10	50
AMBT	80	80	80	80	80	80	80	80
AMBP	29.37	29.37	29.37	29.37	29.37	29.37	29.37	29.37
ANAL	0.580	0.572	0.608	0.735	0.699	1.21	1.20	1.33
ANACC	0.005	0.005	0.005	0.005	0.005	0.01	0.01	0.01
M1	0.4	0.4	0.3	0.2	0.07	0.1	0.2	0.5
M2	0.75	0.75	6.75	0.75	0.75	0.75	0.75	0.75
P1	720	573	426	280	59	132	132	720
P2	1	1	1	1	1	1	1	1
P3	1	1	1	1	1	1	1	1
P4	0.6	0.6	0.6	0.6	0.6	0.6	0.6	0.6
TC-1	170.1	170.0	170.0	170.0	160.1	170.0	170.0	180.0
TC-2	224.8	224.1	226.6	215.2	216.0	205.8	219.7	225.0
TC-3	170.1	170.1	170.2	170.0	160.2	170.1	170.1	180.0
TC-4	170.1	170.1	170.1	170.0	160.2	170.1	170.1	180.0
TC-5	170.0	170.0	170.0	170.0	160.0	170.0	170.0	180.0
TC-6	170.2	170.1	170.1	170.2	160.2	170.1	170.1	180.2
TC-7	170.2	170.1	170.1	170.1	160.1	170.0	170.0	180.1
TC-8	170.0	170.0	170.0	170.0	160.0	170.0	170.0	180.0
TC-9	221.7	215.2	210.5	199.3	191.2	188.6	200.8	220.2
TC-10	171.5	171.4	171.7	171.3	164.0	172.3	172.7	181.2
TC-11	184.7	180.0	179.6	180.8	176.3	180.8	185.3	189.3
TC-12	186.2	182.7	183.3	181.2	181.7	203.3	195.3	193.7
TC-13	79.0	79.0	79.0	79.0	79.0	79.0	79.0	79.0
TC-14	80.5	80.5	81.0	81.0	81.0	80.0	80.5	80.5
TC-15	81.5	81.5	82.0	82.0	82.0	82.0	82.0	82.0
TC-16	80.0	80.0	80.5	80.5	80.5	81.0	81.0	81.0

RUN	B4	B4	B4	B4	B5	B5	B6	B6
TIME	30	30	30	30	50	40	50	40
NOMT	180	180	180	180	180	180	170	170
NOMP	50	40	30	20	100	90	100	90
AMBT	80	80	80	80	81	81	81	81
AMBP	29.37	29.37	29.37	29.37	29.39	29.39	29.39	29.39
ANAL	1.32	1.37	1.51	1.90	1.76	1.61	0.968	0.860
ANACC	0.01	0.01	0.01	0.01	0.01	0.01	0.007	0.007
M1	0.2	0.4	0.3	0.2	0.95	0.83	1.05	0.95
M2	0.75	0.75	0.75	0.75	0.75	0.75	0.75	0.75
P1	720	573	426	279	1460	1310	1460	1310
P2	1	1	1	1	1	1	1	1
P3	1	1	1	1	1	1	1	1
P4	0.6	0.6	0.6	0.6	0.6	0.6	0.6	0.6
TC-1	180.0	180.1	180.0	180.0	180.1	180.0	170.0	170.0
TC-2	223.4	224.7	223.9	225.4	225.4	224.6	225.7	225.0
TC-3	180.0	180.2	180.1	180.1	180.2	180.1	170.2	170.1
TC-4	180.0	180.2	180.1	180.1	180.2	180.1	170.2	170.1
TC-5	180.0	180.0	180.0	180.0	180.0	180.0	170.0	170.0
TC-6	180.0	180.2	180.1	180.1	180.2	180.1	170.1	170.1
TC-7	180.0	180.1	180.1	180.0	180.1	180.1	170.1	170.1
TC-8	180.0	180.0	180.0	180.0	180.0	180.0	170.0	170.0
TC-9	216.3	219.2	213.4	211.6	221.5	221.3	217.7	212.9
TC-10	180.8	181.3	180.7	181.4	181.3	180.9	171.1	171.4
TC-11	190.0	189.2	186.8	188.0	187.8	186.7	178.6	179.5
TC-12	197.7	193.3	188.0	195.6	194.7	193.4	187.0	189.2
TC-13	79.0	79.0	79.5	79.5	79.5	79.5	81.0	81.0
TC-14	80.5	81.0	81.0	81.0	81.0	81.0	81.5	81.5
TC-15	82.0	82.0	82.0	81.5	82.0	82.0	82.5	83.0
TC-16	81.0	81.0	81.0	81.5	80.5	80.5	81.0	81.5

RUN	B6	B7	A6	A6	A6	A7	A7	C1
TIME	50	45	50	30	30	45	30	30
NOMT	160	160	150	150	150	140	140	190
NOMP	90	100	100	90	80	90	80	100
AMBT	81	79	79	79	79	79	79	78
AMBP	29.39	28.97	28.97	28.97	28.97	28.97	28.97	28.65
ANAL	0.460	0.536	0.304	0.270	0.221	0.158	0.139	3.40
ANACC	0.007	0.003	0.002	0.002	0.002	0.001	0.001	0.02
M1	0.6	1.05	1.05	1.05	1.05	1.15	1.05	0.83
M2	0.75	0.75	0.75	0.75	0.75	0.75	0.75	0.5
P1	1310	1455	1455	1310	1160	1310	1160	1460
P2	1	1	1	1	1	1	1	1
P3	1	1	1	1	1	1	1	1
P4	0.6	0.6	0.6	0.6	0.6	0.6	0.6	0.6
TC-1	160.0	160.1	150.1	150.1	150.0	140.0	140.1	190.0
TC-2	220.4	224.8	216.7	214.0	214.3	206.1	206.4	245.0
TC-3	160.2	160.2	150.2	150.1	150.2	140.1	140.2	190.0
TC-4	160.2	160.2	150.1	150.1	150.1	140.0	140.2	190.0
TC-5	160.0	160.0	150.0	150.0	150.0	140.0	140.0	190.0
TC-6	160.2	160.1	150.2	150.2	150.2	140.2	140.2	190.1
TC-7	160.1	160.2	150.2	150.1	150.1	140.1	140.1	190.0
TC-8	160.0	160.0	150.0	150.0	150.0	140.0	140.0	190.0
TC-9	211.3	220.5	207.5	205.8	205.5	197.9	197.4	234.3
TC-10	161.4	161.9	151.8	151.9	152.0	143.0	142.7	191.0
TC-11	173.3	173.0	165.2	162.2	162.5	154.7	154.3	200.5
TC-12	182.2	182.8	174.9	170.5	169.8	163.3	163.1	210.3
TC-13	81.0	78.0	77.5	78.0	78.0	78.0	78.0	77.0
TC-14	82.0	79.0	78.0	78.0	78.5	78.0	78.5	78.5
TC-15	83.0	80.0	79.0	79.0	79.0	79.5	79.5	80.0
TC-16	81.5	79.0	79.0	79.0	79.0	79.0	79.0	78.5

RUN	C1	C1	C1	C1	C1	C1	C1	C1
TIME	45	35	30	45	30	30	40	30
NOMT	190	190	190	190	190	190	190	190
NOMP	90	80	90	70	60	50	50	40
AMBT	78	78	79	79	79	79	77	77
AMBP	28.65	28.65	28.65	28.65	28.65	28.65	28.82	28.82
ANAL	3.22	3.03	3.20	2.93	2.90	2.93	2.92	3.11
ANACC	0.02	0.02	0.02	0.02	0.02	0.02	0.02	0.02
M1	0.83	0.83	1.05	0.6	0.6	0.5	0.4	0.4
M2	0.5	0.5	0.5	0.5	0.5	0.5	0.5	0.5
P1	1310	1160	1310	1015	865	720	720	573
P2	1	1	1	1	1	1	1	1
P3	1	1	1	1	1	1	1	1
P4	0.6	0.6	0.6	0.6	0.6	0.6	0.6	0.6
TC-1	190.0	190.0	190.0	190.0	190.0	190.0	190.1	190.0
TC-2	245.2	242.6	245.3	244.8	244.2	246.0	248.4	249.3
TC-3	190.2	190.2	190.1	190.1	190.0	190.2	190.1	190.2
TC-4	190.2	190.2	190.1	190.1	190.0	190.1	190.1	190.1
TC-5	190.0	190.0	190.0	190.0	190.0	190.0	190.0	190.0
TC-6	190.1	190.1	190.1	190.0	190.0	190.0	190.2	190.1
TC-7	190.0	190.1	190.1	190.1	190.0	190.0	190.1	190.1
TC-8	190.0	190.0	190.0	190.0	190.0	190.0	190.0	190.0
TC-9	235.5	232.5	235.9	236.3	236.6	236.7	233.2	237.0
TC-10	191.4	191.2	191.6	191.4	191.6	192.0	191.3	192.3
TC-11	202.0	199.7	199.4	202.0	202.4	204.0	205.3	209.2
TC-12	209.7	205.7	206.4	210.1	210.5	212.1	215.7	223.5
TC-13	78.0	78.0	78.0	78.5	78.0	78.0	76.0	76.0
TC-14	79.0	79.0	78.5	78.5	79.0	78.5	77.0	77.0
TC-15	80.0	80.0	80.0	80.0	79.5	79.5	77.0	77.5
TC-16	79.0	79.0	79.0	79.0	79.0	79.0	77.0	77.0

RUN	C1	C1	C1	C1	C1	C2	C2	C2
TIME	35	30	30	40	35	30	30	30
NOMT	190	190	180	180	170	180	190	190
NOMP	30	30	20	10	5	5	20	10
AMBT	77	77	77	77	77	78	78	78
AMBP	28.82	28.82	28.82	28.82	28.82	28.87	28.87	28.87
ANAL	3.54	3.54	1.89	3.25	2.20	5.95	4.55	7.78
ANACC	0.02	0.02	0.02	0.02	0.02	0.04	0.04	0.04
M1	0.3	0.4	0.14	0.1	0.07	0.07	0.2	0.1
M2	0.5	0.5	0.5	0.5	0.5	0.5	0.5	0.5
P1	426	426	279	132	59	59	279	132
P2	1	1	1	1	1	1	1	1
P3	1	1	1	1	1	1	1	1
P4	0.6	0.6	0.6	0.6	0.6	0.6	0.6	0.6
TC-1	190.0	190.1	180.0	180.0	170.0	180.0	190.0	190.0
TC-2	248.9	248.6	233.7	227.8	220.1	227.3	227.5	228.9
TC-3	190.2	190.2	180.1	180.2	170.1	180.1	190.0	190.1
TC-4	190.1	190.1	180.1	180.1	170.1	180.1	190.0	190.1
TC-5	190.0	190.0	180.0	180.0	170.0	180.0	190.0	190.0
TC-6	190.1	190.2	180.1	180.1	170.1	180.1	190.0	190.0
TC-7	190.0	190.1	180.0	180.0	170.0	180.0	190.0	190.0
TC-8	190.0	190.0	180.0	180.0	170.0	180.0	190.0	190.0
TC-9	232.7	233.5	213.8	203.9	196.4	204.3	213.2	214.3
TC-10	192.0	192.0	182.2	183.0	174.1	184.9	191.4	192.9
TC-11	209.2	205.5	195.3	199.4	196.2	207.2	205.7	205.9
TC-12	215.9	208.4	199.6	209.0	202.9	217.3	210.3	219.5
TC-13	76.0	76.0	77.0	77.5	77.5	77.0	77.0	77.0
TC-14	77.0	77.0	78.0	78.5	78.5	77.5	77.5	77.5
TC-15	77.5	78.0	79.0	79.0	79.0	78.5	78.5	78.5
TC-16	77.0	77.0	77.5	78.0	78.0	78.0	78.0	78.0

BIBLIOGRAPHY

1. Hannay, J. B. and Hogarth, J. Proc. Roy. Soc. (London), 30, (1880) 178.

2. Pollitzer, F. and Strebel, E. Z. Physik. Chem., 110, (1924) 768.

3. Bartlett, E. P. J. Am. Chem. Soc., 49, (1927) 65.

4. Braune, H. and Strassmann, F. Z. Physik. Chem., 143, (1929) 225.

5. Saddington, A. W. and Krase, N. W. J. Am. Chem. Soc., 56, (1934) 353.

6. Perkins, A. J. J. Chem. Phys., 5, (1937) 180.

7. Kritchevsky, I. R. and Koroleva, M. Acta Physicochim., 15, (1941) 327.

8. Wiebe, R. and Gaddy, V. L. J. Am. Chem. Soc., 63, (1941) 475.

9. Kritchevsky, I. R. and Gamburg, D. Acta Physicochim., 16, (1942) 362.

10. Gratch, S. Project G-9A, University of Pennsylvania Thermodynamics Research Laboratory (1945-6).

11. Diepen, G. A. M. and Scheffer, F. E. C. J. Am. Chem. Soc., 70, (1948) 4085.

12. Ipatev, V. V., Teodorovitch, V. P., Brestkin, A. P. and Artemovitch, V. S. J. Chem. Phys. URSS, 22 (1948) 833.

13. Webster, T. J. J. Soc. Chem. Ind. (London), 69, (1950) 343.

14. Webster, T. J. Proc. Roy. Soc. (London), A214, (1952) 61.

15. Dokoupil, Z., Van Soest, G. and Swenker, M. D. P. Communications from the Physical Laboratories, Leiden University, No. 297 (1955).

16. Ewald, A. H. Trans. Far. Soc., 51, (1955) 347.

17. Poettman, F. H. and Katz, D. L. Ind. and Eng. Chem., 37, (1945) 847.

18. Clark, A. M. and Din, F. Trans. Far. Soc., 46, (1950) 901.

19. Haselden, G. G., Newett, D. M. and Shah, S. M. Proc. Roy. Soc. (London), A209, (1951) 1.

20. Bierlein, J. A. and Kay, W. B. Ind. and Eng. Chem., 45, (1953) 618.

21. Donnelly, H. G. and Katz, D. L. Ind. and Eng. Chem., 46, (1954) 511.

22. Sobocinski, D. P. and Kurata, F. AICh.E. Jour., 5(4), (1959) 545.

23. Thiel, A. and Schulte, E. Z. Physik. Chem., 96, (1920) 328.

24. Quinn, E. L. and Jones, C. L. Carbon Dioxide. Reinhold Publishing Corporation, 1936.

25. Francis, A. W. J. Phys. Chem., 58, (1954) 1099.

26. Ishkin, I. P. and Burbo, P. Z. J. Phys. Chem. (USSR), 13, (1939) 1337.

27. Fedorova, M. F. J. Phys. Chem. (USSR), 14, (1940) 422.

28. Abdulaev, Y. A. J. Phys. Chem. (USSR), 13, (1939) 986.

29. Mills, J. R. and Miller, F. J. L. Can. Chem. Proc. Inds., 29, (1945) 651.

30. Robin, S. and Vodar, B. Disc. Far. Soc., 15, (1953) 233.

31. Webster, T. J. Disc. Far. Soc., 15, (1953) 243.

32. Ewald, A. H., Jepson, W. B. and Rowlinson, J. S. Disc. Far. Soc., 15, (1953) 238.

33. Prausnitz, J. M. AICh.E. Jour., 5(1), (1959) 3.

34. Ziegler, W. T. "Calculation of Solid-Gas and Liquid-Gas Phase Equilibria in Binary Systems," Georgia Institute Technology, August 1959.

35. Beattie, J. A. and Stockmayer, W. H. Phys. Soc. Rept. Prog. Phys., 7, (1940) 195.

36. Beattie, J. A. and Bridgeman, O. C. J. Am. Chem. Soc., 49, (1927) 1665.

37. Beattie, J. A. and Bridgeman, O. C. J. Am. Chem. Soc., 50, (1928) 3133.

38. Beattie, J. A. and Bridgeman, O. C. Proc. Amer. Acad. Arts and Science, 63, (1928) 229.

39. Gillespie, L. J. Phys. Rev., 34, (1929) 1605.

40. Beattie, J. A. and Ikehara, S. Proc. Amer. Acad. Arts and Science, 64, (1930) 127.

41. Gillespie, L. J. Chem. Rev., 29, (1941) 525.

42. Beattie, J. A. Chem. Rev., 44, (1949) 141.

43. Smith, G. E. and Sonntag, R. E. University of Michigan (unpublished), 1960.

44. Haney, R. E. D. and Bliss, H. Ind. and Eng. Chem., 36, (1944) 985.

45. Kritchevsky, I. R. and Markov, V. P. Acta Physicochim., 12, (1940) 59.

46. Michels, A. and Boerboom, A. J. H. Bull. Soc. Chim. Belges., 62, (1953) 119.

47. Zaalishvili, S. D. Uspekhi Khim., 24, (1955) 759.

48. Gillespie, L. J. Phys. Rev., 34, (1929) 352.

49. Gerry, H. T. and Gillespie, L. J. Phys. Rev., 40, (1932) 269.

50. Gillespie, L. J. Chem. Rev., 18, (1936) 359.

51. Onnes, H. K. Commun. No. 71, Leiden University, 1901.

52. de Boer, J. Rept. Prog. Phys., 12, (1949) 305.

53. Hirschfelder, J. O., Curtiss, C. F. and Bird, R. B. Molecular Theory of Gases and Liquids, New York: John Wiley and Sons, Inc., 1954.

54. Lennard-Jones, J. E. Proc. Roy. Soc., A106, (1924) 463.

55. Kennard, E. H. Kinetic Theory of Gases, New York: McGraw-Hill Book Co., Inc., 1938.

56. Hirschfelder, J. O., Bird, R. B. and Spotz, E. L. Trans. ASME, 71, (1949) 921.

57. Kihara, T. J. Phys. Soc. Japan, 3, (1948) 265.

58. Kihara, T. J. Phys. Soc. Japan, 6, (1951) 184.

59. Bird, R. B., Spotz, E. L. and Hirschfelder, J. O. J. Chem. Phys., 18, (1950) 1395.

60. Michels, A., Wouters, H. and deBoer, J. Physica, 1, (1934) 587.

61. Michels, A. and Michels, C. Proc. Roy. Soc. (London), A153, (1936) 201.

62. Gratch, S. Trans. ASME, 70, (1948) 631.

63. Claitor, L. C. and Crawford, D. B. Trans. ASME, 71, (1949) 885.

64. MacCormack, K. E. and Schneider, W. G. J. Chem. Phys., 18, (1950) 1269.

65. Pfefferle, W. C., Joff, J. A. and Miller, J. G. J. Chem. Phys., 23, (1955) 509.

66. Mayer, J. E. J. Phys. Chem., 43, (1939) 71.

67. Lennard-Jones, J. E. Proc. Roy. Soc. (London), A115, (1927) 334.

68. Beattie, J. A. and Stockmayer, W. H. J. Chem. Phys., 10, (1942) 473.

69. Lunbeck, R. J. and Boerboom, A. J. H. Physica, 17, (1951) 76.

70. Rowlinson, J. S., Sumner, F. H. and Sutton, J. R. Trans. Far. Soc., 50, (1954) 1.

71. Guggenheim, E. A. and McGlasham, M. L. Proc. Roy. Soc. (London), A206, (1951) 448.

72. Fox, J. H. P. and Lambert, J. D. Proc. Roy. Soc. (London), A210, (1951) 557.

73. Pitzer, K. S. J. Am. Chem. Soc., 77, (1955) 3427, 3433.

74. Pitzer, K. S. and Curl, R. F., Jr. J. Am. Chem. Soc., 79, (1957) 2369.

75. Prausnitz, J. M. and Gunn, R. D. AIChE. Jour., 4(4), (1958) 430.

76. Meyers, C. H. and Van Dusen, M. S. Bur. Stds. J. Res., 10, (1933) 381.

77. Kobe, K. A. and Lynn, R. E., Jr. Chem. Rev., 52, (1953) 117.

78. Ruhemann, M. The Separation of Gases, Oxford University Press 1949.

79. Froelich, H. C. and Kenty, C. Rev. Sci. Inst., 22, (1951) 214.

80. Marshall, L. Rev. Sci. Inst., 26, (1955) 614.

81. Nelson, L. S. Rev. Sci. Inst., 27, (1956) 655.

82. Scott, R. B. Cryogenic Engineering, D. Van Nostrand Co., Inc., 1959.

83. Hoge, H. J. Temperature, Its Measurement and Control in Science and Industry, Vol. 1, Reinhold Publishing Corporation, New York, 1941.

84. Baker, H. D., Ryder, E. A. and Baker, N. H. Temperature Measurement in Engineering, New York: John Wiley and Sons, Inc., 1953.

85. Scott, R. B. Bur. Stds. J. Res., 25, (1940) 459.

86. Hilsenrath, J., et.al. NBS Circ. 564, 1955.

87. Wiebe, R. and Brevoort, M. J. Rev. Sci. Inst., 2, (1931) 450.